# Spin Systems far from Equilibrium : Aging and Dynamic Phase Transition

Hyunhang Park

Dissertation submitted to the Faculty of the
Virginia Polytechnic Institute and State University
in partial fulfillment of the requirements for the degree of

Doctor of Philosophy
in
Physics

Michel J. Pleimling, Chair
Jean J. Heremans
William Mather
Uwe C. Täuber

March 4, 2013
Blacksburg, Virginia

Keywords: Aging Phenomena, Disordered Ferromagnets, Dynamical Scaling, Dynamic Phase Transition, Surface Critical Phenomena, Surface Phase Diagram

# Spin Systems far from Equilibrium : Aging and Dynamic Phase Transition

(ABSTRACT)

Among the many non-equilibrium processes encountered in nature we deal with two different but related aspects. One is the non-equilibrium relaxation process that is at the origin of 'aging phenomena', and the other one is a non-equilibrium phase transition, called 'dynamic phase transition'. One of the main purposes of our research is to explore more realistic situations than studied previously. Indeed, in the study of aging phenomena certain kinds of disorder effects are considered, and we introduce the 'surface' as a spatial boundary to the system undergoing the dynamic phase transition. In order to observe these processes as clearly as possible, we study in both cases simple spin systems.

Using Monte Carlo simulations we first investigate aging in three-dimensional Ising spin glasses as well as in two-dimensional Ising models with disorder quenched to low temperatures. The time-dependent dynamical correlation length $L(t)$ is determined numerically and the scaling behavior of various two-time quantities as a function of $L(t)/L(s)$ is discussed where $t$ and $s$ are two different times. For disordered Ising models deviations of $L(t)$ from algebraic growth law show up. The generalized scaling forms as a function of $L(t)/L(s)$ reveal a generic simple aging scenario for Ising spin glasses as well as for disordered Ising ferromagnets.

We also study the local critical phenomena at a dynamic phase transition by means of numerical simulations of kinetic Ising models with surfaces subjected to a periodic oscillating field. We examine layer-dependent quantities, such as the period-averaged magnetization per layer $Q(z)$ and the layer susceptibility $\chi(z)$, and determine local critical exponents through finite size scaling. Both for two and three dimensions, we find that the values of the surface exponents differ from those of the equilibrium critical surface. It is revealed that the surface phase diagram of the non-equilibrium system is not identical to that of the equilibrium system in three dimensions.

The study of aging in disordered systems is supported by the U.S. Department of Energy (DOE) through Grant No. DE-FG02-09ER46613. The study of dynamic phase transitions is supported by the U.S. National Science Foundation (NSF) through Grants No. DMR-0904999 and No. DMR-1205309.

# Dedication

To my parents Shintaik Park and Gapsoo Yoon, my sister Myongsun Park, and my wife and baby, Eunkyoung and Ian.

# Acknowledgments

It is incredible that the time to write here has finally come. Now I would like to acknowledge names of people to whom I am indebted.

First of all, I would like to express my gratitude to my advisor Dr. Michel Pleimling for his help and guidance. Without his clear and kind advise I would have been lost in a maze of complicated theories. He taught me to approach the core of the problem step by step. He is a great teacher of physics to me, furthermore, his sense of humor and wisdom will remaine in my mind for a long time. I would like to thank Dr. Uwe Täuber for providing me with invaluable help throughout my whole Ph.D study including my core coursework. I could understand many theoretical concepts completely from his lectures. I am also thankful to my other committee members, Dr. Jean Heremans and Dr. William Mather. Their comments and encouragements were really helpful for me to complete my dissertation.

I am grateful to Ulrich Dobramysl for helping me to understand the vortex dynamics problem in disordered Type-II superconductors. I also thank Yoh Yamamoto for enjoyable discussions about many topics in and out of physics. I would like to thank my graduate friends, Nasrin Afzal, Shahir Mowlaei, Ben Fred M. Intoy, Ahmed Roman, Nick Borchers and Hiba Assi for sharing a pleasant time in the office. Lastly, I am thankful to Yong-jae Kim for giving me priceless help in every aspect of my life here in Blacksburg. Yes, VT life was really awesome.

# Contents

# List of Figures

# List of Tables

# Chapter 1

# Introduction

Equilibrium statistical mechanics is undoubtedly one of the greatest theoretical achievements in Physics of the last 150 years. In principle, this general framework enables us to completely describe equilibrium states and derive thermodynamic quantities such as entropy, pressure or chemical potential through simple mathematical manipulations.

As a matter of fact, however, an equilibrium state is nothing but an exception rather than a rule in the sense that almost every real system in nature persists to be in a non-equilibrium state. Real systems are open to the environment in such a way that exchanges of energy, particles or other quantities occur at all time. There have been huge efforts to seek a general framework applicable to large classes of non-equilibrium systems, but unfortunately these efforts were only partially successful. Thus one can pay attention to the temporal change of the probability distribution of the microstates of the non-equilibrium system of interest. A usual way to do so is to write down stochastic equations such as a Fokker-Planck equation or a master equation for given transition probabilities. Of course, if the system is brought out of equilibrium by an 'infinitely' small external perturbation, then it remains near equilibrium. It is well known that in this case linear response theory can be employed to describe the behavior of the system.

In contrast, strong perturbations kick the system 'far from' equilibrium. Whereas probability currents decay away fast near equilibrium, there is a tenacious non-vanishing flow of probability in the system far from equilibrium. As a result the dynamics far from equilibrium displays a very rich behavior. Even in simple ferromagnetic spin systems, for instance, a sudden change of the temperature from the high temperature paramagnetic phase to the low temperature ferromagnetic phase leads the system to exhibit an extremely slow relaxation to equilibrium. It is known that the typical relaxation time is proportional to the size $L$ of the growing spin domains with some positive exponent $z$, i.e. $t \sim L^z$, which means complete relaxation never finishes in the thermodynamic limit. Furthermore, time translation invariance is broken during the relaxation; two-time quantities such as correlation and response functions depend on both times $t$ and $s < t$, where the time $t$ is called 'observation'

time while the time $s$ is called 'waiting' time. These features show a typical non-equilibrium relaxation phenomenon, referred to as 'aging behavior': Older samples respond more slowly to a change. Remarkably, this statement can be summarized through simple dynamical scaling relations for the correlation and response functions. In the 'simple aging scheme', these quantities can be expressed as a function of the ratio between the two times, $t/s$, assuming the existence of the single characteristic length scale $L(t) \sim t^{1/z}$.

Another example of a strong perturbation is the presence of a periodic reversal of an applied external field. This oscillation can keep the spin system in a dynamical non-equilibrium phase. When the external field is turned on, each spin responds to it and tries to align to the direction of the field. However, the global ordering is not achieved immediately, instead spin droplets are nucleated and coalesce together after some time. The metastable lifetime $\langle\tau\rangle$, the time it takes for the system to escape from the metastable state, defines the intrinsic time scale. Now imagine that the field changes its sign periodically. If the period of the field is larger than $\langle\tau\rangle$, almost all spins flip and the system is able to *follow* the field, so the magnetization will oscillate symmetrically about zero. On the other hand, when the period is much shorter than $\langle\tau\rangle$, then this symmetry is broken and the averaged magnetization over a period takes on a non-zero value. This period-averaged magnetization $Q$ plays the role of the dynamic order parameter which allows to recognize two distinct dynamical phases. One can study the critical region between these two phases by changing the dimensionless parameter $\Theta$ given by the ratio between the metastable lifetime and the half period of field. This transition is called 'dynamic phase transition' (DPT) and is a genuine non-equilibrium phase transition. Surprisingly, the estimation of the critical exponents reveals that for the two-dimensional bulk Ising model the dynamic phase transition belongs to the universality class of the equilibrium Ising model.

In the following we present a detailed investigation of the effects additional constraints have on the model systems described above. This is done in order to study the effect of disorder and surfaces on these non-equilibrium phenomena. In Chapter 2, different types of quenched disorder are added to the ferromagnetic system and the effects disorder has on aging are explored. Adding disorder or impurities to a pure material is a very important problem as already small amounts of impurities can strongly modify properties of the material. In general, it is expected that quenched disorder breaks spatial translational symmetry of the system, thereby yielding a tendency to pin domain walls in certain favorable locations. However, in the past there have been considerable debates, based on analytical predictions and numerical results, about various specific issues such as the growth law of the dynamical correlation length $L(t)$, the scaling form of two-time quantities or the concept of superuniversality. For two different types of disordered systems, namely, the random-site and random-bond Ising models, we perform intensive numerical simulations to monitor the temporal changes of various two-time quantities. Our simulations reveal that the apparent power-law growth of $L(t)$ only holds in the early stages of the coarsening process and that notable deviations are already encountered for moderate values of the correlation length. As a consequence one cannot naively assume that $L(t) \sim t^{1/z}$, and the correct time dependence

$L(t)$ has to be used in the investigation of the scaling behavior of two-time quantities. When doing this, a (modified) simple aging behavior emerges for all the quantities of interest in the scaling limit. Furthermore, we also address superuniversality and show that in certain regimes scaling functions are to a large extend independent of disorder. Finally, we apply method of analysis, obtained from disordered ferromagnets, to Ising spin glasses where frustration effects and disorder are combined.

In the second part of this thesis we focus on systems displaying a dynamic phase transition and add a surface as the simplest geometric boundary. It is readily understood that a surface breaks spatial translational invariance of the system so that the critical behavior near the surface is strongly modified when compared to the conventional bulk critical behavior observed deep inside the bulk. Actually, great progress in our understanding of equilibrium surface critical phenomena has been achieved in the last two decades, and one of the main discoveries is that there are different surface universality classes for a given bulk universality class. For example, for the three-dimensional Ising model the surface phase diagram consists of the ordinary transition, the surface transition, the special transition point and the extraordinary transition, as explained in detail in section 3.1.2. Therefore, in Chapter 3 we focus on whether the dynamic phase transition in presence of a surface shows the same behavior as an equilibrium phase transition close to a surface. Defining a dynamic order parameter $Q$, the susceptibility $\chi$ as well as the Binder cumulant $U$ both in the bulk and at the surface, we monitor the critical behavior of $Q$ and $\chi$ and also determine the critical value of $\Theta$. We then employ the finite size scaling analysis to estimate local critical exponents. Surprisingly, it is revealed that the measured sets of local critical exponents are different from the corresponding equilibrium exponents, and this both for two and three space dimensions. Furthermore, the surface phase diagram in the three-dimensional case is remarkably simple, as only the ordinary transition is encountered.

This thesis is organized in the following way. In Chapter 2 we discuss how aging behavior in the ferromagnetic system is modified due to the presence of disorder. First, phenomenological concepts and the theory of physical aging are developed in the perfect, i.e. non-disordered and non-frustrated, Ising model. Then two different types of disordered Ising models as well as Ising spin glasses are introduced. For all disordered systems, the growth of the dynamical correlation length $L(t)$ is numerically determined and an extended simple aging scenario using $L(t)$ is tested for various two-time quantities. Chapter 3 is devoted to the surface critical behavior at a dynamic phase transition. After a brief review of the dynamic phase transition in the bulk system and local equilibrium critical phenomena, we discuss the critical properties of the surface layer in the semi-infinite Ising model displaying a dynamic phase transition. Relevant quantities such as dynamic order parameter and susceptibility in the bulk and in the surface layer are introduced, and values of critical exponents are estimated by finite size scaling. Both for two and three space dimensions, the obtained values of the critical exponent are compared to those of equilibrium surface universality classes, and the novel type of surface phase diagram that emerges in three dimensions is discussed. Finally, Chapter 4 gives our conclusion.

# Chapter 2

# Aging Phenomena with Disorder

This chapter discusses aging phenomena in various Ising spin systems with a focus on the effect of disorder. In section 2.1 the general concepts of physical aging and some theoretical tools are reviewed, and the simple aging scaling scenario is introduced. The subsequent sections are devoted to the effects that disorder has on the simple aging scenario. This is the main part of the chapter. In section 2.2 two different kinds of disorder are introduced as agents which hinder the domain coarsening so that the growth of the dynamical correlation length $L(t)$ becomes slower. For these cases we show that the simple aging scheme remains valid after a slight generalization. This changed aging scenario is then tested in the Edwards-Anderson Ising spin glass in section 2.3. In section 2.4 we give our conclusions.

## 2.1 Aging in Perfect Ferromagnets

The term 'Aging' is already used in the context of Biology or Chemistry, roughly meaning as 'accumulation of changes in properties of a system over time'. Even though this term in Physics basically shares the same meaning, there is a crucial difference between physical aging and the others : reversibility. In other words, in Biology or Chemistry the aging of the system is characterized as inherently irreversible process, but physical aging is reversible experimentally by heating up the system again. This feature is called 'thermoreversibility'.

Within Physics, aging is a generic concept which describes a typical behavior of a many-body system when it undergoes a non-equilibrium relaxation process. Imagine that we force the system, initially prepared in a disordered high temperature state, into a far from equilibrium state by changing temperature $T$ so suddenly and strongly (or 'quench' in technical terms) that the system ends up in a far from equilibrium state deep inside the coexistence region of the equilibrium phase diagram. After the quench the system will try to return to a new stationary state. However, if there are equivalent and competing free energy minima, then the global relaxation of the system will be complicated and the system will display an intrinsic

non-equilibrium behavior which can be summarized through the following three defining properties : First, slow (non-exponential) relaxation dynamics. Because of competing free energy minima it is very difficult to force the system to relax to the stationary state rapidly. Second, breaking of time-translation-invariance. Right after the quench the system is not in a stationary state, so obviously its properties will not be invariant under time-translations. This suggests that we need physical quantities depending on multiple times in order to describe the relaxation completely. Third, the existence of dynamical scaling. Domains which are locally in equilibrium develop after the quench after some initial transient regime. The geometrical patterns of the domains turn out to be statistically self-similar which suggests that there is a growth of a single time-dependent length scale $L(t)$ and that the behavior of the multiple time quantities is governed by simple dynamical scaling forms. Surprisingly, it has been demonstrated experimentally that this dynamical scaling arises in many different kinds of material. This implies that aging phenomena depend only on a few general characteristics of the systems, thereby displaying a large degree of universality that should allow us to develop in a deep theoretical understanding of aging.

The characteristics of aging phenomena described above are rather general and have initially been discovered and developed in the study of glassy systems [1]. In the following, we consider one of the simplest spin systems : the ferromagnetic Ising model. Let us imagine a perfect i.e. non-disordered and non-frustrated Ising model in a completely disordered (or infinitely high temperature) state as an initial set-up. We then instantaneously decrease (or 'quench') the temperature so that the system is brought out of the equilibrium state. As a further specification, we restrict ourselves to phase-ordering kinetics where we quench the temperature far below the critical temperature $T_c$ with a non-conserved order parameter. (If the system is quenched right to $T_c$ then the system is said to undergo non-equilibrium critical dynamics. Instead, if it is quenched below $T_c$ but with a conserved order parameter then the observed ordering is called phase-separation. All of these situations are not further discussed in this thesis.) Even though the system is quenched into the region of the equilibrium ferromagnetic phase, right after the quench instantaneous equilibriation of the system is not achieved. What happens instead here is the continuous local coarsening of numerous spin domains. Because of the effective field generated by neighboring spins, each spin begins its ordering in such a way that the local domain around the spin chooses one of the equivalent equilibrium states associated with the minimum free energy. Thus, several ordered domains will grow throughout the system and the domain walls move slowly as time goes on. Using the coarse-grained description, the surface tension between the spin domains pushes the domain walls to move in the direction normal to the wall with a force proportional to the mean curvature. This fact is formulated as the celebrated Allen-Cahn equation [2] for phase-ordering kinetics with a non-conserved order parameter. In order to quantify the growth of the domains, we measure the time dependence of the average size of the domains which we shall call the dynamical correlation length $L(t)$. With the help of the Allen-Cahn equation, it can be shown that $L(t)$ is the only characteristic length scale in systems undergoing phase-ordering kinetics which follows an algebraic growth law $L(t) \sim t^{1/z}$, where $z$ is called the dynamic exponent. This exponent has the value $z = 2$ for systems undergoing phase-

ordering, whereas for systems undergoing phase-separation, its value is $z = 3$. This algebraic growth is particularly interesting because in the thermodynamic limit the growth of the domains never stops and the system cannot reach the final equilibrium state on a finite time scale.

In order to properly capture this slow coarsening of the domains, which ultimately is responsible for the aging phenomena, one needs to define and measure multiple-time quantities. The first quantity of great importance is the two-time space-time correlation function

$$C(t, s; \boldsymbol{r}) := \langle \phi(t, \boldsymbol{r}) \phi(s, \boldsymbol{0}) \rangle - \langle \phi(t, \boldsymbol{r}) \rangle \langle \phi(s, \boldsymbol{0}) \rangle \ . \tag{2.1}$$

where $\phi(t, \boldsymbol{r})$ is the order parameter (the magnetization density in the Ising model) at time $t$ and at the spatial point $\boldsymbol{r}$. Here $s$ is called the waiting time or aging time whereas the time $t \geq s > 0$ is called the observation time, and both times are measured after the quench. Since we always prepare our system in the infinitely high temperature state that is invariant under spatial translations, we have that $\langle \phi(t, \boldsymbol{r}) \rangle = \langle \phi(0, \boldsymbol{r}) \rangle = 0$, and then the correlation function reduces to

$$C(t, s; \boldsymbol{r}) := \langle \phi(t, \boldsymbol{r}) \phi(s, \boldsymbol{0}) \rangle \ . \tag{2.2}$$

We also consider another important quantity, the (linear) two-time space-time response function

$$R(t, s; \boldsymbol{r}) := \left. \frac{\delta \langle \phi(t, \boldsymbol{r}) \rangle}{\delta h(s, \boldsymbol{0})} \right|_{h=0} \ . \tag{2.3}$$

where $h(t)$ is the external magnetic field conjugated to the order parameter $\phi$. In numerical simulations (on which the present work is mostly based) the response function is difficult to measure because of the weakness of the signal when measuring the local response to a local perturbation. This is in contrast to the measurement of the correlation function which is straightforward. Thus in practice, researchers making use of simulations preferably use an alternative approach and compute the time integrated response function rather than the response function itself. Two different protocols are mainly used which differ in the time-history of the applied magnetic field $h(t)$. In the thermoremanent (TRM) protocol $h(t)$ is applied from the moment of quench $t = 0$ until the waiting time $t = s$, before being turned off. In the zero-field cooled (ZFC) protocol the field remains zero until the time $s$ has elapsed and is turned on after that time. For both protocols, the magnetization $M$ is measured at a later time $t$. If the field $h(t)$ is small enough, then the susceptibility $\chi$ is directly proportional to the magnetization which is given in the two protocols by

$$M_{\mathrm{TRM}}(t, s; \boldsymbol{r}) = h \chi_{\mathrm{TRM}}(t, s; \boldsymbol{r}) = h \int_0^s \mathrm{d}u \, R(t, u; \boldsymbol{r}) \ , \tag{2.4}$$

$$M_{\mathrm{ZFC}}(t, s; \boldsymbol{r}) = h \chi_{\mathrm{ZFC}}(t, s; \boldsymbol{r}) = h \int_s^t \mathrm{d}u \, R(t, u; \boldsymbol{r}) \ . \tag{2.5}$$

The quantities introduced above depend both on space and time, but purely time-dependent quantities are also very helpful in order to understand the temporal behavior of the system.

These two quantities are called the autocorrelation function and the autoresponse function respectively :

$$C(t,s) := C(t,s;\mathbf{0}) \ , \ R(t,s) := R(t,s;\mathbf{0}) \ . \tag{2.6}$$

As already mentioned, there exists a single characteristic length scale $L(t) \sim t^{1/z}$ in a system with phase-ordering kinetics. This statement implies that the correlation and response functions are independent of the time variables if the lengths are scaled by the correlation length $L(t)$. In other words, all lengths in these quantities can be expressed through $|\boldsymbol{r}|/L(s)$ and $|\boldsymbol{r}|/L(t)$ yielding the common scaling forms

$$C(t,s;\boldsymbol{r}) = [L(s)]^{-B}\mathcal{F}_C\left[\frac{|\boldsymbol{r}|}{L(s)},\frac{|\boldsymbol{r}|}{L(t)}\right] \ , \ R(t,s;\boldsymbol{r}) = [L(s)]^{-A'}\mathcal{F}_R\left[\frac{|\boldsymbol{r}|}{L(s)},\frac{|\boldsymbol{r}|}{L(t)}\right] \ . \tag{2.7}$$

where $\mathcal{F}_C(y,w)$ and $\mathcal{F}_R(y,w)$ are space- and time-dependent scaling functions which are valid in the scaling regime $L(t) \gg L(s) \gg 1$ and $A'$ and $B$ are non-equilibrium exponents which shall be determined later. Then one can immediately rewrite the scaling relations in the following forms which involve the ratio between the length variables

$$C(t,s;\boldsymbol{r}) = [L(s)]^{-B}\tilde{F}_C\left[\frac{L(t)}{L(s)},\frac{|\boldsymbol{r}|}{L(t)}\right] \ , \tag{2.8}$$

$$R(t,s;\boldsymbol{r}) = [L(s)]^{-A'}\tilde{F}_R\left[\frac{L(t)}{L(s)},\frac{|\boldsymbol{r}|}{L(t)}\right] \ . \tag{2.9}$$

These scaling relations are one of the main conclusions in this section and clearly show one aspect of aging, namely the existence of dynamical scaling. Furthermore, if the aging behavior of the system can be completely described by the above scaling relations, the system is said to display a 'simple aging' or 'full aging' scheme in the sense that the scaling function simply depends on the ratio of the two variables. Using the relation $L(t) \sim t^{1/z}$, the scaling forms may be also expressed in terms of the time variables only

$$C(t,s;\boldsymbol{r}) = s^{-b}F_C\left[\frac{t}{s},\frac{|\boldsymbol{r}|}{L(t)}\right] \ , \tag{2.10}$$

$$R(t,s;\boldsymbol{r}) = s^{-1-a}F_R\left[\frac{t}{s},\frac{|\boldsymbol{r}|}{L(t)}\right] \ . \tag{2.11}$$

where $a = \frac{A'}{z} - 1$ and $b = B/z$ are called the aging exponents.

In addition, if we take $\boldsymbol{r} = \mathbf{0}$ the scaling forms for the autocorrelation and autoresponse functions are also derived. In terms of length variables,

$$C(t,s) = [L(s)]^{-B}\tilde{f}_C\left[\frac{L(t)}{L(s)}\right] \ , \tag{2.12}$$

$$R(t,s) = [L(s)]^{-A'}\tilde{f}_R\left[\frac{L(t)}{L(s)}\right] \ . \tag{2.13}$$

Using again the algebraic growth relation the scaling takes on a simple form

$$C(t,s) = s^{-b} f_C\left(\frac{t}{s}\right) \ , \tag{2.14}$$

$$R(t,s) = s^{-1-a} f_R\left(\frac{t}{s}\right) \ . \tag{2.15}$$

One remarks that usually the autocorrelation and autoresponse scaling functions show a power law decay : $\tilde{f}_{C,R}(y) \sim y^{-\lambda_{C,R}}$ and $f_{C,R}(y) \sim y^{-\lambda_{C,R}/z}$ for $y \gg 1$ where $\lambda_{C,R}$ are called the autocorrelation and autoresponse exponents respectively, which are non-trivial exponents associated with the phase-ordering kinetics.

Finally, additional scaling forms for the thermoremanent susceptibility, which will be also used in this work, are derived from (2.4) :

$$\chi(t,s) = [L(s)]^{-A} \tilde{f}_\chi\left[\frac{L(t)}{L(s)}\right] \ , \ \chi(t,s) = s^{-a} f_\chi\left(\frac{t}{s}\right) \ . \tag{2.16}$$

where the two relations describe the expression in terms of the length and time variables respectively. The non-equilibrium exponent $A$ has the following relationship with the aging exponents : $a = \frac{A'}{z} - 1 = A/z$. As we shall see in section 2.2for the disordered ferromagnets, it is notable that if there is no algebraic dependence of $L(t)$ on time $t$ then the expressions in terms of the time variables such as (2.10), (2.11), (2.14) and (2.15) lose their meanings and one needs to use the scaling forms expressed in terms of the length variables only, see (2.8), (2.9), (2.12) and (2.13).

## 2.2 Aging in Disordered Ferromagnets

### 2.2.1 The Effect of Quenched Disorder

As briefly shown in the previous section, the phenomenology of aging in perfect i.e. non-disordered and non-frustrated ferromagnetic systems, is quite well understood by the simple aging scaling scheme and the corresponding scaling forms. For a more fundamental understanding of simple aging, one can refer to the concept of 'Local Scale Invariance (LSI)' [3], which is the dynamical version of attempts to extend in equilibrium critical phenomena scale-invariance to conformal invariance.

The next natural question is whether this ideal scheme is also applicable to more 'realistic' systems. Among the many ways to make 'realistic' systems, introduction of quenched disorder is of great importance. Whereas the effect of disorder on equilibrium critical phenomena was intensively discussed for nearly 50 years since the work on the random-bond Ising model by McCoy and Wu [5], the study of the effects of disorder on non-equilibrium processes such

as ordering processes or relaxation phenomena, began only rather recently. One first notes that disorder makes the system to be inhomogeneous as it breaks the spatial translational invariance of the system. In addition, disorder has a tendency of pinning domain wall of energetically favorable positions. In other words, disorder introduces energy barriers which disturb the domain growth.

An important theoretical prediction in this field comes from the pioneering work by Huse and Henley (HH) [6]. They considered an Ising ferromagnetic system with randomly placed disorder generating random exchange couplings. The Allen-Cahn equation, which was the central equation in the simple aging scaling, is then extended to be able to contain a length- and temperature-dependent diffusion coefficient

$$\frac{\mathrm{d}L(t)}{\mathrm{d}t} = \frac{D(L,T)}{L(t)} \tag{2.17}$$

where the length $L(t)$ indicates the average size of the domain or the dynamical correlation length. Based on the renormalization group analysis and numerical simulation, the authors argued that the asymptotic dynamics at late times, when the impurities begin to effectively pin the domains, is driven by thermal activation process and that the diffusion should depend on temperature $T$ in the following way :

$$D(L,T) \sim \mathrm{e}^{-E_b(L)/k_B T} \tag{2.18}$$

where $E_b(L)$ is the barrier energy and $k_B$ is the Boltzmann constant. Also, as suggested by scaling forms, the barrier energy was assumed to have a power-law dependence on the domain size i.e. $E_b(L) \sim L^{\psi}$ with an exponent $\psi = \frac{2\zeta+d-3}{2-\zeta}$ where $\zeta$ is the domain-wall roughness exponent. This reasoning leads to slow, logarithmic growth of the typical size of the domains $L(t) \sim (\log t)^{1/\psi}$. For example, in two dimensions it is known that $\zeta = 2/3$ and so $\psi = 1/4$. It is remarkable that this logarithmic growth of $L(t)$ is predicted to be independent of the specific realization of the disorder provided that the system has only short-range interactions and that disorder is not too strong to destroy the ferromagnetic phase-ordering itself. This result is also consistent qualitatively with experimental works done for some materials such as $Rb_2Co_{0.60}Mg_{0.40}F_4$ [7] or ZLI 4792 (liquid crystal) [8] which can be described by diluted antiferromagnetic or random-bond Ising models in two dimensions respectively. They have the values of $\psi = 0.28$ and $1/4$ respectively, and $L(t)$ indeed follows the logarithmic growth $(\ln t)^{1/\psi}$ for both of them.

One specific issue that we are going to address concerns the growth law of the length scale $L(t)$. However, before going deeper into this issue, let us describe different kinds of disorder. For simplicity, only two kinds of disorder will be considered throughout this presentation : bond disorder and site disorder. Whereas in the former case the exchange coupling strength is permitted to have random (but positive) values taken from some distribution, in the latter case the concentration of the magnetic sites is diluted in such a way that a given fraction of randomly selected sites is not occupied by an Ising spin.

Contrary to the work by HH, the early Monte Carlo simulations of various disordered ferromagnetic Ising models [4, 9–13] found for the dynamical correlation length $L(t)$ a power-law growth, $L(t) \sim t^{1/z}$, with a non-universal dynamical exponent $z$ that depends on temperature and on the nature of the disorder. This behavior can be explained by assuming that the energy barriers $E_B(L)$ grow logarithmically with $L$ [4, 9]. As a consequence, it follows that the dynamical exponent $z$ should be inversely proportional to the temperature : $z \sim 1/T$. Whereas this temperature dependence has been observed in the Cardy-Ostlund model [14], another study [12] has revealed that in the random-bond Ising model the temperature dependence of the dynamical exponent is more complicated. This fact points to the existence of conceptual problems in the approach of Paul *et al.* [4, 9]. New insights into this matter have come very recently through a series of papers on the dynamics of elastic lines in a random potential [15–18]. These papers provide convincing evidence for a dynamic crossover between a transient regime, characterized by a power-law growth with an effective dynamical exponent that depends on the disorder, and the asymptotic regime where the growth is logarithmic in time. This result strongly suggests the possibility that a similar crossover could take place in disordered ferromagnets and that the observed power-law regime with nonuniversal dynamical exponents is not the asymptotic regime. However, as the transient regime is already extremely long lived for the elastic line [16, 17], it is expected that the asymptotic regime is not easily accessible in simulations of coarsening ferromagnets. Nevertheless, it can well be that on the time scales accessible in relaxation measurements a crossover takes place.

Another important issue concerns the notion of *superuniversality*. In the previous section we already saw that dynamical scaling arises when there exists a unique reference length scale $L(t)$, and two-time quantities such as correlation and response functions can be expressed by scaling forms which include the ratio between the length or time variables, see (2.8), (2.9), (2.10) and (2.11). Furthermore, it has also been suggested that this dynamical scaling should be true even if disorder without frustration is introduced into the system. In other words, scaling functions of space- and time-dependent quantities should be independent of the nature of disorder and of temperature [20]. Some coarsening ferromagnets with weak randomness [19] (as, for example, the random-bond or the random-field Ising models) have been shown to display a *superuniversal* behavior in numerical studies. This has been verified numerically in various coarsening systems both for one-time [11, 13, 21–24] and two-time quantities [12], but it is an open question how general this result really is.

### 2.2.2 Random-Site Ising Model

In addition to two issues stated above, the validity of the hypothetical superaging scenario is another question which needs to be discussed in this subsection. In many systems it is empirically observed that in the aging regime the autocorrelation function $C(t,s)$ behaves like [25]

$$C(t,s) = \mathcal{C}\left[\frac{h(t)}{h(s)}\right] \quad , \quad h(t) = h_0 \exp\left[\frac{1}{c_0}\frac{t^{1-\mu}-1}{1-\mu}\right] \quad , \tag{2.19}$$

where $\mathcal{C}$ is a scaling function, $\mu$ is a free parameter, and $h_0$ and $c_0$ are constants [26]. Depending on the value of $\mu$, different situations are summarized by (2.19). If $0 < \mu < 1$, a subaging behavior prevails, as is, for example, observed in soft matter [27, 28] or in living biological matter [29], with $\mu \approx 0.3 - 0.8$. For $\mu = 1$, one recovers a standard simple aging behavior where the autocorrelation is only a function of the ratio $t/s$. This is the behavior encountered in many systems and, in particular, in the perfect ferromagnets undergoing phase ordering. Finally, for $\mu > 1$ one has a superaging behavior. This is a rather hypothetical scenario as Kurchan has proven an exact lemma [30] that states that under very general conditions a superaging behavior of the autocorrelation cannot exist (this proof can also be extended to response functions [25]). It is therefore intriguing that a study of the autocorrelation in the two-dimensional random-site Ising model [10] yielded data to which one can fit the superaging scaling form

$$C(t,s) = \mathcal{C}\left(\exp\left[\frac{(t-s)^{1-\mu} - s^{1-\mu}}{1-\mu}\right]\right) \tag{2.20}$$

with $\mu$ slightly larger than 1. However, in the random-bond Ising model the autocorrelation displays a simple aging behavior [12] in full analogy to what is observed in the pure model [31]. These differences in the observed scaling behavior of different disordered ferromagnets remains to be explained.

### A. Model and Measured Quantities

Now we proceed to introduce one of the disordered ferromagnetic systems that we are going to discuss in detail. The following part in this section has been published in [32]. We consider the two-dimensional random-site Ising model [33] on a square lattice (we set the lattice constant to one) with the Hamiltonian:

$$\mathcal{H} = -\sum_{\langle \mathbf{x},\mathbf{y}\rangle} \rho_{\mathbf{x}}\rho_{\mathbf{y}} S_{\mathbf{x}} S_{\mathbf{y}} \ , \tag{2.21}$$

where the sum is over nearest-neighbor pairs. $S_{\mathbf{x}} = \pm 1$ are the usual Ising spins and $\rho_{\mathbf{x}}$ are quenched random variables taken from the distribution $P(\rho) = p\delta_{\rho,1} + (1-p)\delta_{\rho,0}$. For $p = 1$ we of course recover the standard Ising model on a square lattice. If the system is diluted, i.e., if $p < 1$, one still observes a phase transition between a disordered high-temperature phase and an ordered low-temperature phase for all $p \geq p_c \approx 0.593$.

In our simulations we prepare the system in a fully disordered state, corresponding to infinite temperature, and then bring it in contact with a heat bath at a temperature $T < T_c(p)$, where $T_c(p)$ is the critical temperature for the dilution $p$. After the quench, the system is evolved with the standard single spin-flip Metropolis algorithm (in order to check that our conclusions are independent of the update scheme we also did a large number of runs with the heat-bath algorithm), and the relaxation of the system toward equilibrium is monitored

through the study of the autocorrelation, the space-time correlation, and the thermoremanent susceptibility. The two-time autocorrelation function is given by the expression

$$C(t,s) = \frac{1}{N}\sum_{\mathbf{x}} \overline{\langle S_{\mathbf{x}}(t) S_{\mathbf{x}}(s)\rangle} \ , \tag{2.22}$$

where the sum is over the $N = L^2$ lattice sites and $S_{\mathbf{x}}(t)$ is the value of the spin at site $\mathbf{x}$ at time $t$. For all studied quantities we have to average over both the thermal noise (indicated by $\langle\cdots\rangle$) and the site disorder (indicated by $\overline{\cdots}$). In order to get a more complete picture of the relaxation processes, we extend our study to the two-time space-time correlation function

$$C(t,s;\mathbf{r}) = \frac{1}{N}\sum_{\mathbf{x}} \overline{\langle S_{\mathbf{x}+\mathbf{r}}(t) S_{\mathbf{x}}(s)\rangle} \ . \tag{2.23}$$

Finally, we also investigate how the system reacts to a perturbation by adding a small spatially random magnetic field $h_{\mathbf{x}} = H_0\varepsilon_{\mathbf{x}}$, $\varepsilon_{\mathbf{x}} = \pm 1$, at the moment of the quench [34]. This field is turned off after the waiting time s after which we measure the decay of the time-dependent thermoremanent susceptibility

$$\chi(t,s) = \frac{1}{N}\sum_{\mathbf{x}} \overline{\{\langle \varepsilon_{\mathbf{x}} S_{\mathbf{x}}\rangle\}} \ , \quad t > s \ , \tag{2.24}$$

where an additional average over the random field, indicated by $\{\cdots\}$, has to be performed.

The results reported in this subsection have been obtained for systems composed of $N = 300 \times 300$ spins. We carefully checked that no finite-size effects show up in our simulations for this system size. We considered three different degrees of dilution: $p = 0.9$, 0.8, 0.75, and three different temperatures for every $p$ value: $T = 0.7T_c(p)$, $0.5T_c(p)$, $0.4T_c(p)$ with $T_c(0.9) \approx 1.914$, $T_c(0.8) \approx 1.50$, $T_c(0.75) \approx 1.30$. For the autocorrelation and the space-time correlation we averaged typically over at least 1,000 independent runs, thereby considering waiting times $s$ up to $20,000$ Monte Carlo steps (MCSs), with a total running time of $t = 50s$ MCS (as usual, time is measured in MCSs, one MCS corresponding to $N = L^2$ proposed updates of the system). We also studied the corresponding quantities with $s = 0$, i.e., $C(t, s = 0)$ and $C(t, s = 0; \mathbf{r})$, as well as the one-time quantity $C(t, \mathbf{r}) \equiv C(t, t; \mathbf{r})$. For the autoresponse we used $H_0 = 0.05$ (we checked that we are in the linear-response regime for that strength of the random field) and averaged at least over $10,000$ independent runs. We thereby considered waiting times up to $s = 800$ and observation times again up to $t = 50s$.

### B. Numerical Results

***Dynamical correlation length*** In the following we first discuss the time dependence of the correlation length before studying in a systematic way the scaling behavior of the various two-time quantities introduced in the previous section. We obtain the dynamical correlation

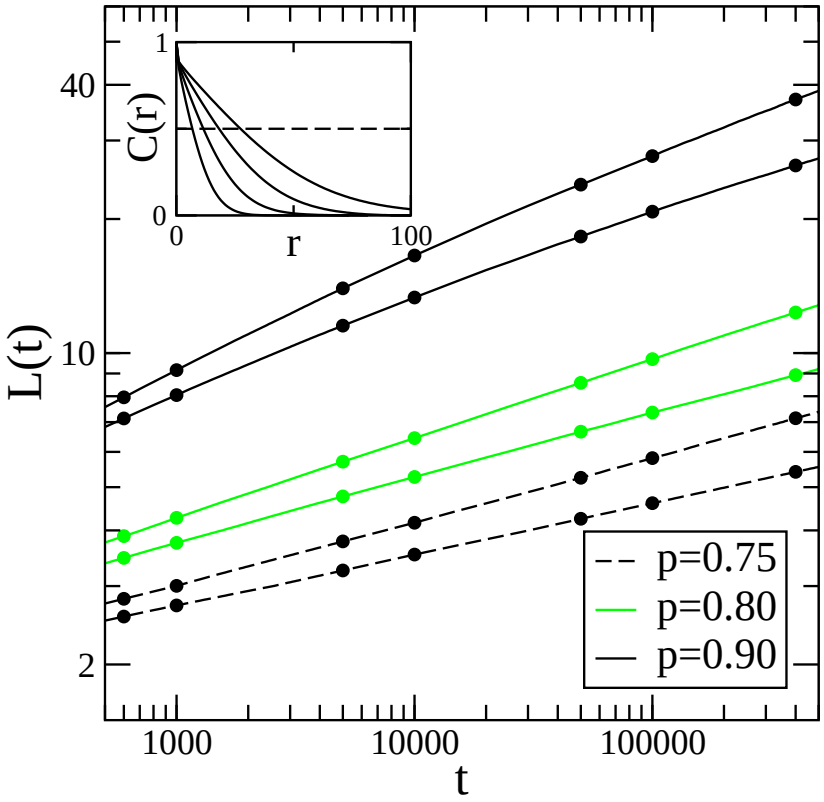


Figure 2.1: Dynamical correlation length $L(t)$ vs time. For every degree of dilution, data for two temperatures are shown: $T = 0.4\,T_C(p)$ and $0.5\,T_C(p)$ (from bottom to top). After an early time regime where $L(t)$ is effectively described by a power-law in time, deviations from a simple algebraic growth start to be manifest already for moderate values of $L(t)$. The inset shows for $p = 0.90$ and $T = 0.4T_c(0.90)$ the decay of the spatial correlation function for $t = 500$, 5000, 50 000, and 500 000 (from left to right). $L(t)$ is obtained from these curves by their intersections with the dashed line $C(r) = 0.5$. After [32]. Copyright (2010) by the American Physical Society.

length $L(t)$ in the usual way [35] by monitoring the one-time space-dependent correlation function

$$C(t, \mathbf{r}) = \frac{1}{N} \sum_{\mathbf{x}} \overline{\langle S_{\mathbf{x}+\mathbf{r}}(t) S_{\mathbf{x}}(t) \rangle} \ . \tag{2.25}$$

We define the correlation length $L(t)$ as the distance at which $C(t, \mathbf{r})$ drops to half of the value it has at $\mathbf{r} = 0$, see the inset in Figure 2.1. The main part of Figure 2.1 shows in a log-log plot $L$ as a function of $t$ for some of the cases studied in this work. In all cases the initial behavior can be described by a power law but deviations from this algebraic growth already show up when the correlation length is on the order of a few lattice constants. These deviations indicate a slowing down of the domain growth after an initial transient behavior. For example, when plotting for $p = 0.90$ (the case where the deviations are the most notable)

$\ln L$ as a function of $\ln(\ln t)$, one observes that the data for large times approach a straight line with an effective slope of approximately 2.5 at the end of the run. Even though this slope is smaller than the value $1/\psi = 4$ expected from the work of Huse and Henley [6], it is worth stressing that the observed behavior is indeed compatible with a slow crossover to a logarithmic growth $L(t) \sim (\ln t)^{1/\psi}$. Still, much longer times are needed in order to unambiguously characterize this asymptotic regime.

As the power-law increase is only a transient one, it is not really meaningful to determine an effective dynamical exponent $z$ from this time-dependent length, as this would only be valid in a certain time window [36]. In fact, as we shall see in the following, it is the naive use of an effective algebraic growth law that is responsible for much of the confusion surrounding the scaling behavior of disordered systems. Indeed, the correct scaling forms are only revealed when the correct growth law $L(t)$ is properly taken into account.

***Autocorrelation function*** In diluted ferromagnets the scaling properties of the autocorrelation function are strikingly different to those in the perfect ferromagnets. For the latter systems the data for different waiting times collapse on a single master curve when plotted as a function of $t/s$ [37], in accordance with the simple aging scaling form (2.14) with $b = 0$. For the random-site system, however, no data collapse is observed when plotting the two-time autocorrelation as a function of $t/s$, see Figures 2.2(a) and 2.2(b). One could try to bring the data to a collapse by letting $b$ to differ from 0, but this yields the unphysical result that $b < 0$, implying that $C$ would grow without bounds when $s \to \infty$ [10]. This observation led Paul *et al.* [10] to fit their numerical data to the superaging scaling ansatz (2.20). As shown in Figures 2.2(c) and 2.2(d), this fitting ansatz with one free parameter, the exponent $\mu$, indeed yields a data collapse which seems rather convincing. A closer look, however, reveals some problems with this ansatz. Choosing $\mu$ such that the collapse is best for the two largest waiting times considered, one observes systematic and increasing deviations when going to lower waiting times. As shown in the inset of Figure 2.2(c) for the case $p = 0.90$ and $T = 0.77$, whereas for small values of the scaling variable the data for the smaller waiting times are lying below the $s$ =20 000 data (the largest waiting time considered in our study), for larger values of the scaling variable the same data lie above the $s$ =20 000 data. This is also seen in the inset of Figure 2.2(d) where we show for the case $p = 0.80$ and $T = 0.75$ the autocorrelation function for the different waiting times and large values of the scaling variable. The same behavior being observed for all studied cases, it follows that the superaging scaling ansatz (2.20) (which, we recall, is problematic by itself as Kurchan's lemma [30] forbids a superaging behavior of the autocorrelation) is a reasonable good fitting function but that it does not capture the true scaling behavior of the two-time autocorrelation.

Faced with this problem, one should remember that the simple aging scaling form (2.19), which obviously does not work in Figures 2.2(a) and 2.2(b), *assumes* an algebraic growth of the dynamical correlation length. For a nonalgebraic growth, as we have in our system, see

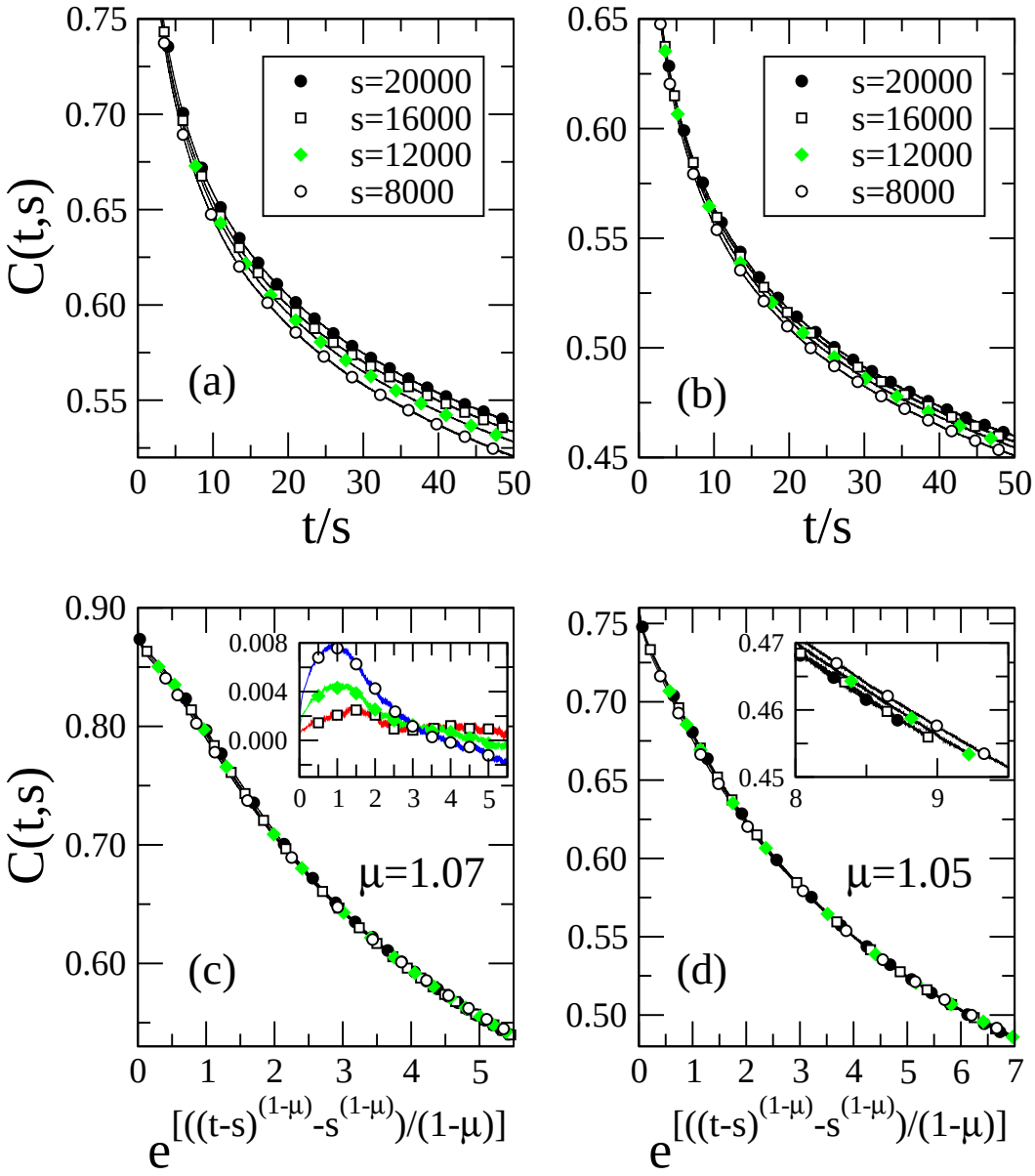


Figure 2.2: Scaling plots of the two-time autocorrelation function for [(a) and (c)] $p = 0.90$, $T = 0.77$ and [(b) and (d)] $p = 0.80$, $T = 0.75$. In traditional full aging plots (where a power-law growth of the correlation length is assumed), see (a) and (b), data for different waiting times $s$ are plotted as a function of $t/s$. In the superaging scaling plots, as proposed in Ref. [10], see (c) and (d), the fitting parameter $\mu$ is chosen such that the data collapse is optimal. The inset of (c) shows systematic deviations when subtracting from the $s$ =20 000 data the data obtained for $s$ =16 000 (red line and open squares), $s$ =12 000 (green line and diamonds), or $s$ =8000 (blue line and open circles). Choosing $\mu$ such that the data collapse is best for the two largest waiting times, systematic deviations are observed both for small and for large values. This is illustrated in the inset of (d) where we show the waiting time-dependent correlation function for the largest values of the scaling variable. Here and in the following error bars in the main panels are much smaller than the sizes of the symbols. After [32]. Copyright (2010) by the American Physical Society.

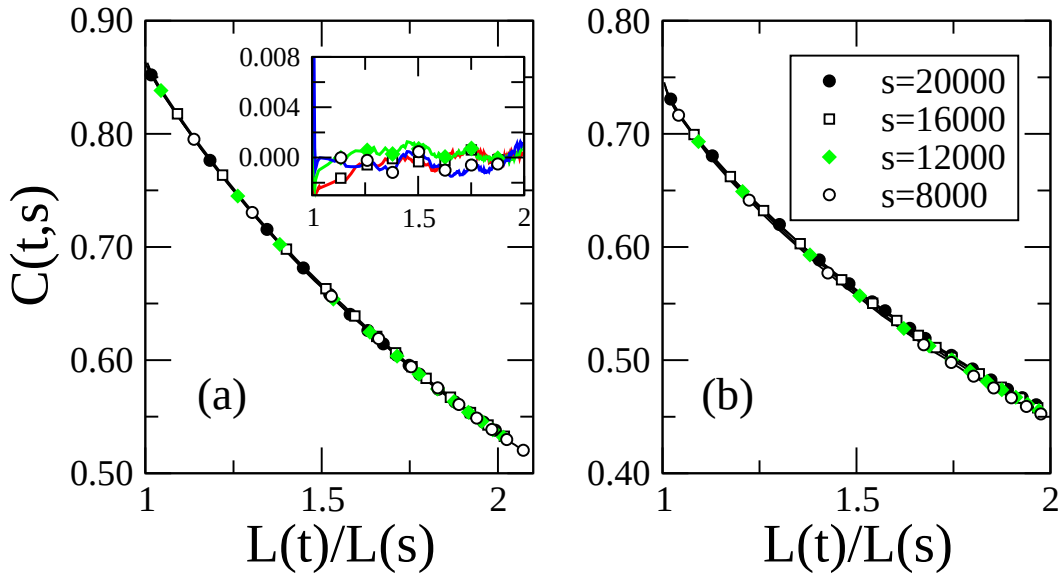


Figure 2.3: Two-time autocorrelation as a function of the ratio $L(t)/L(s)$, where $L(t)$ is the value of the correlation length at time $t$: (a) $p = 0.90$, $T = 0.77$ and (b) $p = 0.80$, $T = 0.75$. This parameter-free scaling yields a data collapse superior to the superaging scaling, see inset in (a) where the data obtained for $s$ =16 000 (red line and open squares), $s$ =12 000 (green line and diamonds), and $s = 8000$ (blue line and open circles) have been subtracted from the $s$ =20 000 data. In order to facilitate a direct comparison, the range of values along the $y$-axis is the same for this inset than for the inset in Figure 2.2(c). After [32]. Copyright (2010) by the American Physical Society.

Figure 2.1, the correct scaling form should be the scaling form (2.12) where the correlation lengths $L(t)$ and $L(s)$ at times $t$ and $s$ are used. We test this scaling form in Figure 2.3 for the same data as in Figure 2.2 and indeed find a perfect scaling behavior with $B = 0$. As shown in the inset, no systematic deviations show up when subtracting from the $s$ =20 000 data the data obtained for the smaller waiting times. Therefore, also in the random ferromagnets a simple aging behavior is observed for the autocorrelation function, provided that the *correct* growth $L(t)$ is taken into account.

Based on this result, we can now give a simple explanation for the origin of the apparent differences in the scaling properties of the autocorrelation in the random-bond and random-site models. Whereas in the random-site model deviations from an algebraic growth law already show up when the correlation length is on the order of a few lattice constants, this could be different for the random-bond model, as various investigations have revealed for that model an effective algebraic growth over many time decades for most of the studied cases. When both the waiting and observation times are in the time window where the growth is effectively algebraic, a simple aging scaling $C(t, s) = f(t/s)$ can be expected [12]. In some case, however, the algebraic power-law growth is presumably not valid during the whole simulation, which would explain why deviations from the $t/s$ scaling show up [38]. A

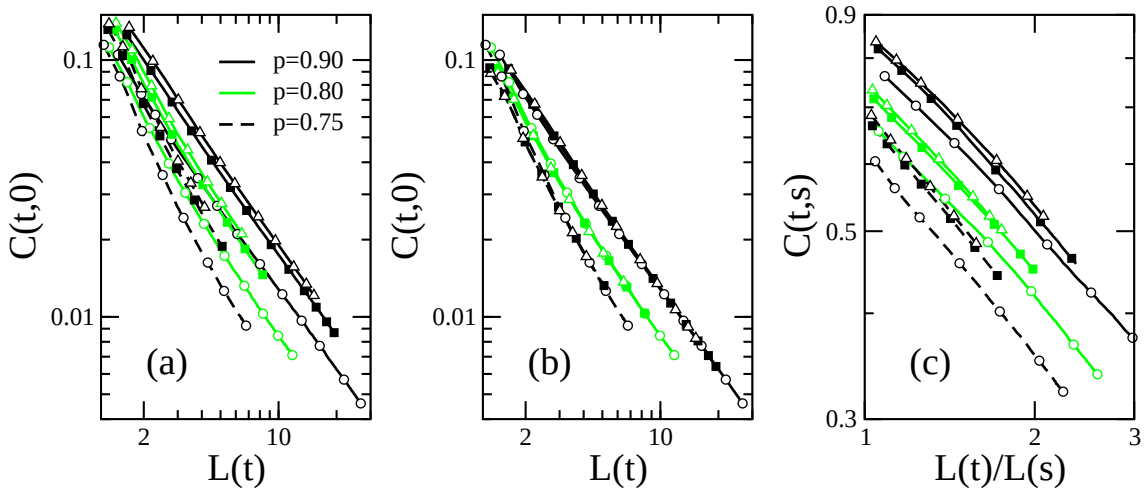


Figure 2.4: (a) $C(t,0)$ as function of $L(t)$ for times up to $t$ =20 000. The symbols (open circles: $T = T_c(0.7)$, filled squares: $T = T_c(0.5)$, open triangles $T = T_c(0.4)$) are guides for the eyes. In all cases the data rapidly display a simple power-law decay. (b) The slopes of $C(t,0)$ are the same for a fixed value of the dilution $p$ but different temperatures, see Table 2.1. In order to illustrate this, we multiplied the data for $T = T_c(0.5)$ and $T = T_c(0.4)$ by a constant thus that they fall on the $T = T_c(0.7)$ data for large $L(t)$. (c) $C(t,s)$ as a function of $L(t)/L(s)$ with $s$ =8000 and $t$ up to $50s$. The two-time autocorrelation function has not yet reached the asymptotic power-law regime $L(t) \gg L(s)$ at the end of the run. After [32]. Copyright (2010) by the American Physical Society.

thorough investigation of the random-bond Ising model, where the numerically determined length $L(t)$ is used in the scaling, would fully clarify the situation and help to understand whether or not there are any fundamental differences between the scaling properties of the random-bond and the random-site Ising models. This will be done in subsection 2.2.3.

It is also of interest to determine the autocorrelation exponent that governs the scaling function of the autocorrelation function for large arguments,

$$C(t,s) \sim \left[\frac{L(t)}{L(s)}\right]^{-\lambda_C} , \tag{2.26}$$

for $L(t)/L(s) \ll 1$. However, in order to reliably measure $\lambda_C$ one usually looks at $C(t,0)$ which for long times decays as $[L(t)]^{-\lambda_C}$. Figure 2.4(a) shows $C(t,0) = C[L(t)]$ for all studied cases in a log-log plot. $C(t,0)$ rapidly approaches a power law which makes the measurement of $\lambda_C$ very easy. A simple inspection already reveals that the curves for a given value of the disorder $p$ decay with similar slopes in the log-log plot, the slopes being steeper for smaller values of $p$. In order to make this better visible we have shifted in Figure 2.4(b) the curves for $0.5T_c(p)$ and $0.4T_c(p)$ by multiplying $C(t,0)$ by a constant thus that these curves fall on the $0.7T_c(p)$ curves for larger values of $L(t)$. The measured values of $\lambda_C$ gathered in Table

| $p$ | $T$ | $\lambda_C$ | $\lambda_R$ | $A$ |
|---|---|---|---|---|
| 0.75 | $0.4\,T_C(0.75)$ | 1.21(3) | 1.32(3) | 0.30(1) |
| | $0.5\,T_C(0.75)$ | 1.21(2) | 1.31(3) | 0.26(1) |
| | $0.7\,T_C(0.75)$ | 1.18(2) | 1.22(3) | 0.15(2) |
| 0.80 | $0.4\,T_C(0.80)$ | 1.11(1) | 1.14(2) | 0.47(1) |
| | $0.5\,T_C(0.80)$ | 1.10(1) | 1.12(2) | 0.38(1) |
| | $0.7\,T_C(0.80)$ | 1.10(1) | 1.11(2) | 0.30(1) |
| 0.90 | $0.4\,T_C(0.90)$ | 1.06(1) | 1.05(2) | 0.65(1) |
| | $0.5\,T_C(0.90)$ | 1.05(1) | 1.04(2) | 0.63(1) |
| | $0.7\,T_C(0.90)$ | 1.05(1) | 1.06(2) | 0.53(1) |

Table 2.1: Values of the autocorrelation exponent $\lambda_C$, the autoresponse exponent $\lambda_R$, and the scaling exponent $A$ of the response for all studied cases. After [32]. Copyright (2010) by the American Physical Society.

2.1 indeed show that within error bars the autocorrelation exponent is independent of the temperature for a fixed value of the dilution.

It is worth noting that for all studied cases the value of the autocorrelation exponent is in agreement with the lower bound $d/2$ derived in [20] and [39]. This is in marked contrast to the claim in [10] that this lower bound is violated in the random-site Ising model. In fact, in their analysis the authors of that paper not only assumed that $C(t,s) \sim t^{-\lambda_C/z}$, which is not valid in the absence of an algebraic growth law, they also tried to extract the autocorrelation exponent from $C(t,s)$, which is a notoriously difficult task. This is shown in Figure 2.4(c) where we plot for the different cases $C(t,s)$ as a function of $L(t)/L(s)$ for $s$ =8000 and $t$ up to $50s$. One immediately remarks that the values of $L(t)/L(s)$ remain very small and that the autocorrelation displays a marked curvature for even the largest values of $t$. Obviously, one is not yet in the scaling regime where $L(t) \gg L(s)$, and a naive measurement at the end of the run would yield effective values for the autocorrelation exponent that are systematically lower than the asymptotic values readily measured when using $C(t,0)$.

***Space-time correlation function*** It has been noted in the past [12, 40], that space- and time-dependent quantities are often better suited than quantities that only depend on time if one aims at studying the scaling properties of an aging system. Taking into account what we learned from the autocorrelation, namely, that the correct growth law $L(t)$ has to be used and that the observed simple scaling behavior means that the exponent $B = 0$, we should have that the space-time correlation function $C(t,s;\mathbf{r})$ is only a function of $L(t)/L(s)$ and $r/L(t)$ [or, alternatively, of $L(s)/L(t)$ and $r/L(s)$],

$$C(t,s;\boldsymbol{r}) = \tilde{F}_C\left[\frac{L(t)}{L(s)}, \frac{r}{L(t)}\right] \tag{2.27}$$

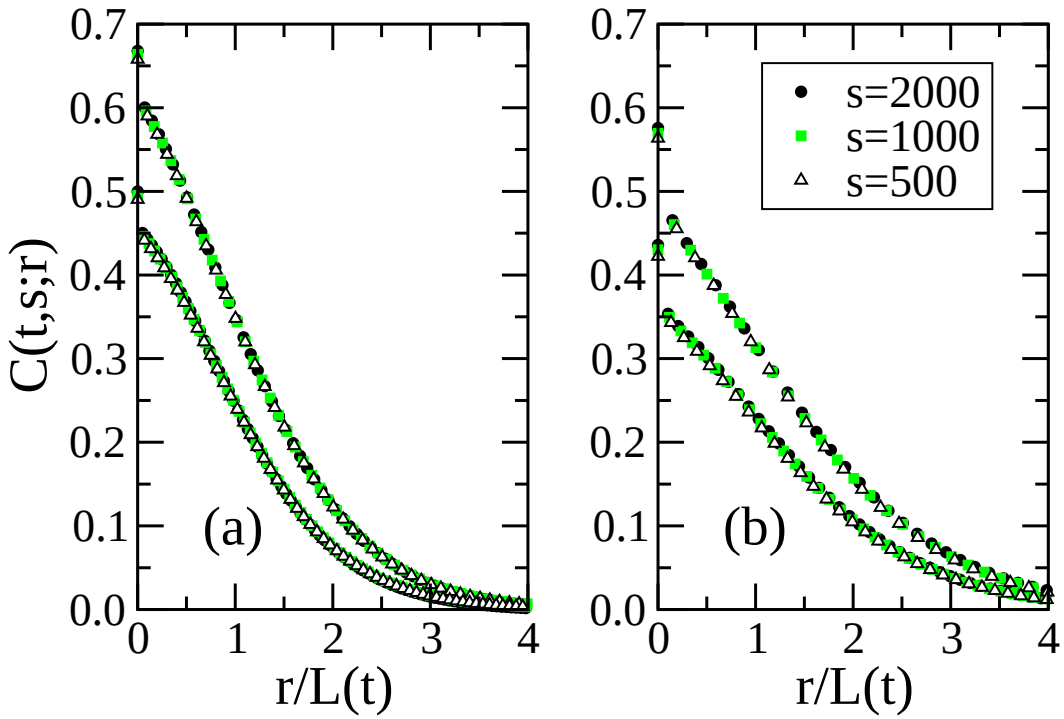


Figure 2.5: Space-time correlation function for various waiting times as a function of $r/L(t)$: (a) $p = 0.90$ and $T = 0.77$, with $L(t)/L(s) = 1.46$ (top) and $L(t)/L(s) = 2.15$ (bottom), and (b) $p = 0.80$ and $T = 0.75$, with $L(t)/L(s) = 1.40$ (top) and $L(t)/L(s) = 2.00$ (bottom). After [32]. Copyright (2010) by the American Physical Society.

with $r = |\mathbf{r}|$. We probe this simple scaling in Figure 2.5 for the cases $p = 0.90$, $T = 0.77$ and $p = 0.80$, $T = 0.75$ (we obtain the same behavior for the other studied cases) where we plot the space-time correlation as a function of the reduced length $r/L(t)$ for fixed values of $L(t)/L(s)$. The observed data collapse again proves that the correlation function in the random-site Ising model displays a simple aging scaling behavior.

At this point one might pause a moment and wonder whether our system has a *superuniversal* scaling behavior. Here superuniversality means that the scaling functions should be independent of disorder and temperature once the unique reference length scale has been chosen to be $L(t)$ [20]. This intriguing behavior has indeed been observed in systems with weak randomness as, for example, the random-bond Ising model or the random-field Ising model. For our model, the disorder has a very strong impact on the coarsening process, as too much disorder completely destroys phase ordering, and it is *a priori* not clear whether a superuniversal behavior is to be expected. As shown in Figure 2.6(a) for the temperature $T = 0.4T_c(p)$, systems with different dilutions $p$ and fixed value of the ratio $L(t)/L(s)$ do not show a common master curve when plotting the space-time correlation as a function of $r/L(t)$. This is in agreement with an earlier study by Iwai and Hayakawa [41] of a diluted system where, using a cell-dynamical system method, the scaling function of the structure

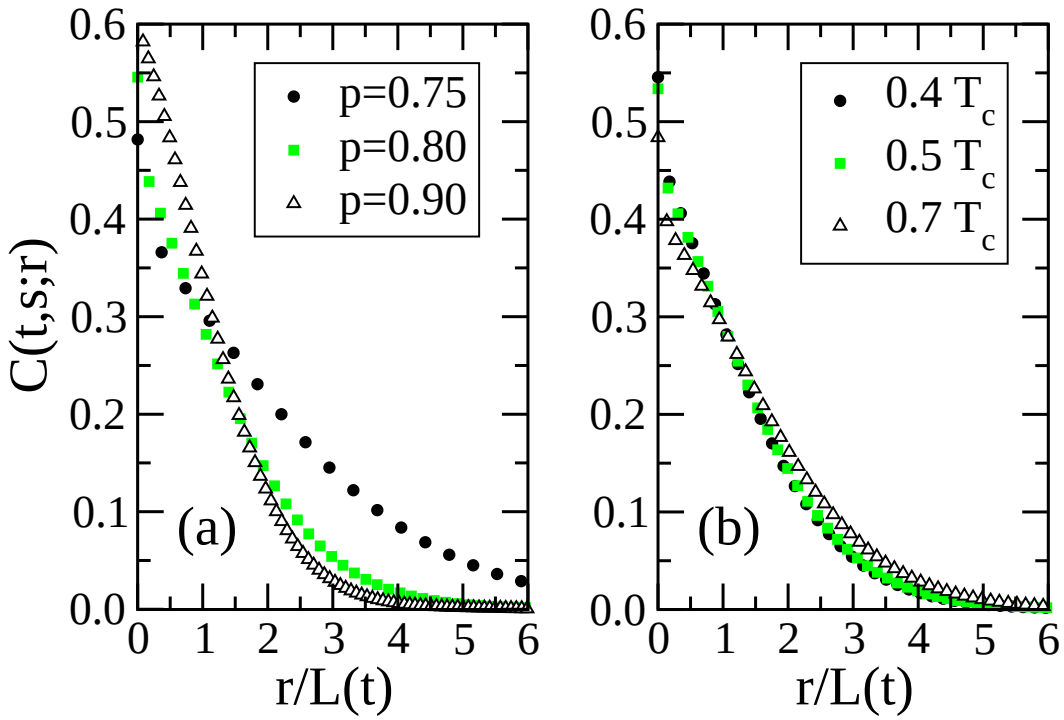


Figure 2.6: (a) Space-time correlation function at $T = 0.4T_c(p)$ for the different degrees of dilution $p$, with $s = 1000$ and $L(t)/L(s) = 1.52$. (b) Space-time correlation function for $p = 0.8$, $s = 1000$, and $L(t)/L(s) = 1.52$, for three different temperatures. After [32]. Copyright (2010) by the American Physical Society.

factor was found to depend on the degree of dilution. Interestingly, we achieve an approximate data collapse, which gets better the lower the temperatures, when the dilution is kept fixed and the temperature is changed, see Figure 2.6(b) for the case $p = 0.8$. This approximate superuniversal behavior is in agreement with the expectation that the dynamics for fixed disorder only weakly depends on temperature, as long as one is not too close to the critical point. Still, the observed strong dependence of the scaling function of the space-time correlation on the degree of dilution indicates that some aspects of the phase ordering of diluted systems remain to be better understood.

***Thermoremanent susceptibility*** Finally, we have also extended our study to the thermoremanent susceptibility (2.24). In order to measure this integrated response one applies a small magnetic field when quenching the system to the temperature $T$. This field is removed after the waiting time $s$ and the relaxation to equilibrium is then monitored by measuring the decay of the magnetization. It is numerically convenient to apply a spatially random magnetic field as a spatially homogeneous field could easily push the (finite) system into one of the two competing equilibrium states. Figure 2.7 and Table 2.1 summarize the observed scaling behavior of the thermoremanent susceptibility. In all cases we have the simple ag-

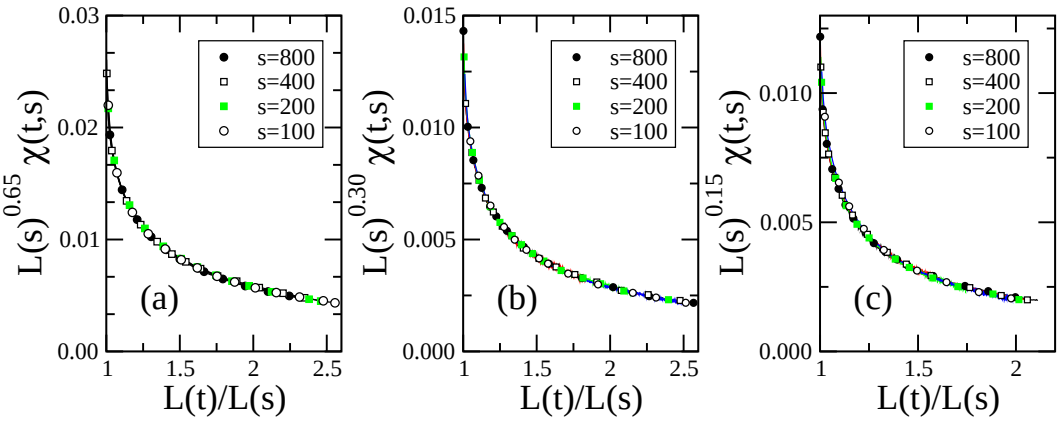


Figure 2.7: Scaling of the thermoremanent susceptibility for (a) $p = 0.90$ and $T = 0.77$, (b) $p = 0.80$ and $T = 1.05$, and (c) $p = 0.75$ and $T = 0.91$. In all cases a simple aging scaling is observed. After [32]. Copyright (2010) by the American Physical Society.

ing scaling (2.16), provided that we use the correct dynamical correlation length $L(t)$. The non-equilibrium exponent $A$ is thereby found to depend on the dilution and on the temperature. For a given dilution, $A$ increases when decreasing the temperature, whereas for a fixed value of $T/T_c(p)$ the value of $A$ decreases when decreasing $p$. As usual the scaling regime is accessed for the response much earlier than for the correlation function. Whereas for the correlation function finite time corrections start to be negligible for waiting times of $s = 1000$ and larger, for the integrated response waiting times of $s = 100$ and larger already yield a perfect data collapse. This is similar to what is observed in the perfect Ising model and in the random-bond Ising model, for example.

We could try to extract from the data shown in Figure 2.7 the autoresponse exponent $\lambda_R$, which governs the power-law decay of the scaling function in the limit $L(t) \gg L(s)$ but we are confronted with the same problem as we encountered when trying to extract the autocorrelation exponent $\lambda_C$ from the two-time correlation function $C(t, s)$: even for an observation time $t$ that is 50 times larger than the waiting time $s$, we have that $L(t)$ is only on the order of $2L(s)$. Consequently, our data still show a slight curvature in a log-log plot, and this only allows to obtain a very rough estimate of $\lambda_R$. For that reason we determined $\lambda_R$ for the smaller waiting time $s = 5$ and $t = 200s$. This allows us to enter the asymptotic power-law regime in most cases. The only exceptions are for $p = 0.75$ and small temperatures, where the growth is the slowest, as here we still have a slight curvature at the end of the run. The values of $\lambda_R$ measured in this way are gathered in Table 2.1. These values show the same dependence on the degree of dilution than $\lambda_C$ and are, in general, consistent with $\lambda_R = \lambda_C$.

Finally, let us briefly comment on the values of the exponent $A$ as this quantity has been of some interest recently. Thus it has been proposed that $A = 1/2$ for coarsening in two dimensions [42], and a numerical study of the random-bond Ising model, that seems to

support this claim, has been published recently [43]. For the random-site Ising model, we can unambiguously conclude that $A$ is not identical to 1/2. It has been argued in Ref. [43] that the thermoremanent magnetization (which is proportional to the thermoremanent susceptibility) suffers from crossover effects that make a reliable estimate of the value of $A$ difficult. However, in our analysis, where we do not assume a power-law growth but use the correct growth law $L(t)$, we do not have any crossover effects, as seen in Figure 2.7, but instead have a very clean scaling behavior with an exponent A that differs from 1/2. We find that $A$ depends on temperature and on the degree of dilution, which is similar to what has been found in an earlier study of the random-bond Ising model [12]. Interestingly, systematic deviations from the value 1/2 are also seen in Figure 5 of Ref. [43], where the exponent $A$ has been determined for the random-bond model under the assumption of an algebraic growth law. Again, a careful study of the random-bond case using the correct growth law $L(t)$ should clarify whether there are any qualitative differences between the random-bond and the random-site models.

### 2.2.3 Random-Bond Ising Model

We saw in the previous subsection that two issues relevant to the disordered ferromagnets i.e. the growth law of length scale $L(t)$ and superuniversality can be clarified to some extent when studying the site disorder case. Whereas no satisfactory scaling is obtained when using the naive assumption that $L(t)$ follows a simple algebraic growth, the expected scaling form (2.8) is in fact recovered when taking into account the crossover from the pre-asymptotic algebraic growth to the slower asymptotic growth by using the numerically determined length $L(t)$. Furthermore, even though there is growing consensus that superuniversality in the strictest sense is not fulfilled, there is strong evidence that in certain regimes scaling functions of one- and two-times quantities show a remarkable independence on the disorder.

In this subsection we apply our analysis to another disordered system, namely the two-dimensional random-bond Ising model. We consider domain growth at temperatures well below the phase transition temperature. In this regime, this model has been characterized in the past by an algebraic growth law. However, notable deviations [9, 12] from the expected simple scaling form (2.8) with $L(t) \sim t^{1/z}$ are observed, which points to the possibility that a situation comparable to that encounter in the random-site model also prevails for the random-bond case. The following part of this section has been presented on our publication [44].

#### A. The Model

The random-bond Ising model in two dimensions studied in the following is characterized by the fact that the disorder is on the level of the bonds connecting the different Ising spins whose couplings are ferromagnetic, albeit with strengths that are taken from a certain

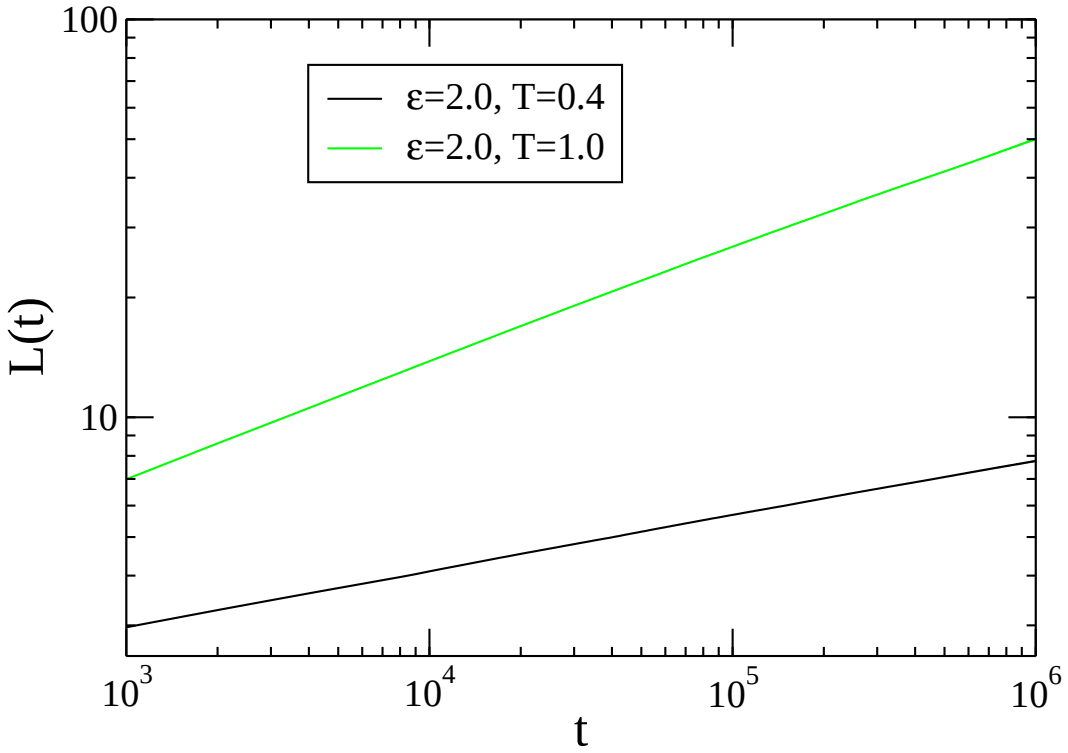


Figure 2.8: Log-log plot of the dynamical correlation length $L(t)$ as a function of time $t$ for the strongest disorder $\varepsilon = 2.0$, with $T = 0.4$ and $T = 1.0$. Clear deviations from a simple power law are observed for larger times. After [44]. With kind permission of The European Physics Journal (EPJ).

distribution. The Hamiltonian is given by

$$\mathcal{H} = -\sum_{\langle \mathbf{x},\mathbf{y} \rangle} J_{\mathbf{xy}} S_{\mathbf{x}} S_{\mathbf{y}} \ , \tag{2.28}$$

where the sum is over nearest neighbor pairs, whereas $S_{\mathbf{x}} = \pm 1$ is the usual Ising spin located at site $\mathbf{x}$. The coupling strengths $J_{\mathbf{xy}}$ are positive random variables uniformly distributed over the interval $[1-\varepsilon/2, 1+\varepsilon/2]$ with $0 < \varepsilon \leq 2$. We recover a perfect, i.e. non-disordered, Ising model when the control parameter $\varepsilon = 0$. Our model has a second order phase transition between the ordered low-temperature ferromagnetic phase and the disordered high-temperature paramagnetic phase at a transition temperature $T_c(\varepsilon) \approx T_c(0) = 2.269\ldots$ that is basically independent of the disorder. In the simulations reported in the following we studied three different cases, namely $\varepsilon = 0.5$, 1.0 and 2.0. Square lattices of $L \times L$ sites where considered, with $L$ ranging from 150 to 900. System sizes were adjusted in order to avoid finite size effects. For all measured quantities we averaged over at least 1000 independent runs. For the determination of the length $L(t)$ we computed the one-time space-time correlation function with up to $t = 10^6$ Monte Carlo steps (MCS), one step consisting of $L \times L$ proposed updates.

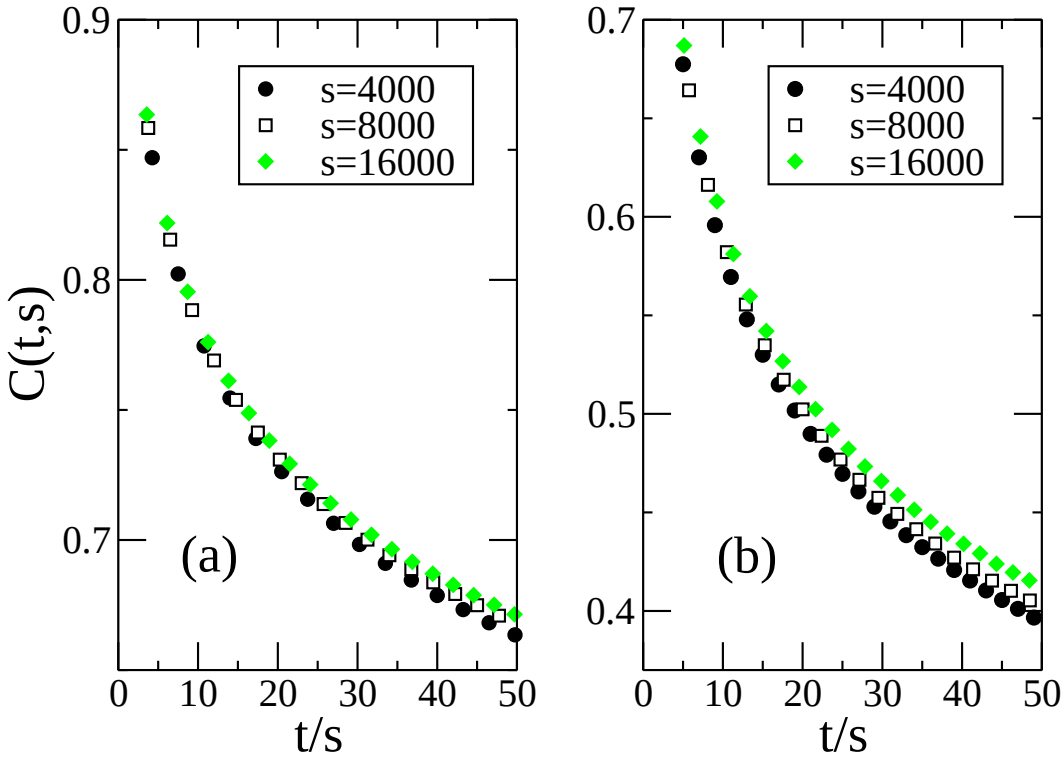


Figure 2.9: Autocorrelation function versus $t/s$ for $\varepsilon = 2.0$, with (a) $T = 0.4$ and (b) $T = 1.0$. The data do not fall on a common master curve. Approximate scaling can only be obtained for unphysical, negative values of the exponent $b$, see equation (2.14). Here and in the following error bars are much smaller than the sizes of the symbols. After [44]. With kind permission of The European Physics Journal (EPJ).

For the two-times quantities we considered waiting times up to $s$ =16 000, with observations times $t = 50s$.

### B. Numerical Results

***Dynamical correlation length*** We extract the dynamical correlation length from the one-time space-time correlation function (2.25). For the random-bond Ising model $C(t, \mathbf{r})$ for fixed $t$ rapidly displays an exponential decay as a function of distance $r = |\mathbf{r}|$. We then determine the dynamical correlation length using the criterion $C(t, L(t)) = \frac{1}{2}$. All conclusions drawn from our study of the random-bond model are independent of the way used to extract the correlation length from the one-time space-time correlation function. As an example we show in Figure 2.8 the time evolution of $L(t)$ for $\varepsilon = 2.0$ and two different temperatures. In both cases clear deviations from an algebraic growth are observed at later times. Our simulations do not allow us to access the asymptotic long time regime, so that we can not affirm that this regime is characterized by a logarithmic growth. Comparing

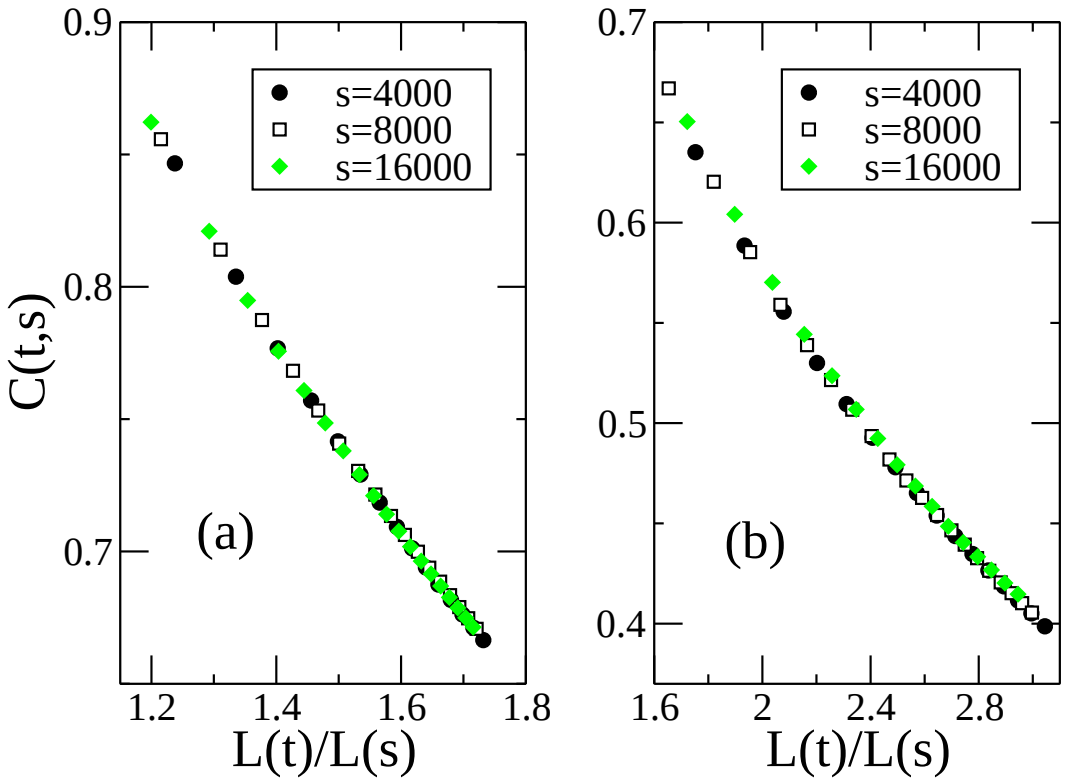


Figure 2.10: Autocorrelation function versus $L(t)/L(s)$ for $\varepsilon = 2.0$, with (a) $T = 0.4$ and (b) $T = 1.0$. The time-dependent lengths $L$ have been determined numerically, see Figure 2.8. The data now collapse on a common master curve, in agreement with the simple aging scaling (2.8). After [44]. With kind permission of The European Physics Journal (EPJ).

with the corresponding lengths obtained in Figure 2.1, we note that the deviations in Figure 2.8 are much less pronounced than those observed for the random-site model. Another way of stating this is that the transient, algebraic-like regime extends to longer times in the random-bond case. Obviously, no theoretical approach is known that allows us to give an analytical expression for the observed crossover of $L(t)$. For that reason we are going to use the numerically determined quantity in the following analysis of the two-times correlation function.

***Two-time autocorrelation function*** As already explained in the previous section, if one assumes an algebraic growth law, $L(t) \sim t^{1/z}$, then the scaling (2.8) reduces to (2.14). However, both for the random-site [10, 32] and random-bond [12, 38] models only an extremely poor scaling is obtained when plotting the autocorrelation function versus $t/s$. An approximate scaling can be achieved with some negative exponent $b$, but this is unphysical [10, 38]. In Figure 2.9 we show the poor scaling for $\varepsilon = 2.0$ for two different temperatures. Deviations are less pronounced at lower temperature, as here the transient algebraic growth

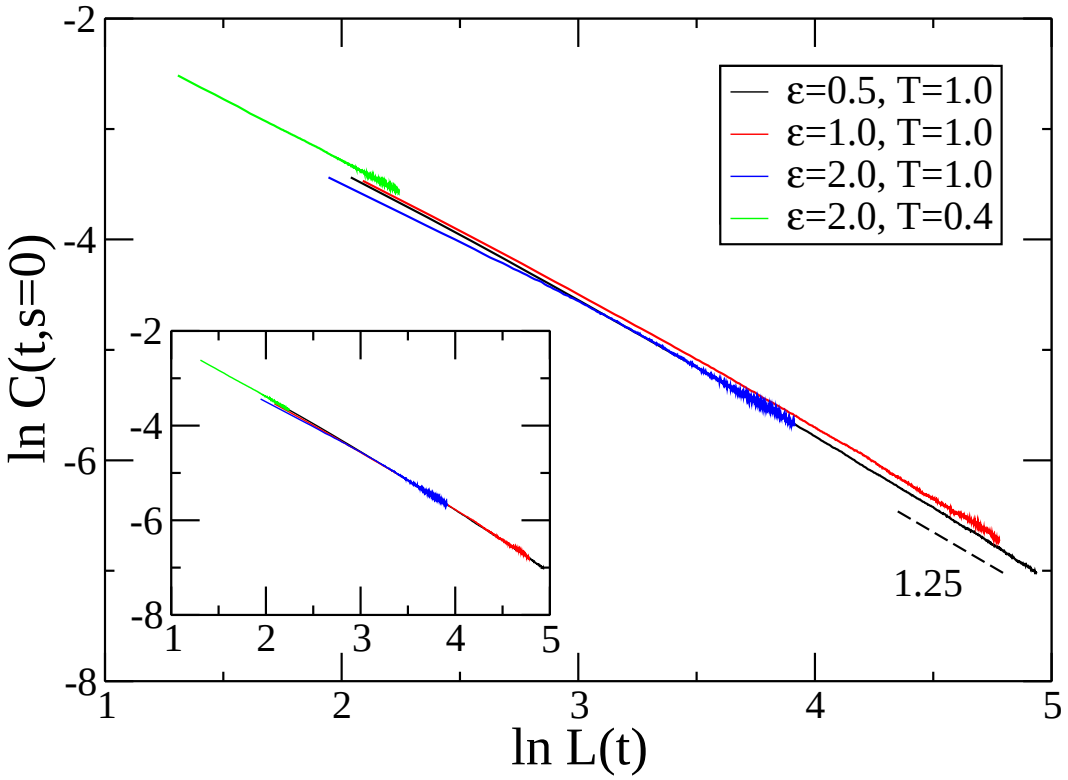


Figure 2.11: Log-log plot of $C(t, s = 0)$ vs. $L(t)$ for four different cases. The dashed line indicates the slope 1.25 measured in the perfect Ising model. As shown in the inset, shifting the different curves vertically makes them overlap, giving some indication that the same slope could emerge for $L(t) \gg 1$ in all cases. After [44]. With kind permission of The European Physics Journal (EPJ).

persists for longer times, see Figure 2.8.

As all this is similar to what is observed in the random-site model [32], we proceed in the same way as in our previous study. Instead of assuming a certain analytical form for $L(t)$ (which we could not derive anyhow, due to the crossover between the two regimes), we use the numerically determined values for $L(t)$ in order to check for scaling. The results of this procedure are shown in Figure 2.10 for the same two cases as those shown in Figure 2.9. In all studied cases, a perfect data collapse is observed when plotting $C$ as a function of $L(t)/L(s)$. It follows that the simple aging scaling (2.8), with $B = 0$, also prevails in the random-bond disordered ferromagnet when using the correct growth law $L(t)$.

In [45] Corberi *et al.* showed that for the random-bond model the autocorrelations for different values of $\varepsilon$ and different temperatures $T$ are in general not identical when plotted against $L(t)/L(s)$ (see also [12]). Instead, a partial collapse is noted, as data with the same ratio $\varepsilon/T$ fall on a common master curve [12, 45]. All this points to the fact that even as superuniversality is not fully realized (for this the autocorrelation should only depend

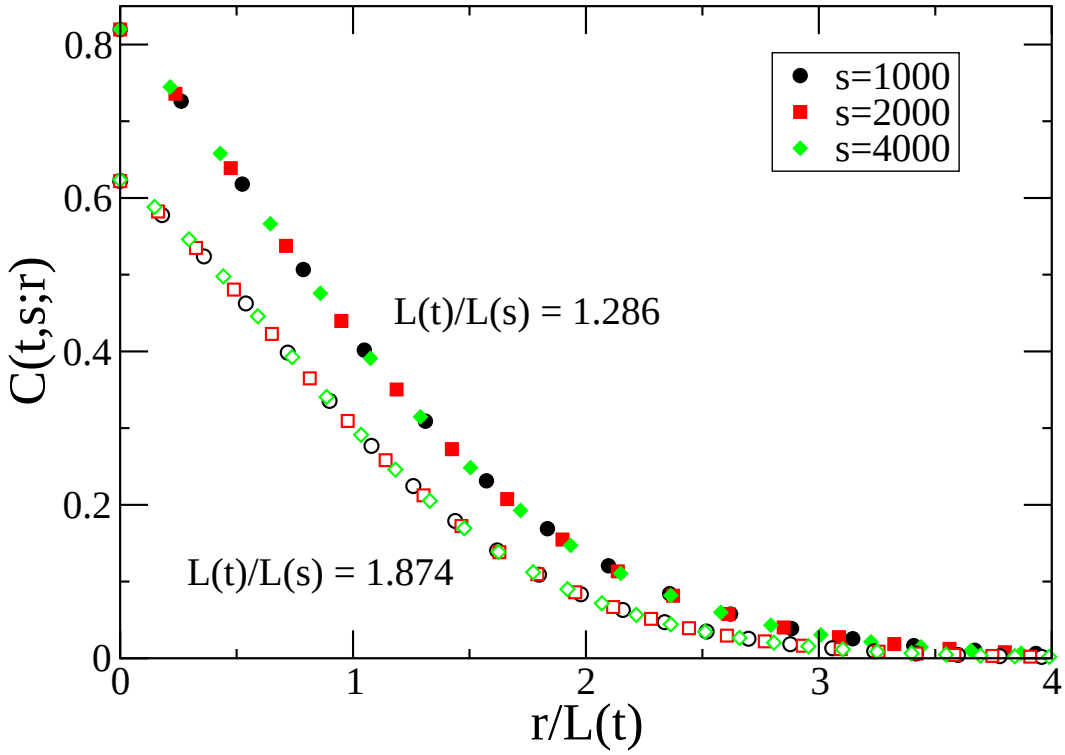


Figure 2.12: Space-time correlation function as a function of $r/L(t)$ for two different ratios $L(t)/L(s) = 1.286$ (filled symbols) and 1.874 (open symbols). The data obtained for different waiting times $s$ fall on a common curve. After [44]. With kind permission of The European Physics Journal (EPJ).

on $L(t)/L(s)$, irrespective of the values of $\varepsilon$ and $T$), there is still a remarkable degree of universality encountered in the disordered ferromagnets.

Another interesting aspect is revealed in Figure 2.11 where we plot $C(t, s = 0)$ as a function of $L(t)$ for four different cases. From the simple scaling picture we expect that for $L(t) \gg 1$ the autocorrelation varies with $L(t)$ in the form of a power-law [25]:

$$C(t, 0) \sim (L(t))^{-\lambda_C} \ , \tag{2.29}$$

with the autocorrelation exponent $\lambda_C$. For the perfect Ising model, different studies have measured this exponent, yielding the value $\lambda_C \approx 1.25$ in two dimensions [20, 46–48]. In Figure 2.11 we show $C(t, s = 0)$ as a function of $L(t)$ for the different disorder distributions and temperatures. Focusing first on the two cases with $\varepsilon = 0.5$ and 1, we note that in the log-log plot the corresponding autocorrelation functions are given by straight lines for the larger values of $L$. For the slopes we obtain 1.25(2), i.e. the same value as for the perfect Ising model. For the two cases with $\varepsilon = 2$, we are not yet completely in the regime of power-law decay (this is especially true for $T = 0.4$ for which only very small values of $L(t)$ are accessible). Still, shifting the curves vertically such that they overlap, see the inset, we

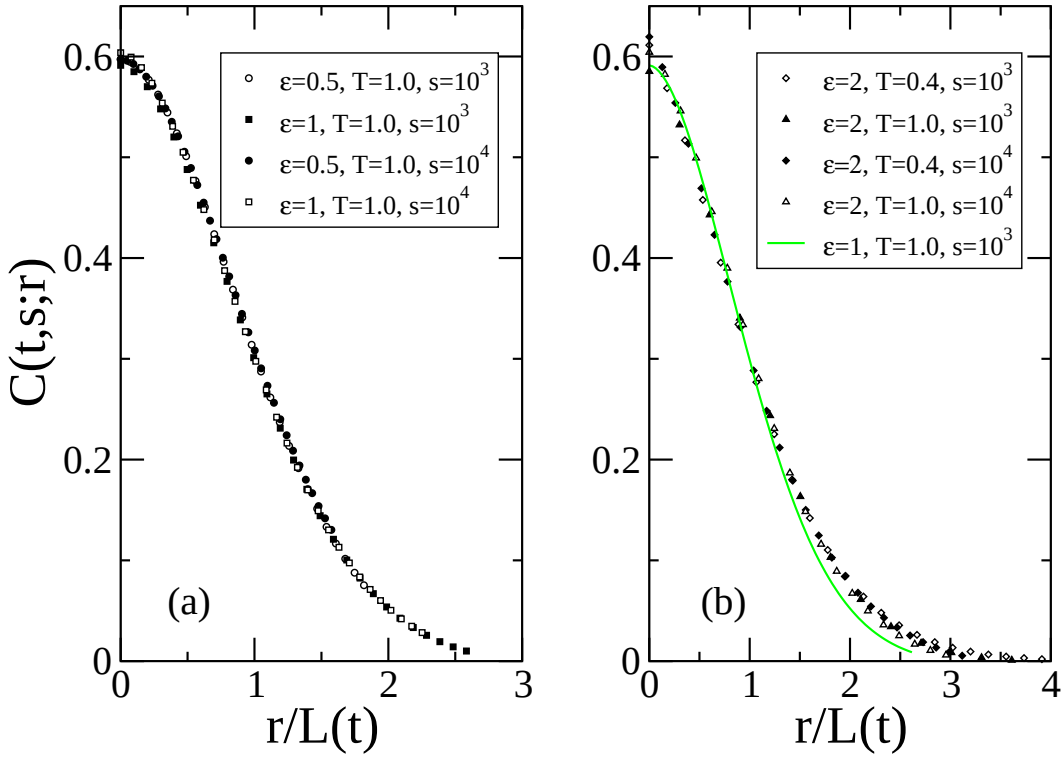


Figure 2.13: Space-time correlation function as a function of $r/L(t)$ for the fixed value $L(t)/L(s) = 1.9$. (a) Comparison of the scaling functions obtained for $\varepsilon = 0.5$ and 1, with $T = 1$ and two different waiting times. (b) The scaling function obtained for $\varepsilon = 2$ differs from the scaling function (green line) shown in (a). After [44]. With kind permission of The European Physics Journal (EPJ).

see that the two $\varepsilon = 2$ curves in fact closely follow the curves for $\varepsilon = 0.5$ and 1. This is at least compatible with a common exponent $\lambda_C \approx 1.25$ irrespective of disorder, even though we are not able to access the algebraic regime in all cases.

***The space-time correlation function*** In an earlier study of the two-times space-time correlation function [12] of the random-bond model, intriguing and yet unexplained results were obtained. On the one hand, looking at $C(t, s; r)$ as a function of $r/L(s)$ for $t/s$ fixed, it was found that the scaling functions for various values of $\varepsilon$ and various temperatures are *identical* to that of the pure model, as would be expected if superuniversality holds, provided the following two conditions are fulfilled: (1) $r/L(s)$ is not too small, $r/L(t) \gtrsim 0.5$, (2) $\varepsilon$ is strictly less than 2. The first condition of course agrees with the observation that superuniversality is absent for the autocorrelation [45], which corresponds to $r = 0$. A possible explanation for the second condition could be that much longer times $t$ (much larger $L(t)$) are needed in order to see the crossover to the scaling function of the pure model for the limiting case where some couplings are very small or even zero.

All these results have been analyzed in [12] under the assumption of an algebraic growth law. We therefore present in the following results for the space-time correlation function $C(t, s; r)$ where the numerically determined length $L(t)$ is used.

We first verify in Figure 2.12 for the case $\varepsilon = 2.0$ and $T = 0.4$ that $C(t, s; r) = C(L(t)/L(s), r/L(t))$, i.e. the space time correlation only depends on $L(t)/L(s)$ and $r/L(t)$. Fixing $L(t)/L(s)$ we see that data obtained for different waiting times $s$ indeed fall on a common scaling curve when plotted against $r/L(t)$.

The scaling functions obtained for different disorder distributions and different temperatures are compared in Figure 2.13. Panel (a) shows for $\varepsilon = 0.5$ and 1, both at temperature $T = 1$, that the data for the space-time correlation obtained for different waiting times collapse at fixed $L(t)/L(s)$. A close inspection shows that the resulting scaling function agrees with that of the perfect Ising model. Noting that the ratio $\varepsilon/T$ is not the same for the two cases shown in panel (a), the observation of a data collapse for our space-time quantity goes beyond the partial collapse discussed in [45] where autocorrelations with the same value of $\varepsilon/T$ are found to agree. In agreement with [45] we observe notable deviations from a common curve also for the space-time correlation when $r/L(t)$ is small. As shown in panel (b) data obtained for $\varepsilon = 2$ and different temperatures show also rather good collapse for a fixed value of $L(t)/L(s)$. However the resulting scaling function still differs from that obtained for smaller values of $\varepsilon$. Using the numerically determined length $L(t)$ does therefore not allow to resolve this issue initially raised in [12].

## 2.3 Aging in Ising Spin Glasses

Spin glasses are roughly described as a collection of interacting magnetic moments whose interactions are random and can be either ferromagnetic or antiferromagnetic. Spin glasses show enormously rich and unexpected physics in every aspect, and thus intensive explorations have been performed both theoretically and experimentally. Nevertheless many fundamental questions still remains open (for a detailed review, see [49]).

In order to understand the complicated behavior of spin glasses, there have been much attempts to propose simple models that capture the most important properties of real spin glasses. A famous example is the mean-field, Sherrington-Kirkpatrick (SK) model [50]. In this model one considers a regular lattice with spins on the lattice sites, and the glassy properties are realized by introducing disorder and frustration effects through the exchange interactions that are randomly distributed following a probability distribution $P(J_{ij})$ that is symmetric about zero. For the purpose of theoretical clarity, $P(J_{ij})$ is chosen to follow the standard Gaussian distribution and the interaction strength is given irrespective of the distance between interacting spin pairs (so-called 'infinite-range' interactions). For this reason a mean-field treatment of this model should be exact. Nevertheless, a comprehensive formulation of the mean-field theory even in equilibrium remains challenging, which is in

contrast to the case of the ferromagnet with infinite-range interactions where the solution is rather trivial.

On the other hand, one can also imagine more realistic type of model by assuming that the interaction strength should depend on the distance between the spins. The simplest case, the 'short-range' version of the SK model, was proposed by Edwards and Anderson [51]. This Edwards-Anderson (EA) model is actually a pioneering model in the history of spin glass study, and it is also called an 'Ising spin glass' since its Hamiltonian is identical to that of Ising ferromagnets with interactions between nearest-neighbor pairs with the exception of random interaction strengths. Unlike the infinite-range (SK) model, there is no accepted theoretical framework for the Ising spin glasses and several competing theories propose rather contradicting scenarios. For example, it is established that Ising spin glasses undergo an equilibrium phase transition between a paramagnetic and a spin-glass phase at a critical temperature $T_c$ in $d > 2$ dimensions [52], however detailed questions about the critical properties such as the behavior of the spin-glass order parameter $q_{\rm EA}$ or the determination of $T_c$ are still under debate. The physics in the ordered low temperature phase also remains very controversial, with different theoretical approaches such as the droplet, the replica symmetry breaking (RSB) or the intermediate Trivial-Non-Trivial (TNT) pictures [20, 53–56].

It is easily conceivable, therefore, that the exploration of the dynamical aspects of Ising spin glasses is even more difficult. Indeed, although many aging phenomena, which are encountered during non-equilibrium relaxation, were originally discovered in experiments on glassy materials, there are not many reliable theoretical results available when studying aging in spin glasses. For instance, already the precise relationship between the time and dynamical length scale in the Ising spin glasses quenched below the critical point is not well understood. The best fitting to the numerical simulation data is given by [57]

$$t(L) \sim L^z \exp\left(\frac{\Delta_0}{k_B T}\left(\frac{L}{\xi_{\rm eq}(T)}\right)^{\psi}\right) \tag{2.30}$$

where $\Delta_0$ is an energy scale of order $k_B T_c$, $\psi$ is the barrier exponent and $\xi_{\rm eq}(T)$ is the equilibrium correlation length at temperature $T$. Equation (2.30) also shows a good fit with the experimental results in some glassy materials such as $CdCr_{1.7}IN_{0.3}S_4$ and Ag:Mn(2.6 at. %)[57]. This form implies that there should be a crossover between a simple power-law growth regime and a logarithmic growth regime $L \sim (\ln t)^{1/\psi}$, but also that it will take a long time to see this crossover.

In this section, we try to apply our simple aging scaling scheme to the Ising spin glasses. In the previous section it was shown that the simple aging scheme is successfully applied to the disordered ferromagnetic systems regardless of the disorder type. Now it would be interesting to see whether this scenario can be extended to the Ising spin glasses, where disorder and frustration effects are combined. The discussion in the following part of this section has been presented on our publication [44].

### A. The Model

The specific model we consider is the three-dimensional Edwards-Anderson (EA) model. The Hamiltonian is identical to (2.28), but the random interactions are now either ferromagnetic or antiferromagnetic. We used the bimodal distribution

$$P(J_{\mathbf{xy}}) = [\delta(J_{\mathbf{xy}} - 1) + \delta(J_{\mathbf{xy}} + 1)]/2 \ , \tag{2.31}$$

symmetric about zero and with $\langle J_{\mathbf{xy}}^2 \rangle = 1$. We focused on the two temperatures $T = 0.833$ and $T = 0.952$, well below the spin glass transition temperature $T_c = 1.12$ [58]. Systems composed of $50 \times 50 \times 50$ to $80 \times 80 \times 80$ spins were studied on a cubic lattice. For all measured quantities we averaged over typically 5000 independent runs. For the two-times quantities waiting times up to $s = 8000$ MCS were considered, with maximal observation times $t = 50s$ MCS.

### B. Numerical Results

***Dynamical Correlation Length*** For the EA spin glass we need to proceed slightly differently than for the disordered ferromagnetic cases in order to obtain the dynamical correlation length. We consider two replicas $S_{\mathbf{x}}^{(\alpha)}(t)$ and $S_{\mathbf{x}}^{(\beta)}(t)$ with the same set of bonds and consider the overlap field as the EA order parameter

$$q_{\mathbf{x}}(t) = S_{\mathbf{x}}^{(\alpha)}(t) S_{\mathbf{x}}^{(\beta)}(t) \ . \tag{2.32}$$

The quantity of interest is then the one-time space-time correlator

$$G(r;t) = \frac{1}{N^3} \sum_{\mathbf{x}} \overline{\langle q_{\mathbf{x}}(t) q_{\mathbf{x}+\mathbf{r}}(t) \rangle} \ , \tag{2.33}$$

where $N^3$ is the total number of sites in our system. One additional complication comes from the fact that the decay of $G(r;t)$ is not given by a simple exponential, but instead one has that

$$G(r;t) \sim \frac{1}{r^a} F\left(\frac{\mathbf{r}}{L(t)}\right) , \tag{2.34}$$

where $a \approx 0.4$ for the three-dimensional case [59], whereas $F(x) = \exp[-x^\beta]$ with $\beta \sim 1.5$ [60]. Using the method of integral estimators proposed in [61], we note that the dynamical correlation length is proportional to the following ratio of integrals:

$$L(t) \propto \frac{I_2(t)}{I_1(t)} \ , \tag{2.35}$$

where

$$I_k(t) \equiv \int_0^{N/2} \mathrm{d}r \, r^k G(t;r) \ . \tag{2.36}$$

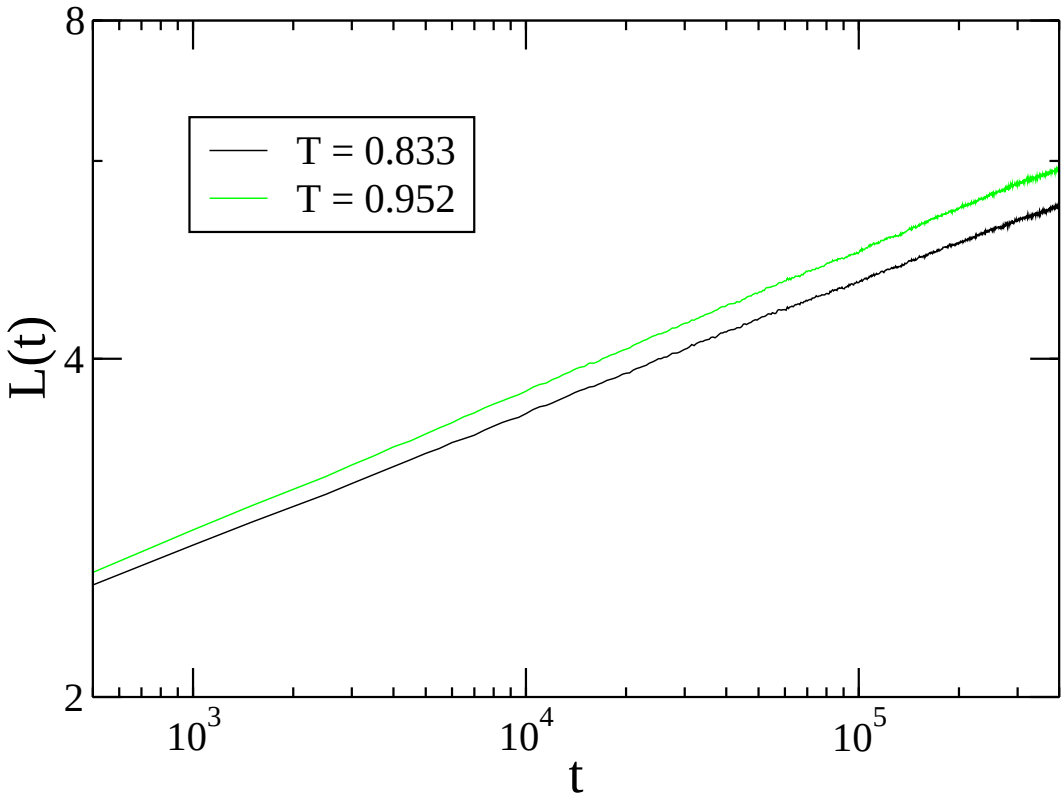


Figure 2.14: Dynamical correlation length versus time for the three-dimensional Edwards-Anderson spin glass, as obtained from equation (2.35). For both temperatures, no strong deviations from an algebraic growth are observed during our simulations. After [44]. With kind permission of The European Physics Journal (EPJ).

We can use $N/2$ as the upper integration boundary as we make sure that $N \gg L(t)$.

In Figure 2.14 we show the dynamical length that we obtain from equation (2.35) for the two temperatures $T = 0.833$ and $T = 0.952$. We note that after 400 000 MCS the dynamical length is still less than 6 lattice constants, which reveals the expected very slow dynamics. Also, only very minor deviations from a straight line are observed in this double logarithmic plot.

***Two-time Autocorrelation Function*** The fact that for our simulation times the length $L(t)$ does not display obvious deviations from an algebraic growth already indicates that two-times quantities should rather well fulfill equation (2.14) obtained under the assumption that $L(t) \sim t^{1/z}$. This is indeed the case, as shown in Figure 2.15 for the two-times spin-spin autocorrelation function $C(t, s)$ at temperature $T = 0.833$. We also note that for the Ising spin glass the exponent $B$ is not zero, as already remarked in earlier studies [62]. However, a closer inspection reveals that there are systematic deviations, both for small and for large

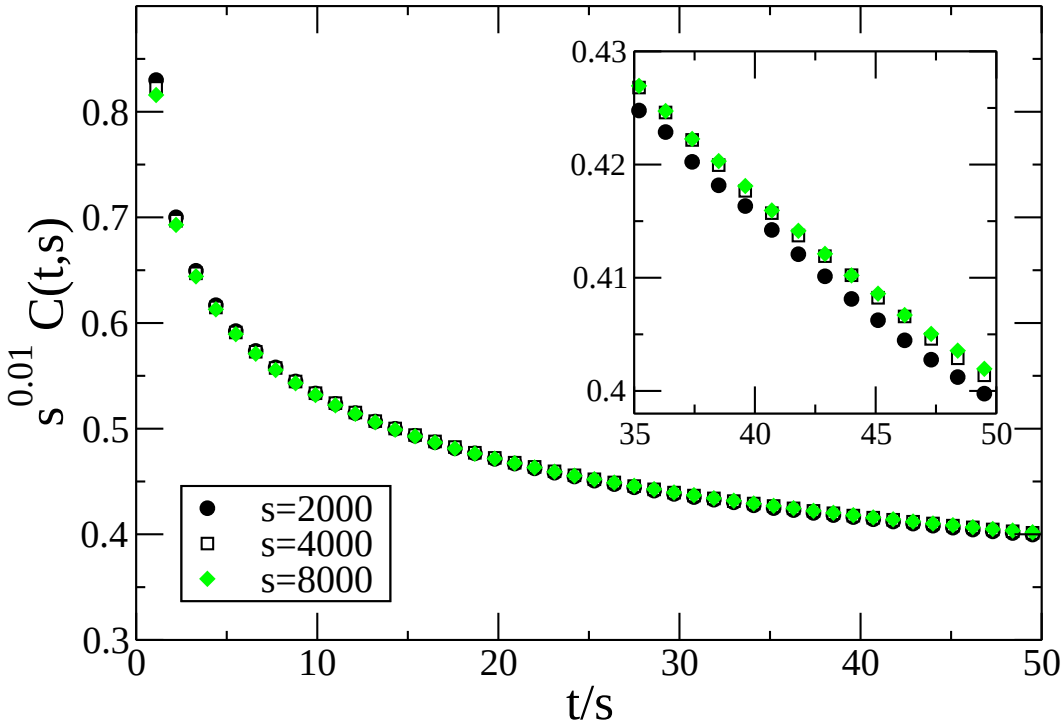


Figure 2.15: Autocorrelation as a function of $t/s$ for the three-dimensional Ising spin glass at temperature $T = 0.833$. Deviations from the scaling (2.14) are observed both for small and for large value of $t/s$, see inset. After [44]. With kind permission of The European Physics Journal (EPJ).

values of $t/s$. Indeed, for small values of $t/s$ the data obtained for the smallest waiting time has the highest value for the autocorrelation function, whereas for large values of $t/s$ the smallest waiting time yields the lowest value (see inset).

We therefore reanalyze the data by using the numerically determined length $L(t)$ of Figure 2.14 instead of simply assuming a perfect power-law increase. For both studied temperatures no systematic deviations are observed any more when plotting $C(t, s)$ as a function of $L(t)/L(s)$. We therefore conclude that also for the Ising spin glass the aging scaling (2.8) with the correct $L(t)$ prevails. Whereas this is the same conclusion as for the disordered ferromagnets, we point out that there is a notable difference between the disordered ferromagnets and the frustrated spin glass: for the former we have that $B = 0$, whereas for the latter the exponent $B$ is different from zero and depends on the temperature, see Figure 2.16.

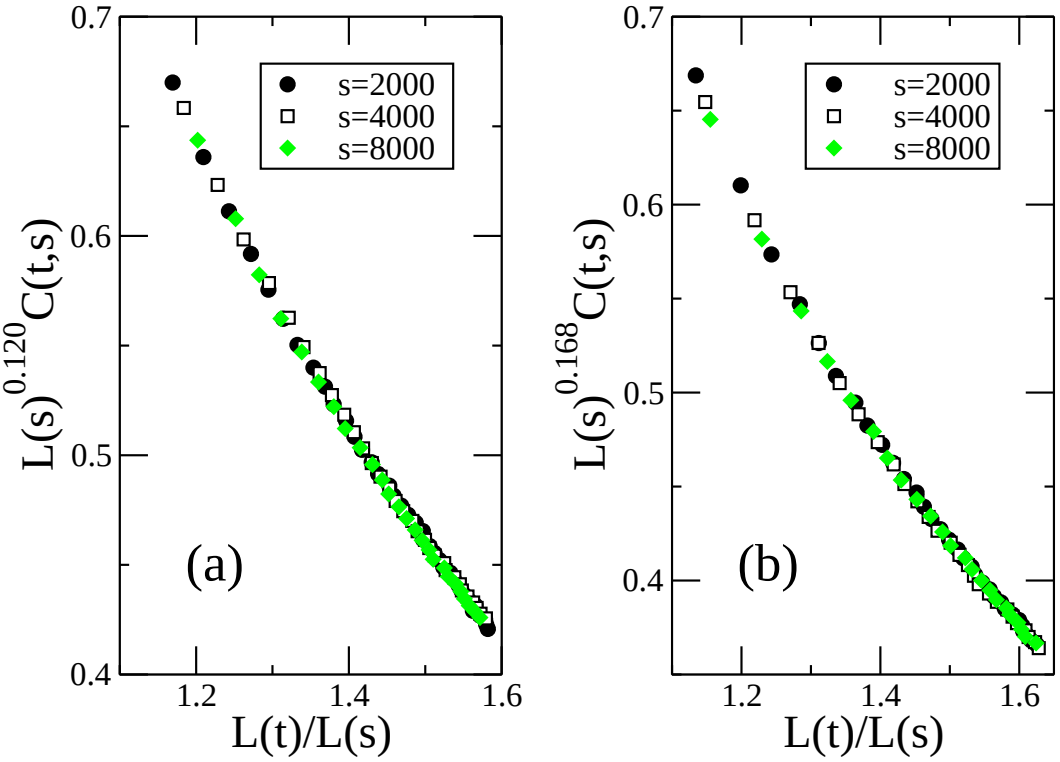


Figure 2.16: Autocorrelation as a function of $L(t)/L(s)$ for the three-dimensional Ising spin glass at temperature (a) $T = 0.833$ and (b) $T = 0.952$. No systematic deviations from the scaling (2.8) are observed. Note that the scaling exponent $B$ is different form zero and that its value depends on the temperature. After [44]. With kind permission of The European Physics Journal (EPJ).

## 2.4 Summary

Aging processes are ubiquitous in Nature. These paradigmatic non-equilibrium collective phenomena were initially studied intensively in glassy materials. However, the investigation of perfect i.e. non-disordered and non-frustrated ferromagnetic spin systems subjected to a direct quenching protocol was extremely helpful for clarifying the theoretical properties of aging processes. Three defining characteristics of aging were stated, and specific dynamical scaling forms were proposed according to the scenario of simple aging.

The fundamental quantity that the simple aging scheme relies on is the dynamical correlation length $L(t)$, and the law governing the growth of $L(t)$ is therefore of great importance in any aging system. In many systems, notably non-disordered systems, an algebraic growth rapidly prevails [25]. This is expected to be different in disordered systems as here a crossover from a transient, preasymptotic, power-law regime to an asymptotic regime with a slower, logarithmic, growth is predicted to happen [6]. There is mounting evidence, due to recent studies of elastic lines in disordered media [16–18], that this crossover indeed takes place. Obviously, this crossover has to be taken into account in order to elucidate the scaling properties of disordered systems relaxing toward equilibrium.

In section 2.2 we dealt with the aging behavior in two kinds of disordered ferromagnetic systems. In the study of the random-site Ising model in two dimensions, deviations from an algebraic growth law, compatible with a crossover to a slower, logarithmic growth, indeed show up on time scales that are accessible in numerical relaxation studies. As a consequence, we do not assume in our scaling analysis any specific form of the growth law but directly use the numerically determined dynamical correlation length $L(t)$. In doing so, a surprisingly simple picture of the relaxation properties of the random-site Ising model emerges. Indeed, for all the studied quantities (autocorrelation, space-time correlation, and autoresponse function) the simple aging scaling behaviors [Eqs. (2.8), (2.12), (2.16)] are observed when plotting the two-time quantities as a function of the ratio of the correlation lengths at times $t$ and $s$: $L(t)/L(s)$. The autocorrelation has been studied previously in Ref. [10] where a superaging scaling ansatz has been used to fit the numerical data. As we showed, this superaging scaling ansatz, which anyhow is in conflict with very general theoretical considerations, is hampered by systematic deviations which do not vanish when optimizing the value of the free parameter $\mu$.

The scaling relations [Eqs. (2.8), (2.12), (2.16)] are characterized by the values of some scaling exponents as well as by the scaling functions themselves. In Table 2.1 we report our estimates for the autocorrelation exponent $\lambda_C$, for the autoresponse exponent $\lambda_R$, as well as for the exponent $A$ of the response function (in addition, we found that the value $B = 0$ for the exponent of the correlation function, as expected for a phase ordering system). Interestingly, the values of $\lambda_C$ and $\lambda_R$ for a fixed dilution are within error bars independent of the temperature, with $\lambda_C \approx \lambda_R$. This is in agreement with the intuitive picture that the dynamical correlations in the diluted ferromagnets are mainly governed by the average size

and shape of ordered clusters. The values of $\lambda_C$ are always found to be larger than the lower bound $d/2$ derived in Refs. [20] and [39], similar to what is observed in the random-bond model. [12] This corrects an earlier claim [10] that in diluted magnets this bound is violated. For the exponent $A$, on the other hand, we find that its value depends on the dilution as well as on the temperature. Due to our high-quality data and our careful analysis, we can exclude for the random-site model that the values of $A$ are independent of dilution and temperature and that they are equal to 1/2.

Next we applied the same analysis to another disordered ferromagnet, the random-bond Ising model in two dimensions, as well as to the three-dimensional Edwards-Anderson spin glass in section 2.3. For the random-bond model notable deviations from simple scaling can be observed when using $t/s$ as scaling variable, similar, but less pronounced, to what is encountered in the random-site case. We find that for both models the simple aging scaling (2.8) is recovered when using as scaling variable $L(t)/L(s)$ with the numerically determined length $L$. Thus even small deviations from an algebraic growth can have a large impact on aging scaling and need to be taken into account in a correct description. However, as we do not have currently analytical expressions of $L(t)$ in disordered systems with a crossover from an algebraic to a slower (logarithmic?) growth, we are bound to use the numerically determined function $L(t)$.

We also briefly discuss some issues related to the concept of superuniversality. Whereas superuniversality, i.e. an independence of scaling functions on disorder when using $L(t)$ in time-dependent quantities, in the strict sense is surely not realized, there is still a remarkable degree of universality that can be encountered in disordered ferromagnets undergoing phase ordering. This universality strongly shows up in the two-times space-time correlation function for not too short distances, as scaling functions are found to be independent of disorder and of temperature in that regime. The only exception is encountered for $\varepsilon = 2$, i.e. the strongest disorder where very weak bonds are present. More extensive studies will be needed in order to fully understand this remarkable behavior of space-time quantities in the aging regime.

# Chapter 3

# Surface Criticality at a Dynamic Phase Transition

This chapter discusses the dynamic phase transition in presence of the surface in two- and three-dimensional kinetic Ising ferromagnetic systems. Section 3.1 gives brief reviews of the dynamic phase transition in general as well as of surface critical phenomena, which are both relevant for our topic. In Section 3.2 we consider kinetic Ising models with free surfaces subjected to a periodic oscillating magnetic field. Whereas the corresponding bulk system undergoes a continuous non-equilibrium phase transition characterized by the exponents of the equilibrium Ising model, we find that the non-equilibrium surface exponents do not coincide with those of the equilibrium critical surface. In addition, in three space dimensions, the surface phase diagram of the non-equilibrium system differs markedly from that of the equilibrium system. Finally, we summarize our results in section 3.3.

## 3.1 Background

### 3.1.1 Dynamic Phase Transition in the Bulk System

In the last fifty years our understanding of equilibrium critical phenomena has developed to a point where well established results are available for a range of different situations. In particular, the origin of and the difference between equilibrium universality classes is now well understood. Far less is known, however, on the properties of non-equilibrium phase transitions taking place in interacting many-body systems that are far from equilibrium. As for the equilibrium situation, a continuous non-equilibrium phase transition is also characterized by a set of critical indices. Absorbing phase transitions encountered in reaction-diffusion systems [63, 64] and phase transitions found in driven diffusive systems [65, 66] are well studied examples of continuous phase transitions taking place far from equilibrium. Even though

the values of the critical exponents have been determined in many cases, a classification of non-equilibrium phase transitions into non-equilibrium universality classes is far from complete.

A different type of non-equilibrium criticality is encountered when kinetic ferromagnets are subjected to a periodically oscillating magnetic field [67, 68]. When increasing the frequency of the field, a phase transition takes place between a dynamically disordered phase at low frequencies, where the ferromagnet is able to follow the changes of the field, and a dynamically ordered phase at high frequencies, where the magnetic system does not have time to adjust to the magnetic field before it changes its orientation. In the dynamically disordered phase the magnetization oscillates around zero, but in the dynamically ordered phase the magnetization keeps oscillating around a non-vanishing average value. Early studies in the field focused on the hysteretic loop between the magnetization $m$ and the field strength $H_0$ and its area encountered in the kinetic Ising model when exposed to a sinusoidally oscillating field. It was then discovered that a symmetry breaking transition between symmetric and asymmetric hysteresis loops occurs as the field frequency changes. Then, fixing the equilibrium temperature $T$ and the field strength $H_0$ so that the system remains in the multidroplet regime, it was discovered that this symmetry breaking indeed corresponds to a genuine non-equilibrium phase transition between dynamically ordered and disordered phases, commonly called 'Dynamic Phase Transition' (DPT).

This series of studies about DPT has been done theoretically in a large range of systems, as for example, the Ising [69–71], Heisenberg [72, 73], or Blume-Emery-Griffiths [74] models, to name a few. Possible experimental realizations have been discussed in Co films on Cu(001) [75] as well as in $[Co/Pt]_3$ magnetic multilayers [76]. Most of these studies looked at general properties of the dynamical ordering, without trying to fully characterize the corresponding continuous transition through the determination of the critical indices. It is only for the two-dimensional kinetic Ising model in a periodically oscillating field that the critical exponents have been measured [71]. Interestingly, even though the studied phase transition is a non-equilibrium transition, the values of the exponents were found to coincide with the values of the universality class of the equilibrium two-dimensional Ising model. This result agrees with an earlier conjecture [77], based on the symmetry of the problem, as well as with an investigation of the time-dependent Ginzburg-Landau model with a periodically changing field [78]. From the symmetry argument given in [77] one expects also for other cases that this dynamic phase transition falls into the universality class of the equilibrium counterpart, but this has not yet been confirmed. Interestingly, as we shall see in the next section (See also [79]), the above mentioned symmetry argument breaks down when the dynamic phase transition takes place in systems with boundaries, yielding surface critical exponents at the non-equilibrium phase transition that do not coincide with the corresponding equilibrium exponents.

In this subsection we present evidence that for the bulk systems both in two and three dimensions the dynamic phase transition falls into the corresponding equilibrium universality class. This is done through a study of the critical properties of the kinetic Ising model in

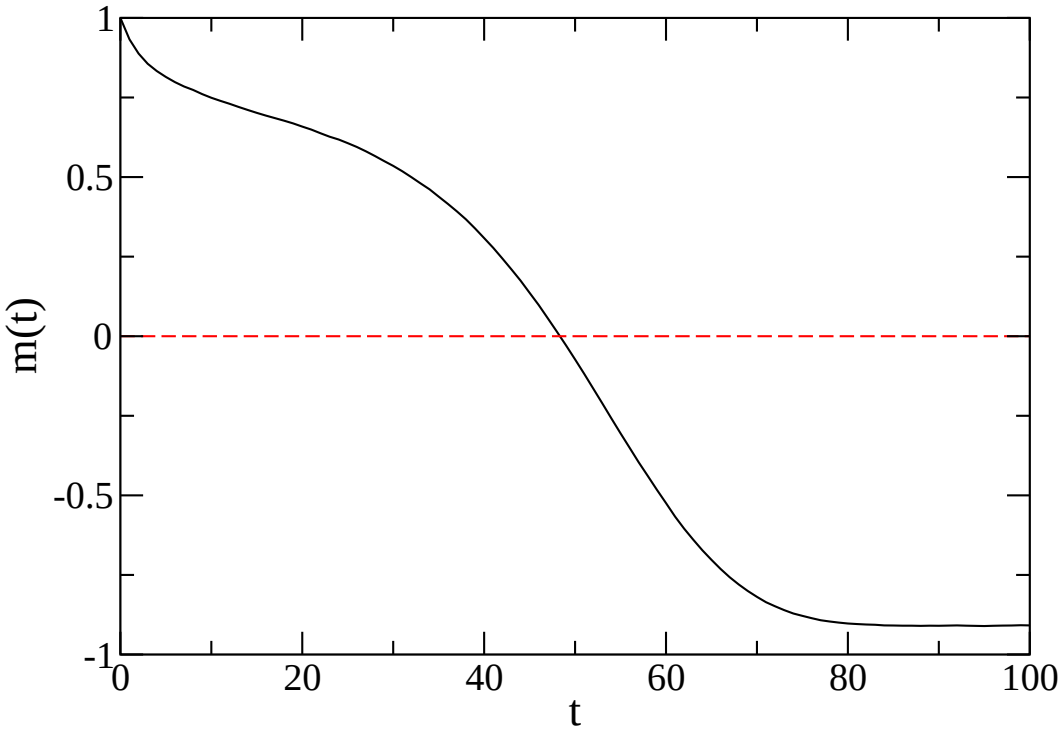


Figure 3.1: Illustration for the determination of the metastable lifetime. After preparing the system in a fully ordered state a constant magnetic field is applied that reverses the magnetization. The metastable lifetime is defined as the first-passage time to zero magnetization. The parameters are $(T, H_0) = (0.8T_c, 0.3J)$ and $(0.8T_c, 0.4J)$ in two and three dimensions respectively, where the system remains in the multidroplet regime for both cases. The data shown have been obtained for the three-dimensional kinetic Ising model composed of $96^3$ sites. The values of metastable lifetime $\langle\tau\rangle_{2\mathrm{d}} = 74.5$ and $\langle\tau\rangle_{3\mathrm{d}} = 47.05$ were confirmed to be independent of the system size by numerical simulations [71, 80]. After [80].

a square wave field. The result in two dimension is due to Korniss *et al.* [71], whereas the three-dimensional result is due to our work [80].

The Hamiltonian of the kinetic Ising model is given by the expression

$$\mathcal{H} = -J \sum_{\langle \mathbf{x},\mathbf{y} \rangle} S_{\mathbf{x}} S_{\mathbf{y}} - H(t) \sum_{\mathbf{x}} S_{\mathbf{x}} \tag{3.1}$$

where $S_{\mathbf{x}} = \pm 1$ is the usual Ising spin located at site $\mathbf{x}$. The first sum in that expression runs over bonds connecting nearest neighbor spins. $J > 0$ is a ferromagnetic coupling and $H(t)$ is a spatially uniform periodically oscillating magnetic field. We use a square wave field of amplitude $H_0$ and half-period $t_{1/2}$. For the data presented in this subsection we choose temperature and magnetic field strength so that the system is in the multidroplet regime: $T = 0.8T_c^{2d}$, $H_0 = 0.3J$ for $d = 2$ and $T = 0.8T_c^{3d}$, $H_0 = 0.4J$ for $d = 3$ respectively, with

the equilibrium critical temperatures $T_c^{2d} = 2.269J/k_B$ and $T_c^{3d} = 4.5115J/k_B$ ($k_B$ is the Boltzmann constant).

The best way to understand the dynamic phase transition is to consider the dynamic competition between $t_{1/2}$ and the metastable lifetime $\langle\tau\rangle$. $t_{1/2}$ is nothing but the inverse of the field frequency, an externally controlled quantity. On the other hand, $\langle\tau\rangle$ is an intrinsic quantity which characterizes the metastability of the bistable system reacting to a single reversal of the external field, see Figure 3.1. This quantity is usually defined as the average first-passage time to zero magnetization, as it takes some time for the system to leave the metastable region of the free-energy landscape. Figure 3.2 shows that assuming the magnetization being aligned with the external field, a reversing of the direction of the field results in a metastable state from which the system tries to escape by nucleating droplets that are pointing in the same direction as the field. Whereas in the dynamically disordered phase the ferromagnet is able to reverse its magnetization before the field is changed again, see Figure 3.2(a), in the dynamically ordered phase the system is still in the metastable state when the field direction switches back, thereby yielding a time dependent magnetization that oscillates around a finite value, as shown in Figure 3.2(c). This competition between the magnetic field and the metastable state is captured by the ratio between two quantities

$$\Theta = \frac{t_{1/2}}{\langle\tau\rangle} \ . \tag{3.2}$$

For the kinetic Ising model the variable $\Theta$ plays the same role as that played by temperature in the equilibrium system. Changing $t_{1/2}$ changes the value of $\Theta$. Consequently, there is a critical value $\Theta_c$ where the dynamic phase transition between the dynamically ordered and the dynamically disordered phases takes place, see Figure 3.2(b).

In order to determine the metastable lifetime we consider an equilibrated system in a field of constant strength $H_0$. Reversing the sign of the field renders the system metastable. The metastable lifetime is then obtained as the average first-passage time to zero magnetization. The system parameters are $(T, H_0) = (0.8T_c\ , 0.3J)$ and $(0.8T_c\ , 0.4J)$ for two and three dimensions respectively, and the corresponding metastable lifetimes are $\langle\tau\rangle_{2d} = 74.5$ and $\langle\tau\rangle_{3d} = 47.05$ where the time is measured in Monte Carlo Step, with one Step corresponding to updating on average every spin once.

In order to elucidate the critical properties of the dynamic phase transition we study a range of different quantities. The main quantity of interest is the period-averaged magnetization

$$Q = \frac{1}{2t_{1/2}} \oint m(t)dt \tag{3.3}$$

where the integration is performed over one period of the oscillating field. The time dependent magnetization is given by

$$m(t) = \frac{1}{N} \sum_{\mathbf{x}} S_{\mathbf{x}}(t) \ . \tag{3.4}$$

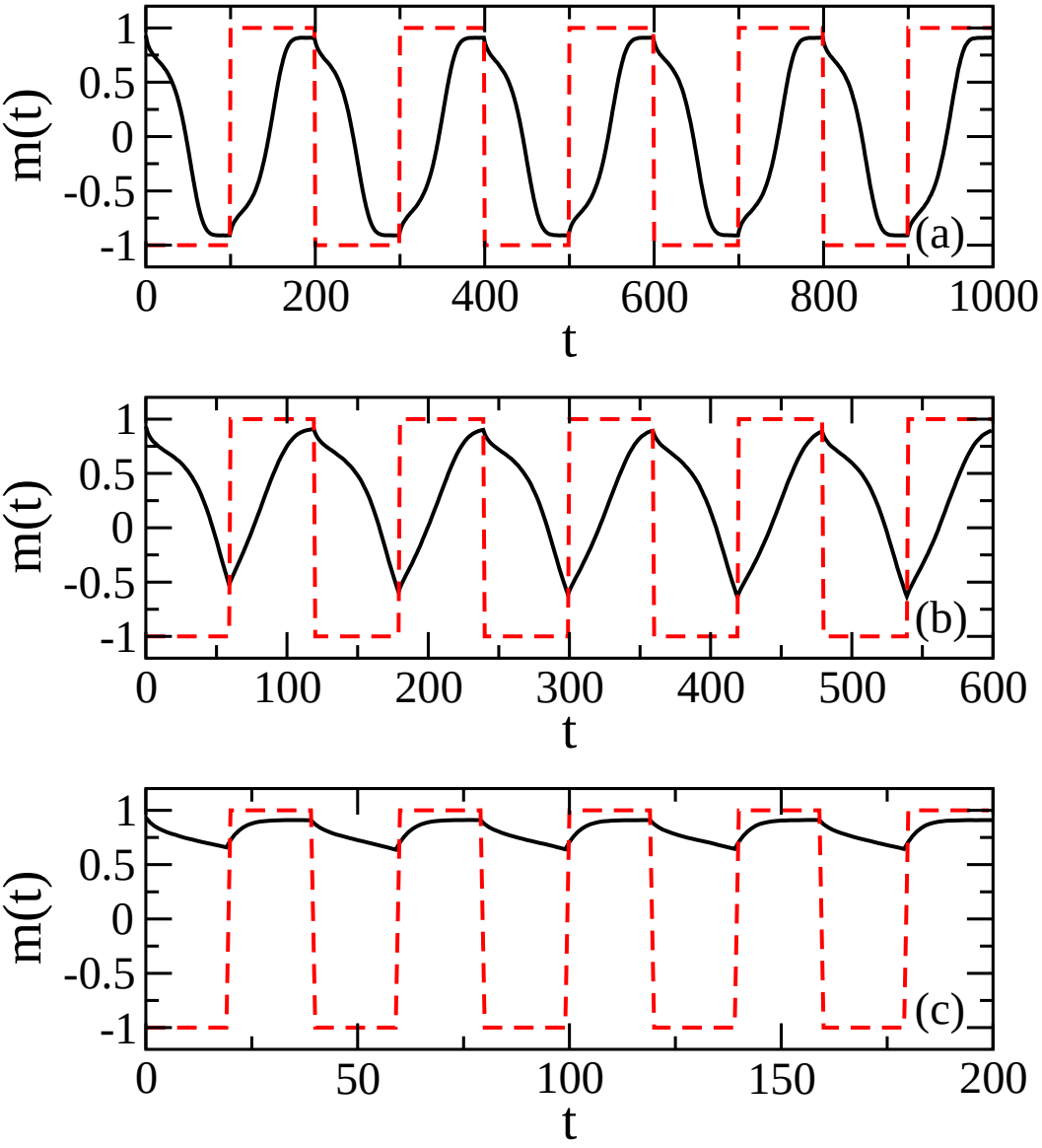


Figure 3.2: Time-dependent magnetization of the three-dimensional kinetic Ising model in a square-wave field of half-period (a) $t_{1/2} = 100$, (b) $t_{1/2} = 60$, and (c) $t_{1/2} = 20$. Starting with the fully magnetized sample, the first five periods are shown for each case. The red dashed line is $H(t)/H_0$ where $H_0$ is the amplitude of the magnetic field. Whereas for case (a) we are in the dynamically disordered phase, for case (c) the system is dynamically ordered. Case (b) is close to the dynamic phase transition. The parameters are $T = 0.8T_c$ and $H_0 = 0.4J$, the system contains $96^3$ spins. After [80].

We consider square and cubic systems with periodic boundary conditions and linear extend $L$, so that $N = L^d$ where $d = 2$ and 3. The order parameter $\langle|Q|\rangle$ is then obtained after averaging both over time (i.e. an average over many periods) and over different realizations of the noise.

Some quantities of interest are directly obtained from the order parameter. Thus we calculate the Binder cumulant

$$U = 1 - \frac{\langle Q^4 \rangle}{3\langle Q^2 \rangle^2} \tag{3.5}$$

that we use to determine the critical point, as shown later. The susceptibility describing the fluctuations of the order parameter is given by

$$\chi^Q = N(\langle Q^2 \rangle - \langle|Q|\rangle^2) \ . \tag{3.6}$$

We also calculated the period-averaged energy

$$E = -\frac{1}{2t_{1/2}} \oint \frac{J}{N} \sum_{\langle \mathbf{x},\mathbf{y} \rangle} S_{\mathbf{x}} S_{\mathbf{y}} \ dt \tag{3.7}$$

and its fluctuation

$$\chi^E = N(\langle E^2 \rangle - \langle E \rangle^2) \ . \tag{3.8}$$

Close to the critical point, the order parameter and the response functions $\chi^Q$ and $\chi^E$ display an algebraic behavior:

$$\langle|Q|\rangle \sim (\Theta_c - \Theta)^\beta \tag{3.9}$$

$$\chi^Q \sim |\Theta_c - \Theta|^{-\gamma} \tag{3.10}$$

$$\chi^E \sim |\Theta_c - \Theta|^{-\alpha} \tag{3.11}$$

with the critical exponents $\beta$, $\gamma$ and $\alpha$.

As a necessary prerequisite for a reliable determination of the critical exponents we need to know the location of the critical point with high precision. As usual for continuous phase transitions the various quantities show a characteristic behavior in finite systems when approaching the critical point. This is illustrated for the Binder cumulant, the order parameter, as well as for the fluctuations of the order parameter in Figures 3.3 and 3.4 for the two and three-dimensional cases respectively. Even though one can get an estimate for the critical value $\Theta_c$ by analyzing the shift of the maximum of the susceptibility when changing the system size, the most reliable way to determine the critical point is to study the Binder cumulant. As seen in Figure 3.3(a), (b) and in Figure 3.4(a), the data sets obtained for different system sizes all cross at common values $\Theta = 0.918$ and $\Theta = 1.285$ for two and three dimensions respectively. These values being compatible with the finite-size shifts of the position of the maxima in $\chi^Q$ and $\chi^E$, one can take these values as the critical values $\Theta_c$ where the dynamic phase transition takes place.

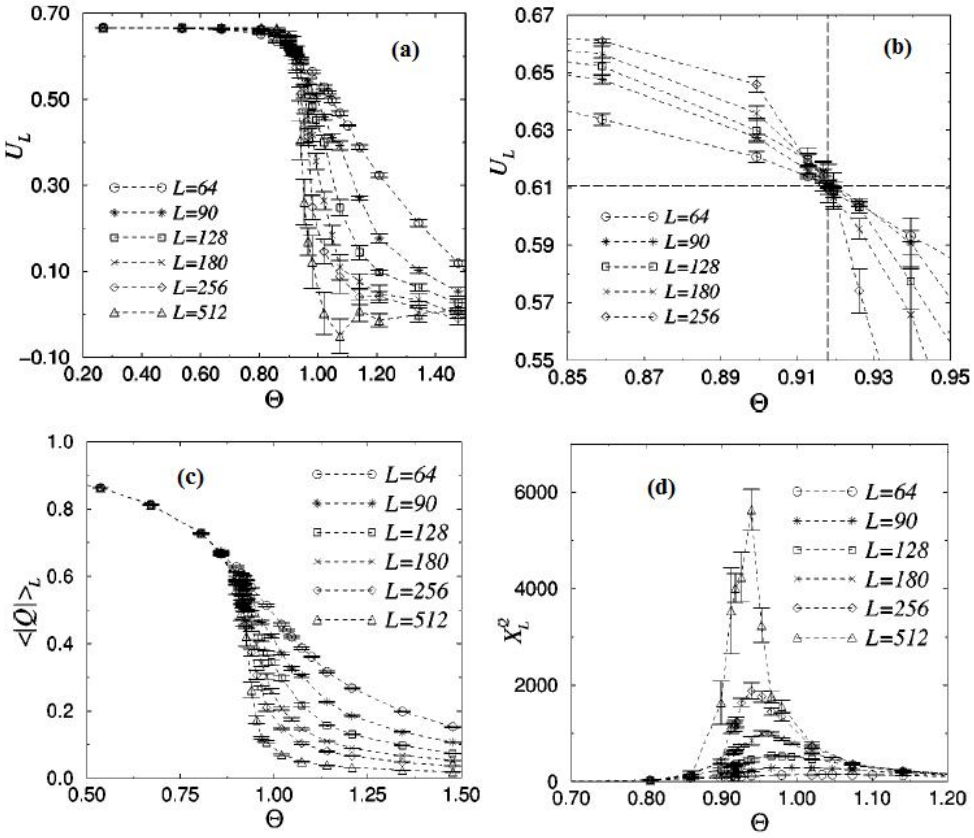


Figure 3.3: Indications of the dynamic phase transition in the two-dimensional kinetic Ising model with $T = 0.8T_c$ and $H_0 = 0.3J$. (a) Binder cumulant and (b) enlarged region near the intersection of the cumulant curves. This quantity makes it possible to find the precise value of the critical point $\Theta_c = 0.918$. (c) The order parameter decreases rapidly and (d) its fluctuation tends to diverge around $\Theta_c$. After [71]. Copyright (2000) by the American Physical Society.

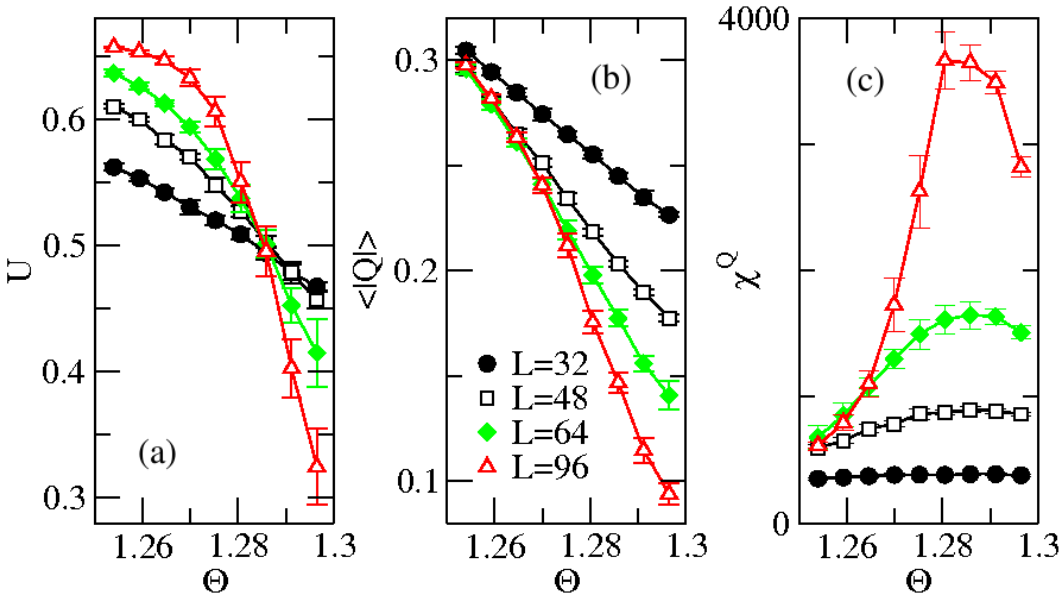


Figure 3.4: (a) Binder cumulant, (b) order parameter, and (c) susceptibility as a function of $\Theta$ for systems with different linear extend $L$ in three dimensions. The cumulants for the different system sizes cross at $\Theta_c = 1.285$. In addition, the susceptibility displays in the finite systems a maximum close to that value of $\Theta$. The data result from averaging over typically 100000 periods. After [80].

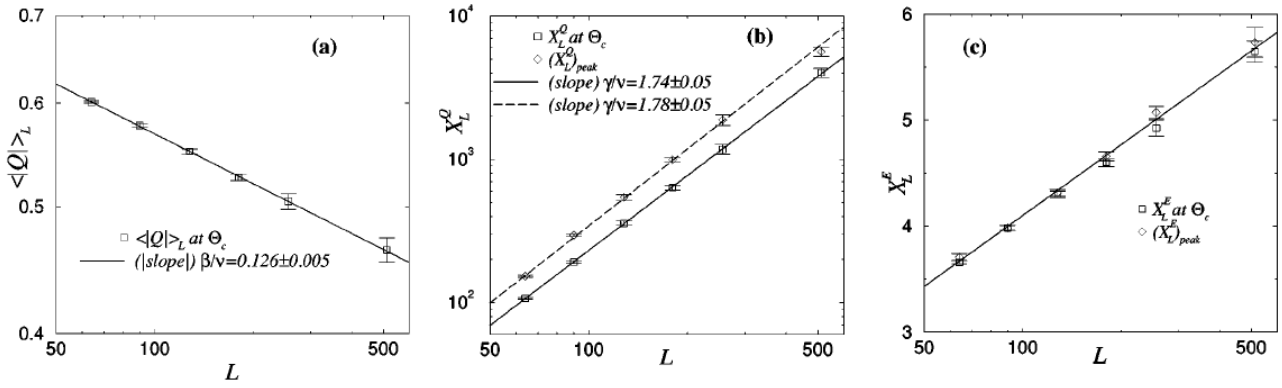


Figure 3.5: Estimation of the critical exponents (a) $\beta/\nu$, (b) $\gamma/\nu$, (c) Check of the logarithmic divergence of $\chi^E$ at a dynamic phase transition with $T = 0.8T_c$ and $H_0 = 0.3J$ in the two-dimensional kinetic Ising model. Finite size scaling analysis represented by (3.12), (3.13) and (3.14) gives values for the critical exponents very close to those of the equilibrium two-dimensional Ising universality class. After [71]. Copyright (2000) by the American Physical Society.

In order to determine the values of the critical exponents, we perform a finite-size scaling analysis [81]. Close to the critical point systems of different sizes should display the following scaling behavior in two dimensions:

$$\langle |Q| \rangle = L^{-\beta/\nu} \mathcal{F}_{\pm}(\theta L^{1/\nu}) \tag{3.12}$$

$$\chi^Q = L^{\gamma/\nu} \mathcal{G}_{\pm}(\theta L^{1/\nu}) \tag{3.13}$$

$$\chi^E = c_1 \ln[L \mathcal{J}_{\pm}(\theta L^{1/\nu})] \tag{3.14}$$

where $\theta = \frac{|\Theta - \Theta_c|}{\Theta_c}$ is the control parameter and $\nu$ is the critical exponent describing the divergence of the correlation length when approaching the critical point. $\mathcal{F}_{\pm}$, $\mathcal{G}_{\pm}$ and $\mathcal{J}_{\pm}$ are scaling functions, where the sign $\pm$ corresponds to $\Theta \gtrless \Theta_c$. The relation (3.14) implies that $\alpha = 0(\log)$, i.e. $\chi^E$ diverges logarithmically, then thus the change of $\chi^E$ as a function of $L$ should give a straight line in a log-linear plot, see Figure 3.5(c). In three dimensions, on the other hand, due to non-zero value of $\alpha$, (3.14) is modified to

$$\chi^E = L^{\alpha/\nu} \mathcal{J}_{\pm}(\theta L^{1/\nu}) \ . \tag{3.15}$$

In that case the data obtained at the critical point $\Theta = \Theta_c$ should yield for all three quantities an algebraic dependence on the system size, which allows to directly determine the critical exponents from the slopes in a double logarithmic plot.

Figure 3.5 shows the estimations for the critical exponent ratios $\beta/\nu$ and $\gamma/\nu$, and the confirmation of the logarithmic divergence of $\chi^E$ for the two-dimensional case. From the slopes in the plots of $\langle |Q| \rangle$ and $\chi^Q$ at $\Theta_c$ one reads off $\beta/\nu = 0.126 \pm 0.005$ (Figure 3.5(a)) and $\gamma/\nu = 1.74 \pm 0.05$ (Figure 3.5(b)). Furthermore, the energy fluctuation $\chi^E$ indeed shows

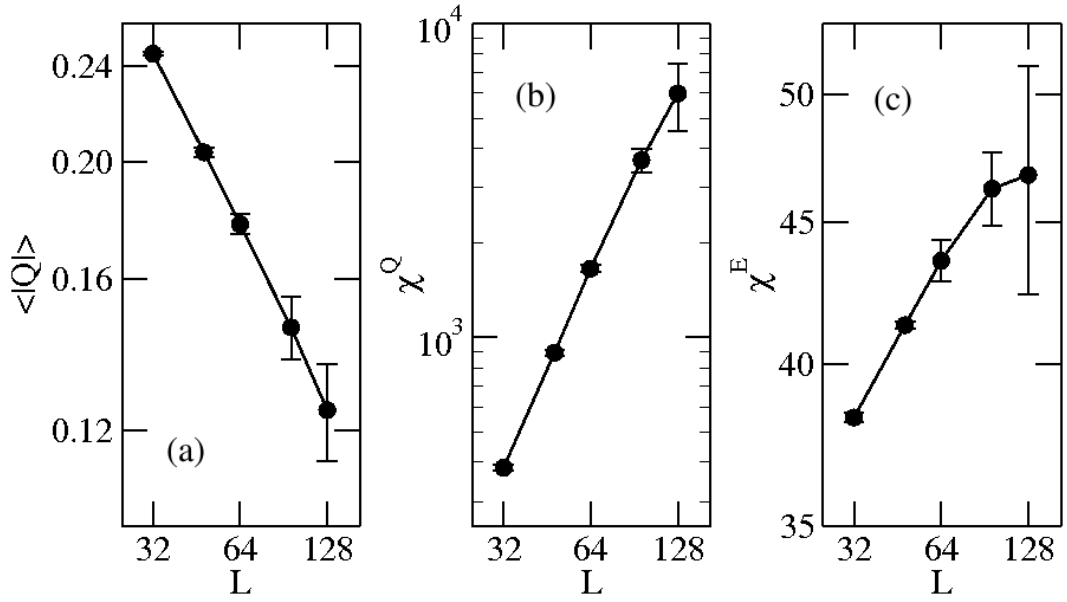


Figure 3.6: (a) Order parameter $\langle|Q|\rangle$, (b) order parameter susceptibility $\chi^Q$, and (c) energy fluctuations $\chi^E$ at the critical point $\Theta = \Theta_c$ as a function of system size in three-dimensional system. The slopes in a double logarithmic plot give the values of the critical exponents $\beta/\nu$, $\gamma/\nu$, and $\alpha/\nu$. The data have been obtained by averaging over at least 200000 periods. After [80].

a logarithmic scaling (Figure 3.5(c)). These values are remarkably similar to the equilibrium critical exponent values $\beta/\nu = 1/8 = 0.125$ and $\gamma/\nu = 7/4 = 1.75$ within error bars. On the other hand, as shown in Figure 3.6, in the three-dimensional case all three quantities indeed depend algebraically on the system size. From the slopes we obtain the values $\beta/\nu = 0.51(2)$, $\gamma/\nu = 1.96(4)$, and $\alpha/\nu = 0.18(3)$ (for the specific heat we did not take into account the largest system size, due to the rather poor quality of the data). Comparing these values with the well known equilibrium values for the three-dimensional Ising model $\beta = 0.33$, $\gamma = 1.24$, $\alpha = 0.108$, and $\nu = 0.63$, we see that the set of exponents we obtain for the dynamic phase transition of the kinetic Ising model indeed agree with the equilibrium values $\beta/\nu = 0.52$, $\gamma/\nu = 1.97$, and $\alpha/\nu = 0.17$. This confirms that for the problem at hand the symmetry argument given in [77] is also valid in three space dimensions.

### 3.1.2 Surface Critical Phenomena

Phase transitions and critical phenomena are usually discussed in the thermodynamic limit. However, one might also consider a finite number of particles or introduce geometrical boundaries. Whereas the former yields finite size corrections to the global thermodynamic quantities, the latter breaks the spatial translation symmetry of the system and changes local

quantities. In this subsection we present a very brief review about the effect of surfaces on the critical properties of the system.

Surface critical phenomena have been studied intensively using analytical techniques (mean field theory, renormalization group theory, conformal invariance), experimental approaches or computational works. The topics of these studies include not only ideal or imperfect surfaces [82–85], but also other inhomogeneous geometries such as wedges, cones or non-flat shapes [86]. However, in this review we limit ourselves to a short discussion of the free energy, Hamiltonian, local quantities, and surface phase diagram in system with a flat, perfect surface.

Just as the bulk free energy contains all necessary information for describing the bulk critical phenomena, the surface critical behavior is completely characterized by the total free energy that includes the bulk and the surface free energies. As a standard continuum description the Landau mean-field theory states that the total free energy comprises the bulk and the surface contributions which are functionals of the order parameter field $\phi(\mathbf{r})$ :

$$F(\phi) = \int_V \mathrm{dV}\, F_b(\phi) + \int_S \mathrm{dS}\, F_s(\phi) \tag{3.16}$$

with the bulk free energy per volume $F_b$ and the surface free energy per surface area $F_s$. dV and dS are the infinitesimal volume and surface elements of the system, respectively. For a ferromagnetic Ising system, in the critical region of the continuous phase transition the bulk free energy is expanded as a function of the scalar order parameter $m$ :

$$F_b(m) = \frac{1}{2}(\nabla m)^2 + \frac{1}{2}\tau_0 m^2 + \frac{1}{4!}u_0|m|^4 - h_0 m \tag{3.17}$$

where the first term shows the extra energy related to a spatial fluctuation of $m$, $\tau_0 \sim T - T_c$ measures the deviation from the critical temperature $T_c$, $u_0 > 0$ guarantees the stability below $T_c$ and the last term is due to the interaction with an external bulk field of strength $h_0$. In the same manner the surface free energy is written as

$$F_s(m) = \frac{1}{2}c_0 m^2 - h_1 m \tag{3.18}$$

where $c_0 = C/\lambda$ is related to the surface enhancement of the coupling constant in the corresponding model with the discrete lattice and $h_1$ is the surface external field. $\lambda$ in the coefficient $c_0$ has the dimension of a length and is often called 'extrapolation length' for reason which we shall see in the following paragraph.

As a matter of fact, when the surface is introduced, the order parameter has a dependence on the position along the $z$ axis perpendicular to the surface lying in the $xy$ plane. The local magnetization density $m(z)$ (local magnetization for brevity) defined in this way is modified by the presence of a surface. Figure 3.7 shows examples of the magnetization profile obtained by Monte Carlo simulations of three-dimensional Ising films with $L = 80$

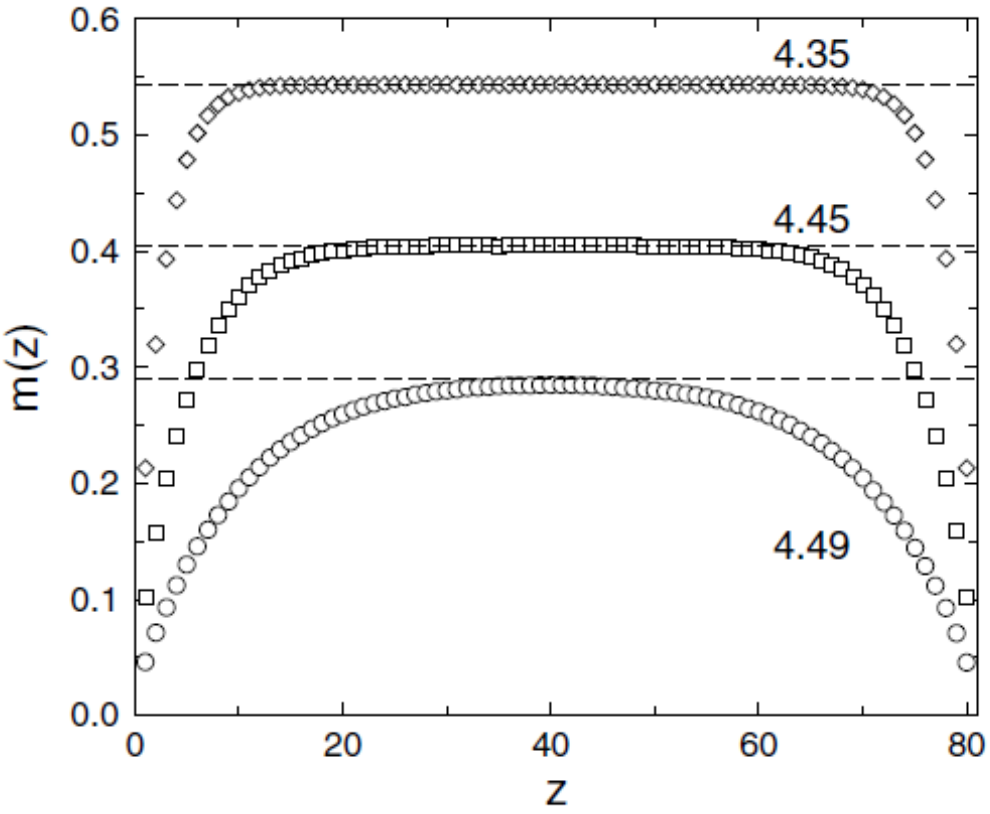


Figure 3.7: Magnetization profiles $m(z)$ of a three-dimensional semi-infinite Ising films with 80 layers with different temperatures $k_bT/J_b$. The dashed lines represent the bulk values $m_b$. After [85]. Reproduced with permission by IOP Publishing.

layers at temperatures below the bulk critical temperature $k_B T_c/J_b = 4.5115$. Deep inside the bulk, $m(z)$ is equal to the bulk value $m_b$ up to corrections $\sim \exp(-z/\xi)$ in the limit $\xi \ll L$ where $\xi$ is the bulk correlation length and $L$ is the system size. On the other hand, due to the reduced coordination number at the surface, one expects that the profile *bends* downwards when it approaches the surface and decreases linearly near $z = 0$. If one extrapolates this linear variation of $m(z)$ to negative $z$, then $m(z)$ vanishes for $z = -\lambda$, which explains the interpretation of $\lambda$ as an extrapolation length. It is also possible to observe an increase of $m(z)$ upon approaching the surface when the surface couplings are strongly enhanced, and then $\lambda$ may become negative. This sign change of $\lambda$ is one of the criteria for classifying the different kinds of phase transitions in presence of a surface [82] : $\lambda > 0$, $\lambda = \infty$, $\lambda < 0$ above $T_c$ and $\lambda < 0$ below $T_c$ correspond to the ordinary transition, the special transition, the surface transition and the extraordinary transition respectively. The established surface phase diagram in three-dimensional Ising model is presented at the end in detail.

For the Ising model on the semi-infinite lattice, the general Hamiltonian is given by [85]

$$\mathcal{H} = -J_b \sum_{\langle \mathbf{x},\mathbf{y} \rangle} S_{\mathbf{x}} S_{\mathbf{y}} - J_s \sum_{\{\mathbf{x},\mathbf{y}\}} S_{\mathbf{x}} S_{\mathbf{y}} - h_0 \sum_{\langle \mathbf{x} \rangle} S_{\mathbf{x}} - h_1 \sum_{\{\mathbf{x}\}} S_{\mathbf{x}} \tag{3.19}$$

where $S_{\mathbf{x}} = \pm 1$ are the usual Ising spins. The parenthesis $\langle\rangle$ in the first sum means the sum runs over nearest neighbor spin pairs where one of them should be a bulk spin at least, whereas the second parenthesis $\{\}$ includes pairs of surface layer spins only (see Figure 3.8). Both the bulk and the surface couplings $J_b$ and $J_s$ are assumed to be ferromagnetic. The bulk field $h_0$ acts on the total spins and the surface field $h_1$ acts only on spins at the surface, which means the surface spins feel the field $h_0 + h_1$.

A bunch of layer-dependent quantities can be used for the investigation of the semi-infinite system. It is enough to introduce magnetization per layer $m(z)$ and its susceptibility per layer $\chi(z)$ as necessary quantities for this review. In particular, magnetizations and susceptibilities in the middle layer (deep in the bulk) and at the surface layer are defined as the derivatives with respect to the bulk and the surface field $h_0$ and $h_1$,

$$m_b = -\frac{\partial F_b}{\partial h_0} \ , \quad \chi_b = -\frac{\partial^2 F_b}{\partial {h_0}^2} \ , \tag{3.20}$$

$$m_1 = -\frac{\partial F_s}{\partial h_0} \ , \quad \chi_1 = -\frac{\partial^2 F_s}{\partial h_0 \partial h_1} \ , \quad \chi_{11} = -\frac{\partial^2 F_s}{\partial {h_1}^2} \tag{3.21}$$

where $m_b$ and $m_1 = m(z = 1)$ are the bulk and the surface magnetization, $\chi_1$ and $\chi_{11} = \chi(z = 1)$ are the response of the surface magnetization to a bulk and a surface field respectively. In the critical regime the behavior of the system is fully described by surface critical exponents associated with the corresponding critical quantities :

$$m_1 \sim t^{\beta_1} \ , \quad \chi_1 \sim |t|^{-\gamma_1} \ , \quad \chi_{11} \sim |t|^{-\gamma_{11}} \quad \text{as} \quad t \to 0 \tag{3.22}$$

where $t$ is the reduced temperature.

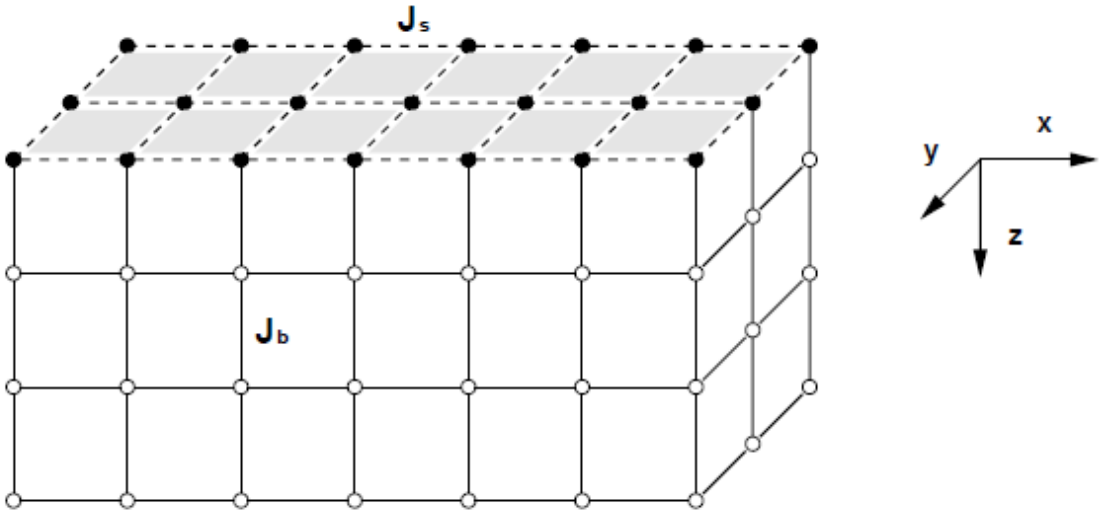


Figure 3.8: Configurations of surface coupling $J_s$ and bulk coupling $J_b$ in three-dimensional semi-infinite Ising model. The top and bottom layers perpendicular to the $z$ direction are regarded as the surface, and the coupling strength $J_s$ is assigned to the links connecting the spins in surface layers. After [87]. With kind permission of The European Physics Journal (EPJ).

The surface phase diagram of the semi-infinite three-dimensional Ising model with vanishing external bulk and surface fields is shown in the Figure 3.9. The ratio $r \equiv J_s/J_b$ on the horizontal axis represents the degree of surface enhancement related to the coefficient $c_0$ in the mean-field description, and the vertical axis shows the temperature $k_BT/J_b$. When the value of $J_s$ is close to $J_b$, the system undergoes an 'ordinary transition' where the bulk and the surface layer order at the same time at the bulk critical temperature $T_c$. At this transition the ordering of the surface is induced by the bulk ordering via the diverging bulk correlation length, and it is known that this transition occurs in all three-dimensional $O(n)$ models for vanishing external fields. Beyond a critical ratio $r > r_{sp}$, where $J_s$ is sufficiently enhanced, the surface may order alone without bulk ordering at a temperature $T_s$ higher than the bulk $T_c$. This novel kind of phase transition is referred to as 'surface transition'. Interestingly, at this transition the surface correlation length diverges by itself as the bulk remains in the paramagnetic phase and the bulk correlation length is finite. Furthermore, if the temperature is lowered to $T_c$ then one encounters a different kind of phase transition, called 'extraordinary transition', where the bulk layer orders in presence of an ordered surface. The presence of an ordered surface implies that the surface keeps its long-range order as $T$ approaches $T_c$. It was revealed that this surface transition due to strongly enhanced surface couplings is equivalent to the bulk ordering in presence of a surface external field $h_0$ which is called 'normal transition' and which occurs in binary fluid mixtures in contact with a boundary [88, 89]. These transition lines meet at the multicritical point which is located at $r_{sp}$. At this

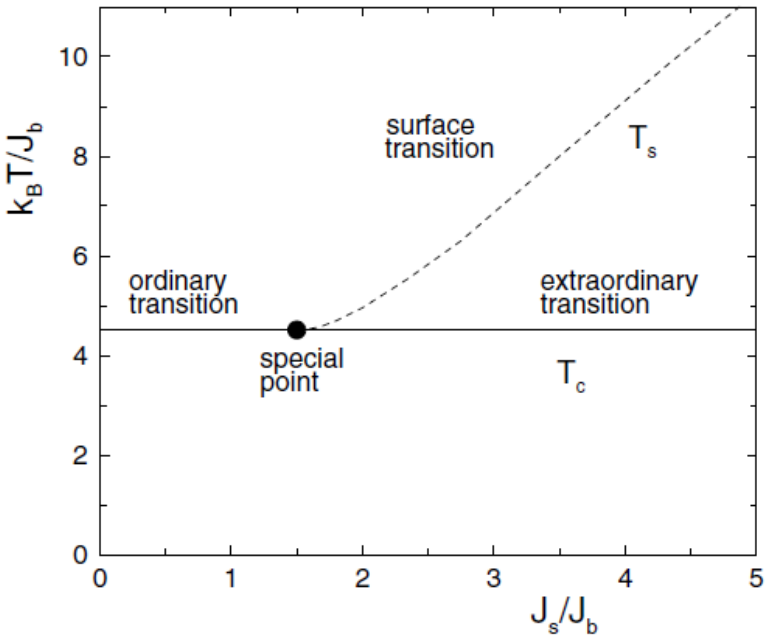


Figure 3.9: The surface phase diagram in three-dimensional semi-infinite Ising model in the absence of the external field. The solid horizontal line is divided into ordinary and extraordinary transition region by the special transition point, and the surface transition denoted by dashed line branches from that point, too. The special point is located near $1.5J_s/J_b$. After [85]. Reproduced with permission by IOP Publishing.

point both the bulk and the surface correlation lengths diverge so that the corresponding layers become critical. The value of $r$ for the special transition point was predicted to be $r_{sp} = 1.25$ in the mean-field approximation, but the simulational works estimate $r_{sp} \approx 1.50$ [90–92] and 1.66 [93] for the three-dimensional semi-infinite Ising and XY models respectively.

It is well established, by both mean-field approximation and renormalization group calculation, that the surface phase diagrams in all semi-infinite $O(n)$ models with isotropic couplings above the upper critical dimension show these three lines of continuous phase transitions as long as the system fulfills the conditions that the pair interactions and the boundary-induced contributions are of short range [84]. Exceptional cases include the following : In the Ising model ($n = 1$) in absence of the external field this surface phase diagram is encountered in dimensions higher than 2 only, in other words, there is only the ordinary transition in two dimensions which immediately makes sense if one remembers that the surface in the two-dimensional Ising model is one-dimensional. Multi-component spin models ($n \geq 3$) with isotropic couplings in dimensions 3 do not exhibit the surface transition where only the surface orders, because of the well-known Mermin-Wagner theorem [94]. A marginal case is the XY model ($n = 2$) which shows quasi-long range order in two dimensions. It was reported that a phase diagram similar to Figure 3.9 was found for the three-dimensional

semi-infinite XY model where the surface does not display any long-range order but undergoes a Kosterlitz-Thouless transition [95–97].

## 3.2 Dynamic Phase Transition in Presence of a Surface

As reviewed in the previous section, both the dynamic phase transition as a far-from-equilibrium phenomena and the surface critical phenomena have been very active research fields which were investigated independently. Very few studies have looked at the impact surfaces can have on the dynamic phase transition, focusing mostly on rather general aspects. For example, the effects of boundaries on magnetization switching in kinetic Ising models were studied in [98]. In [72, 99], the dynamic phase transition was investigated in Heisenberg films with competing surface fields. Combining these two different fields, it is natural to ask what is the effect of a surface on a dynamic phase transition, i.e. on the critical properties of a system undergoing a DPT.

In this section, we present the first study of the surface critical properties at a dynamic phase transition. Using large-scale numerical simulations, we study kinetic Ising models with free surfaces subjected to a square-wave oscillating field. Both in two and three space dimensions we obtain values for the surface critical exponents that differ markedly from the values of the equilibrium surface exponents, thus demonstrating that the dynamic surface universality class differs from that of the equilibrium system, even though the same universality class prevails for the corresponding bulk systems. In addition, we find that the kinetic surface phase diagram in three dimensions is remarkably simple and does not exhibit a special transition point, nor a surface or extraordinary transition, which are all present in the equilibrium surface phase diagram. This section has been published in [79].

### 3.2.1 Quantities and Analysis

In order to study the surface critical behavior at the dynamic phase transition, we consider square and cubic lattices with open boundary conditions in one direction, called $z$ direction in the following, whereas in the directions perpendicular to the $z$ direction we have periodic boundary conditions [85]. In this way, we have in a system of linear extend $L$ two surfaces, located at $z = 1$ and $z = L$. Every lattice site $\mathbf{x}$ is characterized by an Ising spin $S_{\mathbf{x}} = \pm 1$. The Hamiltonian is given by

$$\mathcal{H} = -J_b \sum_{\langle \mathbf{x},\mathbf{y} \rangle} S_{\mathbf{x}} S_{\mathbf{y}} - J_s \sum_{\{\mathbf{x},\mathbf{y}\}} S_{\mathbf{x}} S_{\mathbf{y}} - H(t) \sum_{\mathbf{x}} S_{\mathbf{x}} \ , \tag{3.23}$$

where $J_b > 0$ and $J_s > 0$ are ferromagnetic bulk and surface coupling constants. The first sum is over nearest neighbor sites where at most one of the sites is in a surface layer. The second sum, on the other hand, is over neighboring sites that are both in a surface layer.

We thereby allow for different values of the coupling constants at the surface and inside the bulk. Finally, the last term is the magnetic field term where $H(t)$ is a spatially uniform field that oscillates in time. We follow [71] and use a square-wave field with amplitude $H_0$. Both temperature and magnetic field strength are chosen in such a way that the system is in the multidroplet regime : $T = 0.8T_c^{2d}$, $H_0 = 0.3J_b$ for $d = 2$ and $T = 0.8T_c^{3d}$, $H_0 = 0.4J_b$ for $d = 3$. Here $T_c^{2d} = 2.269J_b/k_B$ and $T_c^{2d} = 4.511J_b/k_B$ are the critical temperatures of the two- and three-dimensional equilibrium systems.

As the surfaces break spatial translation invariance, all quantities of interest depend on the distance to the surface. We therefore define local, i.e., layer-dependent quantities. We can basically utilize the quantities which were introduced in the earlier subsection 3.1.1 and extend them to depend on $z$. Thus, we consider the layer magnetization averaged over one period of the external field ($t_{1/2}$ is the half-period of the oscillating field),

$$Q(z) = \frac{1}{2t_{1/2}} \oint m(t,z)dt \ , \tag{3.24}$$

with the time-dependent magnetization $m(t,z) = \frac{1}{L^{d-1}} \sum_{\mathbf{x}} S_{\mathbf{x}}(t)$ of layer $z$, the sum being taken over all spins in that $(d-1)$-dimensional layer. The local order parameter is then given by $\langle |Q(z)| \rangle$, where $\langle \cdots \rangle$ indicates both a time average (i.e., an average over many periods) and a thermal average (realized in the numerical simulations through multiple independent runs with different random number sequences), yielding typically a total of 500 000 periods over which the average is taken. In a similar way, we define the layer Binder cumulant

$$U(z) = 1 - \frac{\langle [Q(z)]^4 \rangle}{3\langle [Q(z)]^2 \rangle^2} \tag{3.25}$$

and the layer susceptibility

$$\chi(z) = L^{d-1}(\langle Q(z)^2 \rangle - \langle |Q(z)| \rangle^2) \ . \tag{3.26}$$

In the following, the surface quantities will be characterized by an index $s$, whereas an index $b$ will be given to the quantities from the middle of the sample.

An important quantity in the study of the dynamic phase transition is the ratio

$$\Theta = \frac{t_{1/2}}{\langle \tau \rangle_b} \tag{3.27}$$

that quantifies the competition between the metastable state, characterized by the metastable lifetime $\langle \tau \rangle_b$, and the oscillating magnetic field. For small values of $\Theta$, we are in the dynamically ordered phase, whereas for large values the system is dynamically disordered. The quantity $\Theta$ therefore plays the same role as that played by temperature at an ordinary equilibrium phase transition. The metastable lifetime in our systems is again layer-dependent, the value of $\langle \tau(z) \rangle$ being smaller in the surface layer than deep inside the bulk, as surface

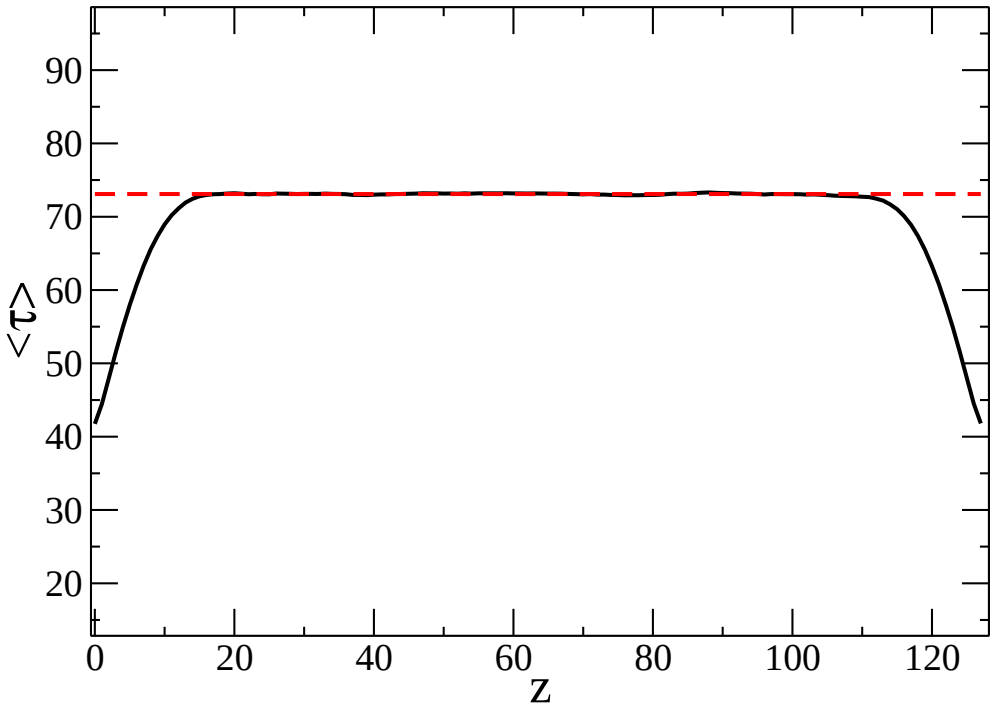


Figure 3.10: The plot of the metastable lifetime $\langle\tau\rangle$ as a function of $z$ for two-dimensional semi-infinite Ising model. The change of $\langle\tau\rangle$ inside the bulk is almost negligible, while the value decreases as one approaches the surface layer. Since sites occupying the surface layer have fewer connections than sites inside the bulk layer, spins near the surface can escape their metastable state faster than the spins inside the bulk. The red dashed line indicates $\langle\tau\rangle_b$ which is identical to $\langle\tau\rangle = 74.5$ of the infinite system, see subsection 3.1.1. The system contains $128^2$ spins.

spins are coupled to fewer spins; see Figure 3.10, for example. As we are interested in the surface properties at the bulk phase transition, we define $\Theta$ with respect to the bulk quantity $\langle\tau\rangle_b$.

In the infinite system, the order parameter and the susceptibility show an algebraic behavior close to the critical point,

$$\langle|Q_b|\rangle \sim (\Theta_c - \Theta)^{\beta} \ , \quad \chi_b \sim |\Theta_c - \Theta|^{-\gamma} \ . \tag{3.28}$$

As already mentioned in the subsection 3.1.1, using finite-size scaling the authors of [71] found in two dimensions the same values for the exponents as those obtained for the equilibrium Ising model, namely $\beta/\nu = 1/8$ and $\gamma/\nu = 7/4$, where $\nu$ is the critical exponent that governs the divergence of the correlation length.

Similarly, surface critical exponents are introduced to describe the behavior of surface quantities close to the bulk critical point (we use here the standard nomenclature of surface critical phenomena, see [82, 83, 85] and also the subsection 3.1.2),

$$\langle|Q_s|\rangle \sim (\Theta_c - \Theta)^{\beta_1} \ , \quad \chi_s \sim |\Theta_c - \Theta|^{-\gamma_{11}} \ . \tag{3.29}$$

Close to a bulk critical point, finite-size scaling theory [82, 83, 85] provides us with scaling relations for our surface quantities,

$$\langle|Q_s|\rangle = L^{-\beta_1/\nu} F_{\pm}(\theta L^{1/\nu}) \ , \tag{3.30}$$

$$\chi_s^Q = L^{\gamma_{11}/\nu} G_{\pm}(\theta L^{1/\nu}) \ , \tag{3.31}$$

where $\theta = \frac{|\Theta - \Theta_c|}{\Theta_c}$, whereas $F_{\pm}$ and $G_{\pm}$ are scaling functions, where the $+(-)$ sign corresponds to $\Theta > (<)\ \Theta_c$. Choosing $\Theta = \Theta_c$, we therefore expect that our quantities depend algebraically on the linear system size.

### 3.2.2 The Results - Critical Exponents and Surface Phase Diagram

To begin with, we discuss the change of the dynamic order parameter and the susceptibility. As shown in Figure 3.11 for the two-dimensional system with $J_s = J_b$, both the bulk and the surface order parameters decrease rapidly when approaching the critical point $\Theta_c$ from below. Concomitantly, the bulk and surface susceptibilities display peaks in the vicinity of $\Theta_c$. Changing the system size yields system size dependencies (shifts of the positions of the maxima of the susceptibilities, increasing peak heights, ...) typical for a continuous phase transition.

From the study of the Binder cumulant in the infinite system we already know that the precise value of $\Theta_c$ equals 0.918 in two dimensions, see subsection 3.1.1. Indeed, the crossing

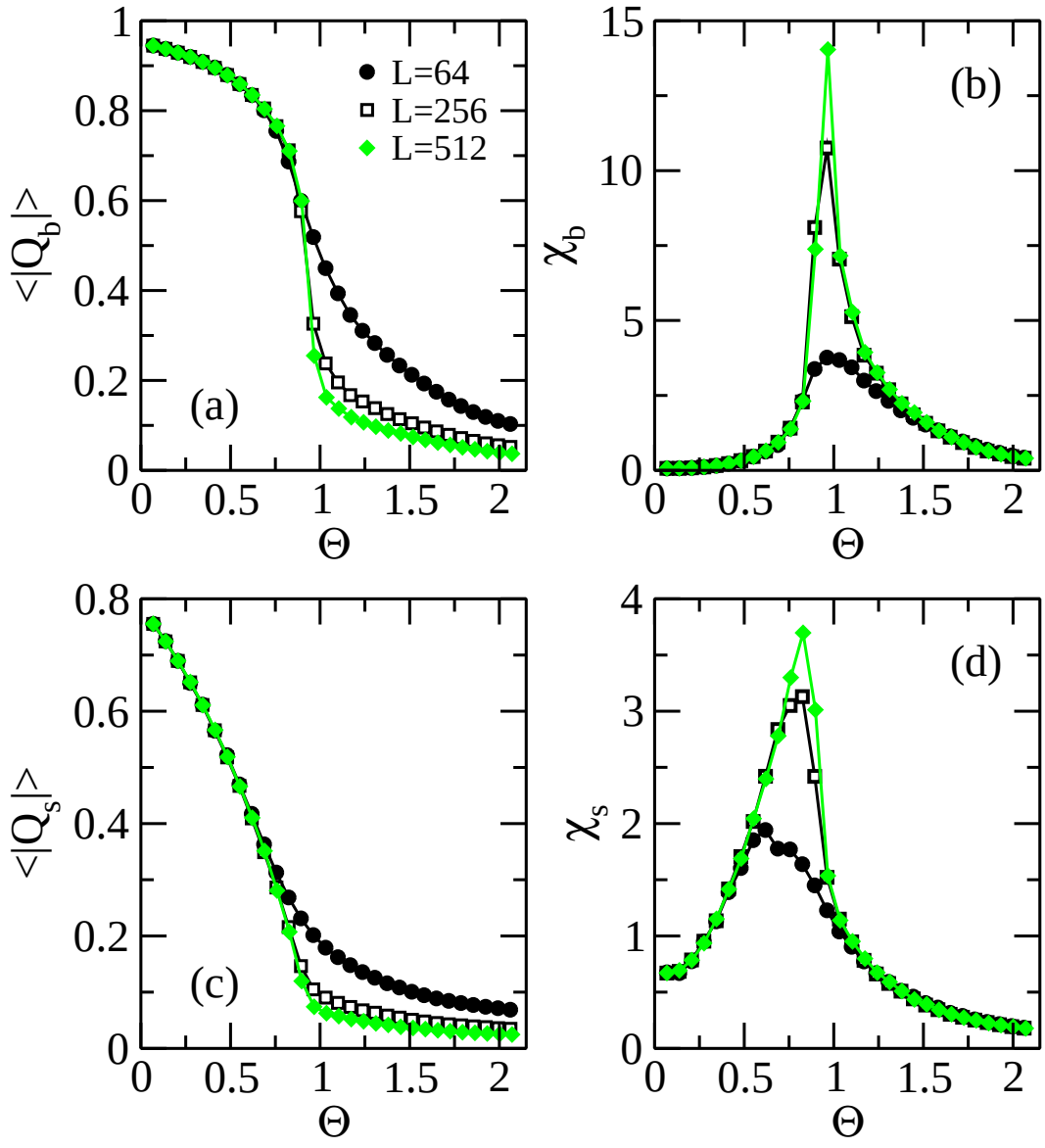


Figure 3.11: Bulk (a, b) and surface (c, d) quantities for the two-dimensional model, composed of $L \times L$ spins, with $J_s = J_b$. Close to the bulk critical point $\Theta_c$, the local order parameters decrease rapidly and the local susceptibilities display pronounced maxima. Here and in the following error bars are smaller than the sizes of the symbols. After [79]. Copyright (2012) by the American Physical Society.

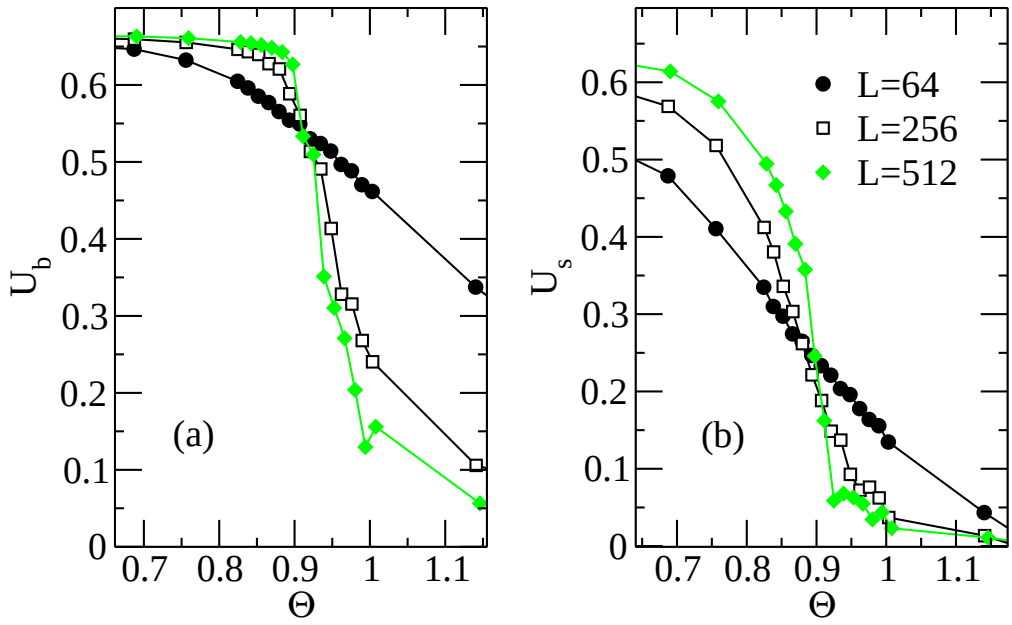


Figure 3.12: The plot of the Binder cumulant function $U$ as a function of $\Theta$ for (a) the bulk and (b) the surface layer. For both layers, curves for all different system sizes cross each other around a specific point, which is estimated as $\Theta_c \approx 0.918$. Note that this estimation is consistent with the result shown in Figure 3.11.

of the Binder curves in the semi-infinite system confirms the estimated value. Figure 3.12 shows the change of Binder curves for different system sizes both in the bulk and in the surface layer. They meet around a specific point, which is estimated as $\Theta_c = 0.918$. But the values of $U$ are different for the bulk and the surface layers i.e. $U_s \approx 0.25$ whereas $U_b \approx 0.53$.

Equations (3.30) and (3.31) imply that our quantities depend algebraically on the linear system size. This is shown in Figure 3.13 for various values of the surface coupling $J_s$. For not too large values of $J_s$ corrections to scaling are negligible, so that we can determine the values of the critical exponents from the slopes. We find $\beta_1/\nu = 0.43(1)$ and $\gamma_{11}/\nu = 0.18(1)$. We immediately remark that these values rather well fulfill the scaling relation $2\beta_1 + \gamma_{11} = d - 1$ that is expected to hold for surface critical exponents. We also note that our values differ strongly from the values of the surface exponents in the equilibrium critical Ising model: $\beta_1^e/\nu = 0.5$ and $\gamma_{11}^e/\nu = 0$ [82, 83, 85]. We therefore have the interesting situation that while

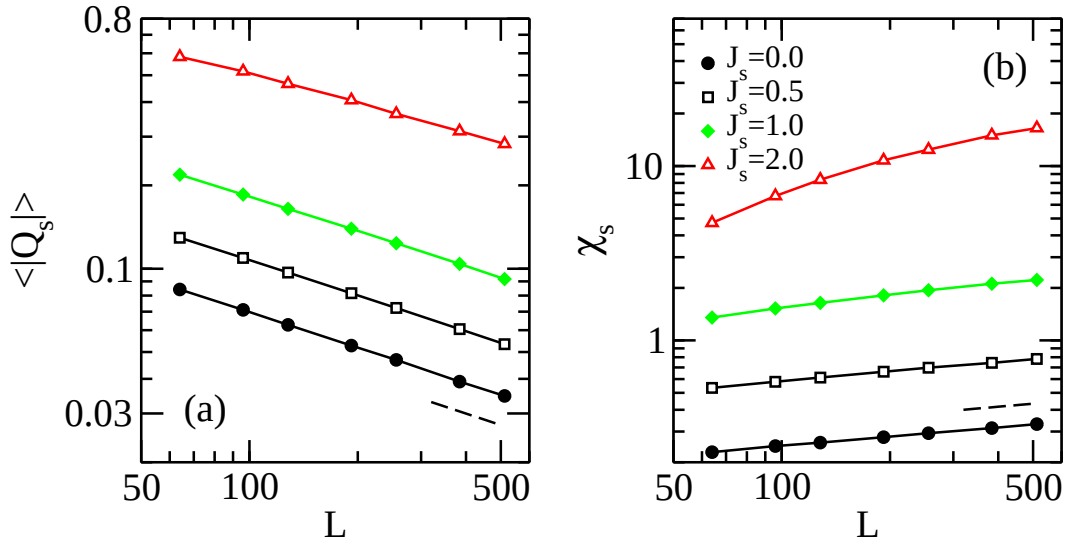


Figure 3.13: Log-log plot of (a) the surface order parameter and (b) the surface susceptibility as a function of the linear system size for the two-dimensional kinetic Ising model at $\Theta = \Theta_c$. The different curves correspond to different values of the surface coupling constant $J_s$ (given in units of $J_b$). The dashed lines have slopes $-0.43$ (a) and 0.18 (b). For large values of $J_s$ corrections to scaling become sizeable. After [79]. Copyright (2012) by the American Physical Society.

the dynamic phase transition in the bulk belongs to the universality class of the equilibrium Ising model, this is not true for the corresponding surface universality class.

For the three-dimensional system, the figure 3.14 shows the change of the order parameter and the susceptibility in the bulk and the surface layer for the case $J_s = J_b$. One can check that the bulk system undergoes again a dynamic phase transition characterized by the critical exponents of the three-dimensional equilibrium critical Ising model, as we verified in the subsection 3.1.1. On the other hand, the surface order parameter decreases steadily, and the susceptibility shows a non-critical peak, which is not located close to $\Theta_c$. This result leads one to expect that for surface in three dimensions the situation is more complicated and thus a more detailed investigation with various surface couplings are needed. For not too small values of the surface coupling, the situation is similar to the two-dimensional case; see the example $J_s = 2J_b$ shown in the first row in Figure 3.15. When reducing $\Theta$, the surface undergoes at the bulk transition value $\Theta_c$ a transition to a dynamically ordered phase. This transition is revealed by a characteristic peak in the surface susceptibility as well as by a crossing at $\Theta_c$ of the surface Binder cumulant computed for different system sizes. However, for values of $J_s < 1.5J_b$, see Figure 3.15(c), the surface spins do not order dynamically at $\Theta_c$, but instead are still able of following the external field, even though this is no longer the case for the bulk spins. At lower values of $\Theta$, the surface order parameter of our finite systems deviates from zero, but this partial dynamical ordering is not related to a phase transition.

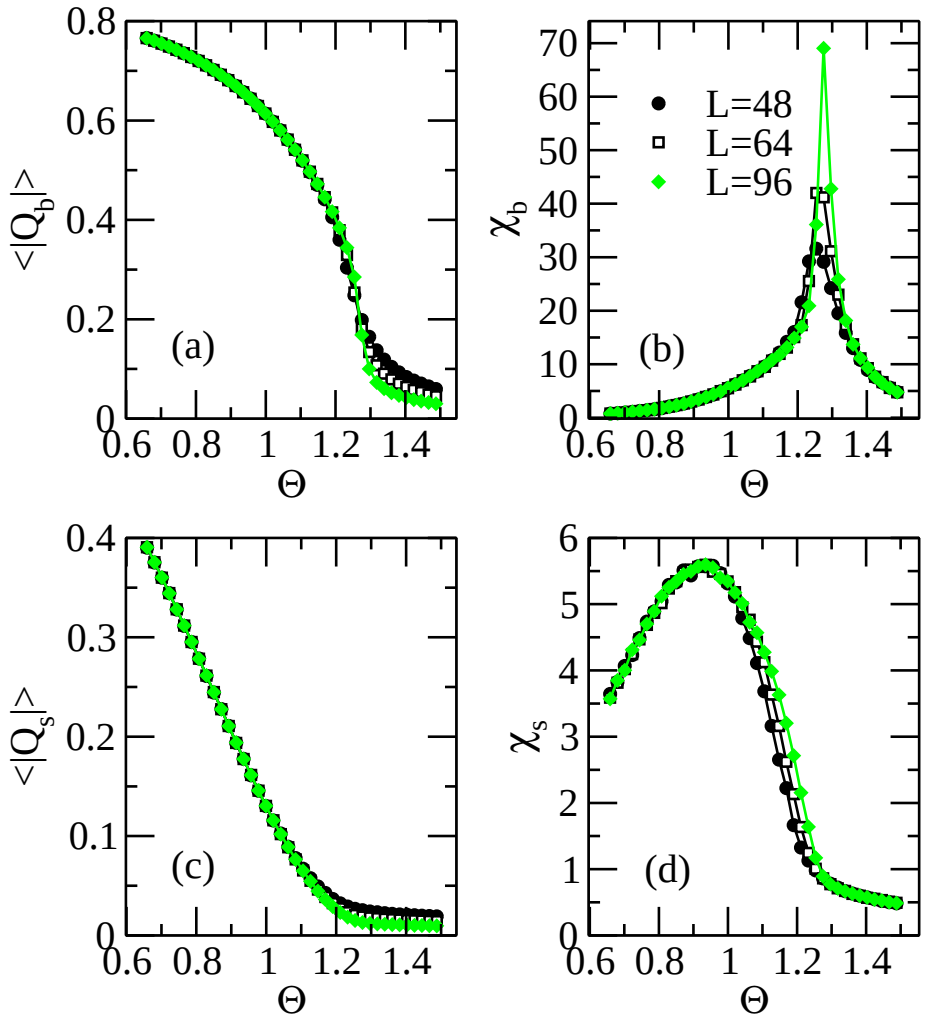


Figure 3.14: The plots of the bulk (a, b) and surface (c, d) quantities for the three-dimensional semi-infinite Ising model with $J_s = J_b$. The bulk layer displays a usual phase transition, whereas the surface layer shows non-critical behavior: the order parameter decreases just continuously, and the maxima of the susceptibility is not divergent.

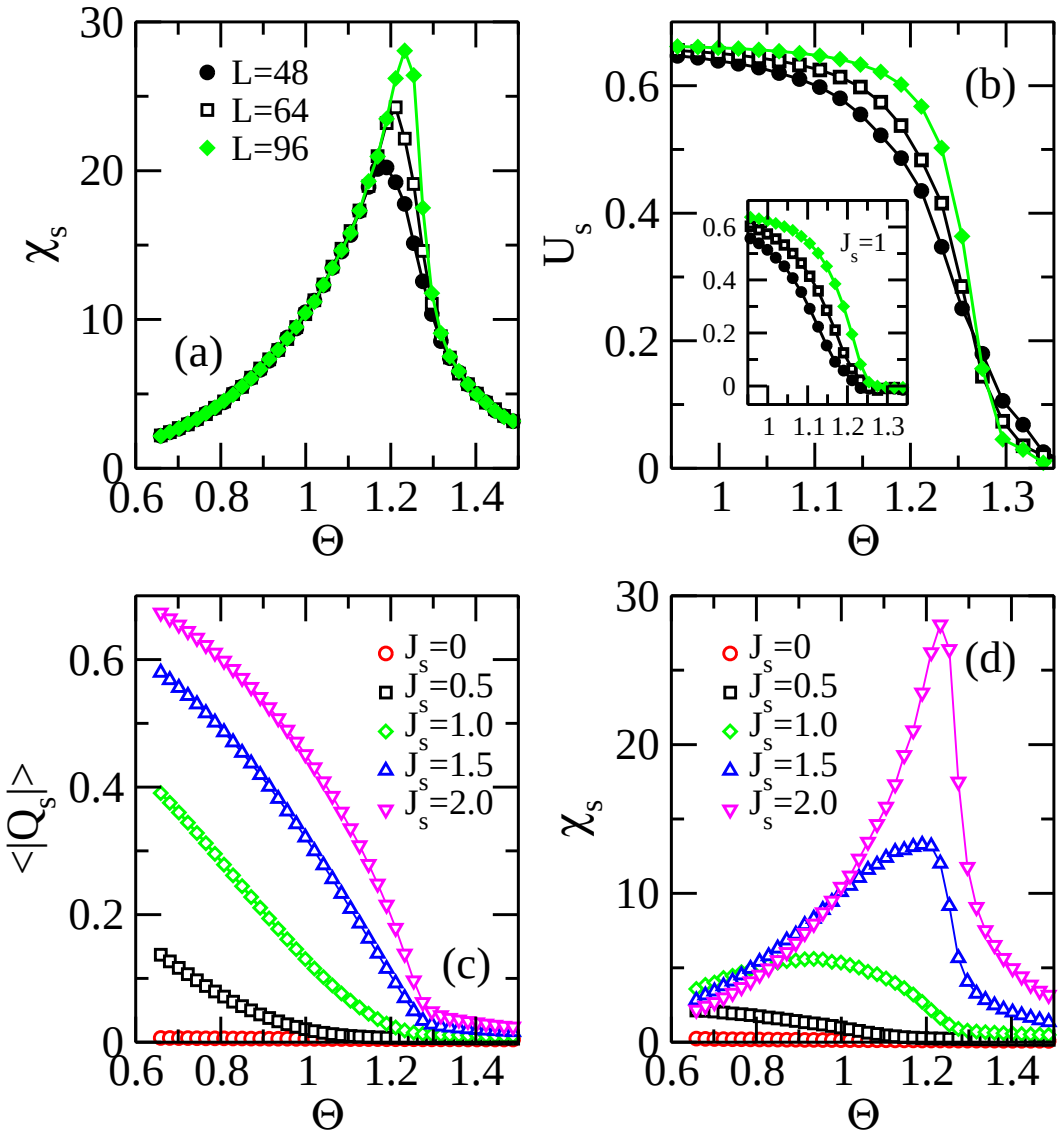


Figure 3.15: Surface susceptibility (a) and surface Binder cumulant (b) for the three-dimensional kinetic Ising model with $J_s = 2J_b$. For small values of $J_s$, the surface does not order dynamically at the bulk critical point, as shown by (c) the surface order parameter and (d) the surface susceptibility. All surface coupling constants are expressed in units of $J_b$. The inset in (b) shows that for $J_s = J_b$ the surface Binder cumulants do not cross at a common value of $\Theta$. The system size in (c) and (d) is $L = 96$. After [79]. Copyright (2012) by the American Physical Society.

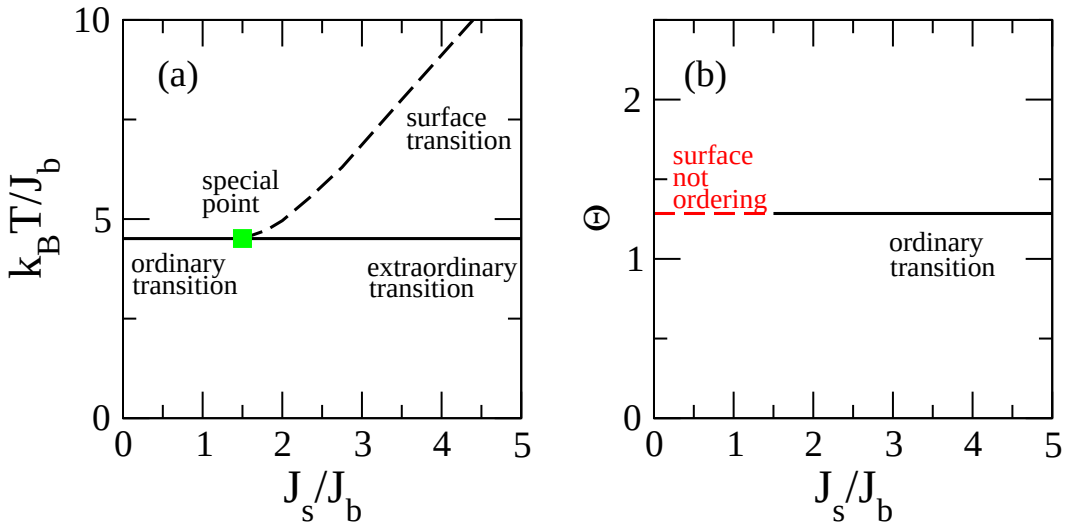


Figure 3.16: Surface phase diagram of (a) the equilibrium three-dimensional Ising model and (b) the non-equilibrium three-dimensional kinetic Ising model. After [79]. Copyright (2012) by the American Physical Society.

This is also revealed by the presence of a noncritical peak (or, for very small values of $J_s$, by the complete absence of any peak) in the surface susceptibility [see Figure 3.15(d)] as well as by the absence of the crossing of the surface Binder cumulants for different system sizes, as shown in the inset of Figure 3.15(b).

Based on our data, where we studied surface couplings from $J_s = 0$ to $J_s = 16J_b$, the surface phase diagram of the three-dimensional kinetic Ising model shown in Figure 3.16(b) differs remarkably from the corresponding diagram of the equilibrium model [82, 83, 85]; see Figure 3.16(a). Not only does the surface not order dynamically at the bulk critical point for $J_s < 1.5J_b$, as just discussed, the kinetic Ising model also does not exhibit a surface transition, where the surface orders alone, whereas the bulk remains disordered. Concomitantly, the special transition point, where both surface and bulk are critical, and the extraordinary transition, where the bulk orders in presence of an ordered surface, are also absent. In fact, whereas for the equilibrium system is it possible to shift the phase transition temperature of the two-dimensional surface $k_B T_c^{2d} = 2.269\cdots J_b$ above the bulk transition temperature $k_B T_c^{3d} = 4.511\cdots J_b$ by sufficiently increasing the ratio $J_s/J_b$ of the couplings, a similar mechanism does not exist in the kinetic Ising model.

Finally, for $J_s > 1.5J_b$, we can again measure the surface critical exponents through a finite-size scaling analysis. As shown in Figure 3.17, corrections to scaling are much more important in three than in two dimensions. Based on our data, we obtain $\beta_1/\nu = 0.88(3)$ and $\gamma_{11}/\nu = 0.29(3)$. These values again differ markedly from the known values $\beta_1^e/\nu = 1.27$ and $\gamma_{11}^e/\nu = -0.40$ of the corresponding surface critical exponents [100]. Most notably, whereas in the equilibrium system the surface susceptibility displays a cusp singularity characterized

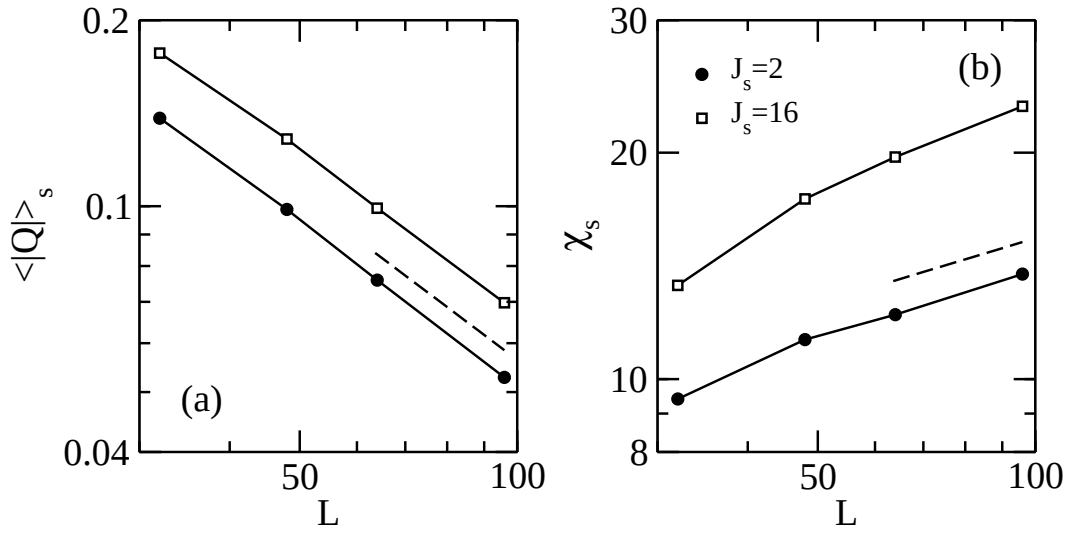


Figure 3.17: (a) Surface order parameter and (b) surface susceptibility as a function of system size at the bulk critical point of the three-dimensional kinetic Ising model. The dashed lines have slopes −0.88 (a) and 0.29 (b). After [79]. Copyright (2012) by the American Physical Society.

by a negative critical exponent, in our system the surface susceptibility diverges with a positive critical exponent.

## 3.3 Summary

As we mentioned in subsection 3.1.1, a symmetry argument put forward in [77] states that continuous transitions with up-down symmetry and non-conserved order parameter should fall into the universality class of the ordinary Ising model. This indeed agrees with our own results (as well as with previous results [71, 78]) that the bulk critical exponents at the dynamic phase transition are the same as that of the equilibrium Ising model, and this both in two and three dimensions.

However, once surfaces are introduced, the lattice symmetry is broken close to the surfaces, and one of the assumptions underlying the argument of [77] is no longer fulfilled. Indeed, our results show that the dynamic surface exponents differ from the surface exponents of the equilibrium model, yielding new non-equilibrium surface universality classes. Using field-theoretical methods similar to those developed for equilibrium critical surfaces [83, 100], it should be possible to compute these new exponents and to classify the possible dynamic surface universality classes.

It follows from our work that our understanding of the role played by surfaces in non-equilibrium systems, and more specifically at non-equilibrium phase transitions, is far from

being complete. Surfaces break lattice symmetries, and this can have many surprising and unexpected effects out of equilibrium, as exemplified in our study of surface critical behavior at a dynamic phase transition. Based on our results, we expect that future in-depth studies of the role of surfaces far from equilibrium will reveal additional new and unexpected phenomena.

# Chapter 4

# Conclusion

Systems far from equilibrium can be found everywhere. Whereas many of them are familiar, ordinary systems, a theoretically satisfactory description of them remains elusive. Physicists often start their studies with simple model systems and proceed to complicated models step by step, thereby trying to mimic real systems. Following this traditional way, we begin our study of two different but related far from equilibrium phenomena with the celebrated Ising model. After reviewing the phenomena in its pure forms, we introduce additional constraints to the model and ask what kind of effects these constraints have on these non-equilibrium phenomena.

In the first part of our work, we try to apply the simple aging scaling scenario to Ising spin glasses as well as to disordered ferromagnets. The simple aging scenario is a well established framework that the perfect Ising model obeys, under the assumption that there is a single characteristic length scale. Therefore, in order to see whether the simple aging scenario is fulfilled also in disordered systems, the first thing to do is to check the assumption of an algebraic growth law for the dynamical correlation length $L(t)$. Indeed, whereas $L(t)$ in the perfect Ising model shows this algebraic growth i.e. $L(t) \sim t^{1/z}$, we numerically confirm that the introduction of disorder leads $L(t)$ to grow much more slowly (maybe logarithmically?) for both cases of site disorder and of bond disorder. Using this numerically obtained value of $L(t)$, we find that two-time quantities again collapse on a single master curve after scaling, but now as a function of the ratio $L(t)/L(s)$. This implies that the simple aging scheme remains true when using $L(t)$ in the scaling analysis, even though some properties of the Ising model change due to disorder effects. Finally we discuss the possibility that the modified simple aging scenario can be applied to Ising spin glasses, where the combination of frustration and disorder yields extremely slow dynamics. Within numerically accessible time windows, we also observe in this case that different autocorrelation curves fall onto a master curve when scaled by $L(t)/L(s)$.

In the second part of the thesis we investigate the surface critical properties of the Ising model displaying a dynamic phase transition. Dynamic phase transition is one example of a genuine

non-equilibrium phase transition, and its critical behavior has been intensively studied in the past for a bulk system. The most important discovery among many interesting results is that the universality class of the two-dimensional non-equilibrium kinetic Ising model turns out to be identical to the equilibrium two-dimensional Ising universality class. It is well known that in equilibrium systems the surface critical behavior is much different from the bulk critical behavior due to a reduced coordination number at the surface. Noticing that in the past the dynamic phase transition was studied in the bulk system only, we study for the first time the dynamic phase transition in presence of a surface. We introduce a dynamic order parameter, the susceptibility and the Binder cumulant both for the bulk and for the surface layer. The change of the order parameter and susceptibility near the critical value of the order parameter $\Theta$ clearly indicates the presence of a dynamic surface phase transition. In order to estimate the surface critical exponents, we use the finite size scaling method to measure the slopes in the plots of the surface order parameter and susceptibility as a function of the system size $L$. The values of local critical exponents that we obtain are unexpected : both in two and three dimensions they differ from the equilibrium set of surface critical exponents. Moreover, in three dimensions, the majority of surface transitions that the equilibrium system exhibits are not found at the dynamic phase transition, with the exception of the ordinary transition. Thus the surface phase diagram is remarkably simple, and the surface universality class of the Ising model undergoing a dynamic phase transition is clearly different from the equilibrium surface universality class. This novel result implies that the surface as a geometrical boundary plays a rather crucial role at a dynamic phase transition, thereby causing many surprising and unexpected effects in non-equilibrium systems.

# Bibliography


[1] L. C. E. Struik. *Physical ageing in amorphous polymers and other materials*. Elsevier, Amsterdam, 1978.

[2] S. M. Allen and J. W. Cahn. A microscopic theory for antiphase boundary motion and its application to antiphase domain coarsening. *Acta Metallurgica*, 27:1085, 1979.

[3] M. Henkel and M. Pleimling. Local scale-invariance as dynamical space-time symmetry in phase-ordering kinetics. *Phys. Rev. E*68:065101(R), 2003.

[4] R. Paul, S. Puri, and H. Rieger. Domain growth in random magnets. *Europhys. Lett.*, 68:881, 2004.

[5] B. M. McCoy and T. T. Wu. Theory of a two-dimensional Ising model with random impurities. I. Thermodynamics. *Phys. Rev.*, 176:631, 1968.

[6] D. A. Huse and C. L. Henley. Pinning and roughning of domain walls in Ising systems due to random impurities. *Phys. Rev. Lett.*, 54:2708, 1985.

[7] H. Ikeda, Y. Endoh and S. Itoh. Ordering kinetics in a two-dimensional percolation magnet. *Phys. Rev. Lett.*, 64:1266, 1990.

[8] D. K. Shenoy, J. V. Selinger, K. A. Grüneberg, J. Naciri and R. Shashidhar. Coarsening of reverse tilt domains in liquid-crystal cells with heterogeneous alignment layers. *Phys. Rev. Lett.*, 82:1716, 1999.

[9] R. Paul, S. Puri, and H. Rieger. Domain growth in Ising systems with quenched disorder. *Phys. Rev. E*71:061109, 2005.

[10] R. Paul, G. Schehr, and H. Rieger. Superaging in two-dimensional random ferromagnets. *Phys. Rev. E*75:030104(R), 2007.

[11] C. Aron, C. Chamon, L. F. Cugliandolo, and M. Picco. Scaling and superuniversality in the coarsening dynamics of the 3D random field Ising model. *J. Stat. Mech.*, :P05016, 2008.

[12] M. Henkel and M. Pleimling. Superuniversality in phase-ordering disordered ferromagnets. *Phys. Rev. B*78:224419, 2008.

[13] M. P. O. Loureiro, J. J. Arenzon, L. F. Cugliandolo, and A. Sicilia. Curvature-driven coarsening in the two-dimensional Potts model. *Phys. Rev. E*81:021129, 2010.

[14] G. Schehr and H. Rieger. Nonequilibrium dynamics below the super-roughning transition. *Phys. Rev. B*71:184202, 2005.

[15] A. Kolton, A. Rosso and T. Giamarchi. Nonequilibrium relaxation of an elastic string in a random potential. *Phys. Rev. Lett.*, 95:180604, 2005.

[16] J. D. Noh and H. Park. Relaxation dynamics of an elastic string in random media. *Phys. Rev. E*80:040102(R), 2009.

[17] J. L. Iguain, S. Bustingorry, A. B. Kolton and L. F. Cugliandolo. Growing correlations and aging of an elastic line in a random potential. *Phys. Rev. B*80:094201, 2009.

[18] C. Monthus and T. Garel. An eigenvalue method for computing the largest relaxation time of disordered systems. *J. Stat. Mech.*, :P12017, 2009.

[19] S. Puri. Ordering dynamics in disordered systems. *Phase Transitions*. 77:469, 2004.

[20] D. S. Fisher and D. A. Huse. Nonequilibrium dynamics of spin glasses. *Phys. Rev. B*38:373, 1988.

[21] A. J. Bray and K. Humayun. Universality class for domain growth in random magnets. *J. Phys. A: Math. Gen.*, 24:L1185, 1991.

[22] S. Puri, D. Chowdhuri and N. Parekh. Non-algebraic domain growth in random magnets: a cell dynamical approach. *J. Phys. A: Math. Gen.*, 24:L1087, 1991.

[23] H. Hayakawa. A cell-dynamics approach to the ordering in a system with quenched random impurities. *J. Phys. Soc. Japan.*, 60:2492, 1991.

[24] B. Biswal, S. Puri and D. Chowdhury. Domain growth in weakly disordered magnets. *Physica A*, 229:72, 1996.

[25] M. Henkel and M. Pleimling. *Nonequilibrium phase transitions: volume 2 - Ageing and dynamical scaling far from equilibrium*. Springer, Heidelberg, 2010.

[26] A. Andreanov and A. Lefèvre. Crossover from stationary to ageing regime in glassy dynamics. *Europhys. Lett.*, 76:919, 2006.

[27] L. Ramos and L. Cipelletti. Ultraslow dynamics and stress relaxation in the ageing of a soft glassy system. *Phys. Rev. Lett.*, 87:245503, 2001.

[28] P. Wang, C. Song and H. A. Makse. Dynamic particle tracking reveals the ageing temperature of a colloidal glass. *Nat. Phys.*, 2:526, 2006.

[29] X. Trepat, L. Deng, S. S. An, D. Navajas, D. J. Tschumperlin, W. T. Gerthoffer, J. P. Butler and J. J. Fredberg. Universal physical responses to stretch in the living cell. *Nature*, 447:592, 2007.

[30] J. Kurchan. Elementary constraints on autocorrelation function scalings. *Phys. Rev. E*66:017101, 2002.

[31] Some systematic deviations, similar to those observed in the random-site model, albeit much less pronounced, have been reported in an early study of the aging properties of the random-bond model for specific realizations of the disorder. (Ref. [38])

[32] H. Park and M. Pleimling. Aging in coarsening diluted ferromagnets. *Phys. Rev. B*82:144406, 2010.

[33] D. Stauffer. Scaling theory of percolation clusters. *Phys. Rep.*, 54:1, 1979.

[34] A. Barrat. Monte Carlo simulations of the violation of the fluctuation-dissipation theorem in domain-growth processes. *Phys. Rev. E*57:3629, 1998.

[35] A. J. Bray. Theory of phase-ordering. *Adv. Phys.*, 43:537, 1994.

[36] In fact, a non-constant effective dynamical exponent is also seen in Fig. 10(b) of Ref. [9], even though the authors of that paper interpret the data differently.

[37] M Henkel, A. Picone and M. Pleimling. Two-time autocorrelation function in phase-ordering kinetics from local scale-invariance. *Europhys. Lett.*, 68:191, 2004.

[38] M Henkel and M. Pleimling. Ageing in disordered magnets and local scale invariance. *Europhys. Lett.*, 76:561, 2006.

[39] C. Yeung, M. Rao and R. C. Desai. Bounds on the decay of the autocorrelation in phase-ordering dynamics. *Phys. Rev. E*53:3073, 1996.

[40] A. Röthlein, F. Baumann and M. Pleimling. Symmetry-based determination of space-time functions in nonequilibrium growth processes. *Phys. Rev. E*74:061604, 2006.

[41] T. Iwai and H. Hayakawa. Simulation of domain growth in a system with random impurities. *J. Phys. Soc. Japan.*, 62:1583, 1993.

[42] F. Corberi, E. Lippiello and M. Zannetti. Interface fluctuations, bulk fluctuations, and dimensionality in the off-equilibrium response of coarsening systems. *Phys. Rev. E*63:061506, 2001.

[43] E. Lippiello, A. Mukherhjee, S. Puri and M. Zannetti. Scaling behavior of response functions in the coarsening dynamics of disordered ferromagnets. *EPL*, 90:46006, 2010.

[44] H. Park and M. Pleimling. Domain growth and aging scaling in coarsening disordered systems. *Eur. Phys. J.*, B85:300, 2012.

[45] F. Corberi, E. Lippielli, A. Mukherjee, S. Puri and M. Zannetti. Growth law and superuniversality in the coarsening of disordered ferromagnets. *J. Stat. Mech.*, :P03016, 2011.

[46] K. Humayun and A. J. Bray. Non-equilibrium dynamics of the Ising model for $T \leq T_c$. *J. Phys. A: Math. Gen.*, 24:1915, 1991.

[47] F. Liu and G. F. Mazenko. Non-equilibrium autocorrelations in phase-ordering dynamics. *Phys. Rev. B*44:9185, 1991.

[48] E. Lorenz and W. Janke. Nnumerical tests of local scale invariance in ageing q-state Potts models. *Europhys. Lett.*, 77:10003, 2007.

[49] K. Binder and A. P. Young. Spin glasses: Experimental facts, theoretical concepts, and open questions. *Rev. Mod. Phys.*, 58:801, 1986.

[50] D. Sherrington and S. Kirkpatrick. Solvable model of a spin-glass. *Phys. Rev. Lett.*, 35:1792, 1975.

[51] S. F. Edwards and P. W. Anderson. Theory of spin glasses. *J. Phys. F: Metal Phys.*, 5:965, 1975.

[52] N. Kawashima and H. Rieger. Recent progress in spin glasses. In H. Diep, editor, *Frustrated magnetic systems*. Singapour, 2004. World Scientific.

[53] D. S. Fisher and D. A. Huse. Ordered phase of short-range Ising spin glasses. *Phys. Rev. Lett.*, 56:1601, 1986.

[54] E. Marinari, G. Parisi, F. Ricci-Tersenghi, J. J. Ruiz-Lorenzo and F. Zuliani. Replica symmetry breaking in short-range spin glasses : theoretical foundations and numerical evidences. *J. Stat. Phys.*, 98:973, 2000.

[55] F. Krzakala and O. C. Martin. Spin and link overlaps in three-dimensional spin glasses. *Phys. Rev. Lett.*, 85:3013, 2000.

[56] M. Palassini and A. P. Young. Nature of the spin glass state. *Phys. Rev. Lett.*, 85:3017, 2000.

[57] J. P. Bouchaud, V. Dupuis, J. Hammann and E. Vincent. Separation of time and length scales in spin glasses: Temperature as a microscope. *Phys. Rev. B*65:024439, 2001.

[58] H. G. Katzgraber, M. Korner and A. P. Young. Universality in three-dimensional Ising spin glasses: A Monte Carlo study. *Phys. Rev. B*73:224432, 2006.

[59] E Marinari and G. Parisi. Effects of a bulk perturbation on the ground state of 3D Ising spin glasses. *Phys. Rev. Lett.*, 86:3887, 2001.

[60] S. Jimenez, V. Martin-Mayor and S. Perez-Gaviro. Rejuvenation and memory in model spin glasses in three and four dimensions. *Phys. Rev. B*72:054417, 2005.

[61] F. Belleti *et al.* An in-depth view of the microscopic dynamics of Ising spin glasses at fixed temperature. *J. Stat. Phys.*, 135:1121, 2010.

[62] J. Kisker, L. Santen and M. Schreckenberg. Off-equilibrium dynamics in finite-dimensional spin-glass models. *Phys. Rev. B*53:6418, 1996.

[63] M. Henkel, H. Hinrichsen and S. Lübeck. *Nonequilibrium phase transitions: volume 1 - Absorbing phase transitions*. Springer, New York, 2008.

[64] G. Ódor. *Universality in nonequilibrium lattice systems: Theoretical foundations*. World Scientific, Singapore, 2008.

[65] B. Schmittmann and R. K. P. Zia. Statistical Mechanics of Driven Diffusive Systems. In C. Domb and J. L. Lebowitz, editors, *Phase Transitions and Critical Phenomena,* volume 17, New York, 1995, Academic Press.

[66] G. L. Daquila and U. C. Täuber. Nonequilibrium relaxation and critical aging for driven Ising lattice gases. *Phys. Rev. Lett.*, 108:110602, 2012.

[67] B. Chakrabarti and M. Acharyya. Dynamic transitions and hysteresis. *Rev. Mod. Phys.*, 71:847, 1999.

[68] M. Acharyya. Nonequilibrium phase transitions in model ferromagnets: A review. *Int. J. Mod. Phys. C*, 16:1631, 2005.

[69] M. Acharyya. Nonequilibrium phase transition in the kinetic Ising model: Critical slowing down and the specific-heat singularity. *Phys. Rev. E*56:2407, 1997.

[70] S. W. Sides, P. A. Rikvold and M. A. Novotny. Kinetic Ising model in an oscillating field: Finite-size scaling at the dynamic phase transition. *Phys. Rev. Lett.*, 81:834, 1998.

[71] G. Korniss, C. J. White, P. A. Rikvold and M. A. Novotny. Dynamic phase transition, universality, and finite-size scaling in the two-dimensional kinetic Ising model in an oscillating field. *Phys. Rev. E*63:016120, 2000.

[72] H. Jang, M. J. Grimson and C. K. Hall. Dynamic phase transitions in thin ferromagnetic films. *Phys. Rev. B*67:094411, 2003.

[73] M. Acharyya. Axial and off-axial dynamic transitions in uniaxially anisotropic heisenberg ferromagnet: A comparison. *Int. J. Mod. Phys. C*, 14:49, 2003.

[74] O. Canko, B. Deviren and M. Keskin. Dynamic phase transition in the kinetic spni-3/2 Blume-Emery-Griffiths model in an oscillating field. *J. Phys. Condens. Matter*, 18:6635, 2006.

[75] Q. Jiang, H.-N. Yang and G.-C. Wang. Scaling and dynamics of low-frequency hysteresis loops in ultrathin Co films on a Cu(001) surface. *Phys. Rev. B*52:14911, 1995.

[76] D. T. Robb, Y. H. Xu, O. Hellwig, J. McCord, A. Berger, M. A. Novotny and P. A. Rikvold. Evidence for a dynamic phase transition in $[Co/Pt]_3$ magnetic multilayers. *Phys. Rev. B*78:134422, 2008.

[77] G. Grinstein, C. Jayaprakash and Y. He. Statistical mechanics of probabilistic cellular automata. *Phys. Rev. Lett.*, 55:2527, 1985.

[78] H. Fujisaka, H. Tutu and P. A. Rikvold. Dynamic phase transition in a time-dependent Ginzburg-Landau model in an oscillating field. *Phys. Rev. E*63:036109, 2001.

[79] H. Park and M. Pleimling. Surface criticality at a dynamic phase transition. *Phys. Rev. Lett.*, 109:175703, 2012.

[80] H. Park and M. Pleimling. Dynamic phase transition in the three-dimensional kinetic Ising model in an oscillating field. Submitted to *Phys. Rev. E*.

[81] K. Binder. In V. Privman, editor, *Finite-size scaling and numerical simulations of statistical systems*. Singapore, 1990. World Scientific.

[82] K. Binder. Critical behavior at surfaces. In C. Domb and J. L. Lebowitz, editors, *Phase Transitions and Critical Phenomena,* volume 8, London, 1983, Academic Press.

[83] H. W. Diehl. Field-theoretical approach to critical behaviour at surfaces. In C. Domb and J. L. Lebowitz, editors, *Phase Transitions and Critical Phenomena,* volume 10, London, 1986, Academic Press.

[84] H. W. Diehl. The theory of boundary critical phenomena. *Int. J. Mod. Phys. B*, 11:3503, 1997.

[85] M. Pleimling. Critical phenomena at perfect and non-perfect surfaces. *J. Phys. A: Math. Gen.*, 37:R79, 2004.

[86] F. Iglói, I. Peschel and L. Turban. Inhomogeneous systems with unusual critical behaviour. *Adv. Phys*, 42:683, 1993.

[87] M. Pleimling and W. Selke. Critical phenomena at perfect and non-perfect surfaces. *Eur. Phys. J.*, B1:385, 1998.

[88] A. J. Bray and M. A. Moore. Critical behaviour of semi-infinite systems. *J. Phys. A: Math. Gen.*, 10:1927, 1977.

[89] T. W. Burkhardt and H. W. Diehl. Ordinary, extraordinary, and normal surface transitions: extraordinary-normal equivalence and simple explanation of $|T-T_c|^{2-\alpha}$ singularities. *Phys. Rev. B*50:3894, 1994.

[90] K. Binder and D. P. Landau. Crossover scaling and critical behavior at the "surface-bulk" multicritical point. *Phys. Rev. Lett.*, 52:318, 1984.

[91] C. Ruge, A. Dunkelmann and F. Wagner. New method for determination of critical parameters. *Phys. Rev. Lett.*, 69:2465, 1992.

[92] C. Ruge, A. Dunkelmann, F. Wagner and J. Wulf. Study of the three-dimensional Ising model on film geometry with the cluster Monte Carlo method. *J. Stat. Phys.*, 73:293, 1993.

[93] Youjin Deng, Henk W. J. Blöte and M. P. Nightingale. Surface and bulk transitions in three-dimensional $O(n)$ models. *Phys. Rev. E*72:016128, 2005.

[94] N. D. Mermin and H. Wagner. Absence of ferromagnetism or antiferromagnetism in one- or two-dimensional isotropic Heisenberg models. *Phys. Rev. Lett.*, 17:1133, 1966.

[95] J. Fröhlich and C. E. Pfister. Classical spin systems in the presence of a wall: multi-component spins. *Commun. Math. Phys.*, 107:337, 1986.

[96] D. P. Landau, R. Pandey and K. Binder. Monte Carlo study of surface critical behavior in the XY model. *Phys. Rev. B*39:12302, 1989.

[97] O Peczak and D. P. Landau. Monte Carlo study of the surface special transition in the XY model in three dimensions. *Phys. Rev. B*43:1048, 1991.

[98] H. L. Richards, M. Kolesik, P. -A. Lindgard, P. A. Rikvold and M. A. Novotny. Effects of boundary conditions on magnetization switching in kinetic Ising models of nanoscale ferromagnets. *Phys. Rev. B*55:11521, 1997.

[99] H. Jang and M. J. Grimson. Hysteresis and the dynamic phase transition in thin ferromagnetic films. *Phys. Rev. E*63:066119, 2001.

[100] H. W. Diehl and M. Shpot. Massive field-theory approach to surface critical behavior in three-dimensional systems. *Nucl. Phys.*, B528:595, 1998.